Functional consequences of unilateral and sequential bilateral cortical infarcts in the adult rat brain

DISSERTATION

zur Erlangung des akademischen Grades
doctor rerum naturalium (Dr. rer. nat.)

vorgelegt dem Rat der Biologisch-Pharmazeutischen
Fakultät der Friedrich-Schiller-Universität Jena

von Dipl.-Biochem. Elena Chanina
geboren am 01.01.1974 in Kaluga, Russland

Gutachter 1: Prof. Dr. O.W. Witte

Gutachter 2: Prof. Dr. J. Bolz

Gutachter 3: Prof. Dr. T. Jones

Tag der mündlichen Prüfung: 5. Juli 2006

Tag der öffentlichen Verteidigung: 28. Juli 2006

Jena, den 4. August 2006

Table of contents

Zusammenfassung

Die Auswirkungen von Schlaganfällen sind nicht auf die geschädigte Hirnregion beschränkt sondern betreffen auch die Umgebung des Hirninfarktes sowie ipsi- und kontralaterale Hirnregionen. Die vorliegende Studie beschäftigt sich mit den strukturellen und funktionellen Folgen von kortikalen Hirninfarkten im sensomotorischen Vorderpfotenkortex der Ratte (FL SMC). Um die Rolle funktioneller Veränderungen im kontralateralen Kortex zu klären wurde diese Hirnregion systematisch zu verschiedenen Zeitpunkten durch einen zweiten Hirninfarkt lädiert, wobei zur Auslösung der Infarkte das Photothrombose-Modell verwendet wurde. Mit Hilfe einer sensomotorischen Verhaltenstestbatterie wurde die Entwicklung des sensomotorischen Defizits und die Funktionserholung beider Pfoten analysiert und so der Einfluss der zweiten Läsion auf die Erholung der initial geschädigten Vorderpfote bestimmt. Darüber hinaus wurde immunhistochemisch das Ausmaß der neuronalen Degeneration sowie entzündlicher Veränderungen in entfernten Hirnregionen analysiert und die Langzeitfolgen von einzelnen und wiederholten Hirninfarkten mit Hilfe von volumetrischen Messungen und kognitiven Verhaltenstests charakterisiert.

In einer ersten Serie von Experimenten konnte in den vorliegenden Untersuchungen nachgewiesen werden, dass das Ausmaß der neuronalen Degeneration nach Hirninfarkten vom zeitlichen Abstand zwischen den Infarkten abhängt. Degenerative Veränderungen der Nervenzellen waren im Striatum und Thalamus jeweils von einer massiven Aktivierung von Mikrogliazellen und Astrozyten begleitet, wobei diesbezüglich keine Unterschiede zwischen Tieren mit einem einzelnen bzw. zwei bilateralen Infarkten beobachtet wurden. Die Untersuchungen der sensomotorischen Vorderpfotenfunktion zeigten in einer weiteren Serie von Experimenten

interessanterweise keine Unterschiede in der Funktionserholung zwischen Tieren mit einzelnen oder bilateralen Hirninfarkten. Auch wenn der zeitliche Abstand zwischen den Infarkten variiert wurde (direkt hintereinander, 2 Tage, 7 Tage oder 10 Tage), störte der zweite kontralaterale Infarkt nicht die Funktionserholung der initial beeinträchtigen Pfote. Diese Befunde deuten daraufhin, dass der kontralaterale Kortex zur Funktionserholung der initial beeinträchtigen Vorderpfote keinen wesentlichen Beitrag leistet. In einer dritten Untersuchungsserie zeigte sich allerdings bei Tieren mit bilateralen Hirninfarkten eine erhebliche Reduktion des globalen Hirnvolumens im Vergleich zu Tieren mit einem Hirninfarkt und den Kontrolltieren. In Verhaltensuntersuchungen im Wasserlabyrinth konnte nachgewiesen werden, dass dieser Verlust an globalem Hirnvolumen mit schlechteren Leistungen in diesem kognitiven Test einhergehen. Die diesen degenerativen Prozessen zugrunde liegenden Mechanismen sind allerdings noch weit gehend unbekannt und machen so weitere Untersuchungen erforderlich.

Abstract

The effects of focal brain ischemia are not limited to the lesion itself but also involve perilesional and widespread ipsilateral and contralateral brain areas. The present study was designed to characterize the structural and behavioral consequences of cortical infarcts in the forelimb sensorimotor cortex (FL SMC) of rats. In order to analyze the role of functional alterations in the contralateral cortex the homotopic contralesional areas were systematically lesioned at different time points after the first infarct using a photothrombosis model. A battery of sensorimotor tests was used to assess the effect of different time intervals between the cortical bilateral infarcts in the FL SMC on the forelimb sensorimotor deficit and functional recovery. Neuronal degeneration and inflammation were immunohistochemically studied in remote subcortical areas. Furthermore, the long-term effects of single and sequential cortical infarcts on brain volume and cognitive function were assessed in this study.

In a first set of experiments it was demonstrated that the extent of remote neuronal degeneration following bilateral infarcts was dependent on the time interval between the lesions. Neuronal degeneration detected in the striatum and thalamus was accompanied by massive activation of microglia and astrocytes that, however, did not differ between SL and DL groups. Investigations of forelimb sensorimotor functions in a second set of experiments using glass cylinder and foot-fault tests demonstrated no difference in time course and extent of functional recovery in SL and DL-animals. Even when the intervals between the infarcts were varied (0, 2, 7, or 10 days), the second infarct did not impair the functional recovery of the initially impaired forelimb. This finding provides further evidence that the contralesional cortex did not significantly contribute to the functional recovery of the impaired forelimb. However,

in the third study evaluation of brain volume in DL-animals detected a reduction of global brain volume compared to SL-animals. Behavioral studies in the water maze further demonstrated that this loss of brain volume corresponded to a slight but significant cognitive impairment. Additional investigations are needed to elucidate the pathophysiological mechanisms causing degenerative processes after repetitive ischemic infarcts.

Belief begins where science leaves off and ends where science begins.

Rudolf Virchow (1821-1902)

1. Introduction

Stroke is the third biggest cause of death in the industrialized world after heart disease and cancer and is one of the main causes of morbidity and invalidity. Depending on the lesion type, topography, and size a wide range of motor and sensory deficits as well as cognitive and behavioral abnormalities are observed after stroke. Pharmacological treatment is directed onto the acute phase after stroke and consists mainly of thrombolysis using a recombinant tissue plasminogen activator treatment for early restoration of brain perfusion. Because of a limited time window for acute therapy only a subgroup of patients reaching the hospital within 3 hours can benefit from this treatment, whereas for others only symptomatic therapy is available. Therefore, most patients show remaining neurological deficits requiring long-term rehabilitation or institutional care. Functional recovery varies depending on the size and location of the initial stroke and it is often difficult to predict the long-term outcome within the first days after the insult (Chollet and Weiller, 1994). The mechanisms of poststroke functional recovery are only poorly understood and investigations of the underlying processes are very important for the development of appropriate rehabilitative strategies.

Ischemic stroke results from a transient or permanent reduction in cerebral blood flow that is restricted to a territory of a major brain artery. The reduction in flow is, in most cases, caused by the occlusion of a cerebral artery either by an embolus or by local thrombosis. Following the cessation of blood supply, metabolic deprivation, excitotoxicity and peri-infarct depolarizations emerge and contribute to the ischemic

brain damage within the first hours after stroke (for review see Dirnagl et al., 1999) (Fig.1.1). Excitotoxicity causes not only cellular death in the infarct core but also initiates molecular events that lead to apoptosis and inflammatory processes.

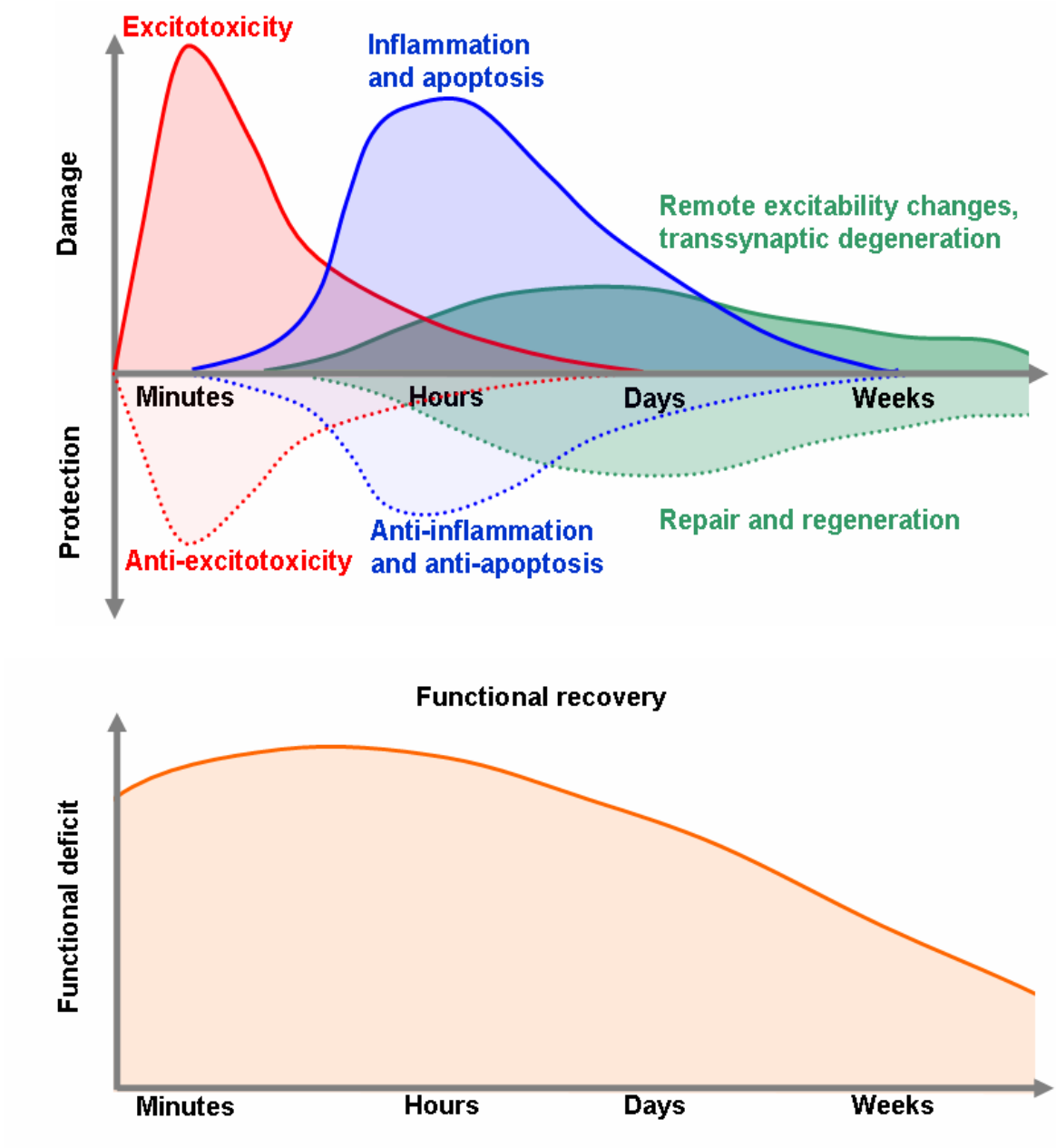

Fig. 1.1. Correlation of time course of putative cascades in focal brain ischemia (modified from Dirnagl et al., 2003) and functional recovery. **A:** Here, the x-axis illustrates the evolution of the cascades over time and the y-axis reflects the impact of each element of the destructive (top) and protective (bottom) cascades on functional outcome. **B:** Time course of functional recovery after focal brain ischemia. It is suggested that functional recovery depends on time course and interaction between neurotoxic and neuroprotective mechanisms. Here, the x-axis illustrates the evolution of functional recovery over time and the y-axis reflects the level of functional deficit after ischemia onset.

Inflammation occurs within a few hours after the onset of ischemia and lasts for weeks and even months and is characterized by an activation of glial cells (astrocytes, microglia) and leukocytes. These cells produce proinflammatory cytokines and chemokines that trigger different pathophysiological cascades deleterious for cell survival (Dirnagl and Priller, 2005; Mergenthaler et al., 2004). Focal cerebral ischemia induces not only destructive cascades, but also activates endogenous protective mechanisms. Anti-inflammatory cytokines such as transforming growth factor-beta and interleukin-10 are induced (Bogdan et al., 1992). Furthermore, the expression of antiapoptotic Bcl2-proteins after focal brain ischemia may suppress cellular death (Linnik et al., 1995; Wiessner et al., 1999). The activation of these endogenous protective mechanisms could increase the resistance of the brain to subsequent ischemic injury (Dirnagl et al., 2003; Kirino, 2002; Kitagawa et al., 1990). This so-called “ischemic tolerance” or “ischemic preconditioning” can be observed in a limited time window. It is widely assumed that the interactions between these damaging and neuroprotective cascades influence the functional deficit after stroke, but only little is known how these processes can be influenced to improve the functional outcome.

Accumulating evidence indicates that primarily uninjured tissue surrounding the ischemic lesion as well as remote ipsilateral and contralateral brain regions play a crucial role in long-term recovery. Various functional alterations occur within these structurally intact regions that may be favourable and/or disadvantageous, compensating for lesion-induced deficits while causing a deterioration of functional impairment or even postlesional epilepsy. Experimental studies in rats indicate widespread and partially persistent alterations in cortical excitability immediately adjacent to the focal ischemic infarct and also in remote ipsilateral and contralateral brain regions. Electrophysiological recordings using the paired-pulse protocol in brain

slice preparations revealed an impairment of functional cortical inhibition in both hemispheres (Buchkraemer-Ratzmann et al., 1996) accompanied by a reduction of γ-aminobutyric acid $(GABA)_A$ dependent inhibitory function (Neumann-Haefelin et al., 1995). Redecker et al. (2002) further demonstrated a reduced expression as well as dysregulation of the $GABA_A$ receptors up to 30 days after focal cortical ischemia in the cortex, hippocampus, and thalamus of both hemispheres for nearly all receptor subunits. Furthermore, inhibitory $GABA_B$ and excitatory N-metyl-D-aspartate (NMDA) receptor binding is up-regulated bilaterally in widespread cortical regions (Qu et al., 1998; Que et al., 1999). In addition, long-term potentiation that is commonly associated with plasticity and learning was facilitated in the ipsilesional hemisphere after cortical ischemic infarcts (Hagemann et al., 1998). These data suggest that the alterations in neurotransmission might influence the functional deficit and long-term recovery, although the underlying mechanisms are not well understood. Anatomically, cortical lesions induce axonal sprouting and dendritic arborization within the ipsilesional and unimpaired contralesional hemisphere (Biernaskie et al., 2001; Jones et al., 2003; Jones and Schallert, 1992; 1994; Napieralski et al., 1996) suggesting that these regions take part in the recovery process. Interestingly, the postlesional axonal sprouting could be prevented by blockade of neuronal activity (Carmichael and Chesselet, 2002). Moreover, the increase in axonal sprouting and dendritic arborization in the contralesional cortex might be due to compensatory motor activity since immobilization of the unimpaired forelimb has been shown to block these changes (Schallert et al., 2000a).

It is suggested that the widespread postlesional plastic alterations might facilitate the reorganization of brain connections or maps that, in turn, may cause, to some degree, the restoration of functions after focal somatosensory and motor cortical damage (Nudo and Friel, 1999). From the functional point of view, the topography of

the remote alterations after stroke is difficult to explain. However, experimental and clinical studies describe two main reorganization patterns observed in the ipsilesional and/or contralesional hemisphere indicating that these brain regions contribute to functional recovery. Several studies in humans and animal models clearly demonstrate that significant adaptive changes take place in the direct vicinity of the infarct (Butz et al, 2004; Chollet et al, 1991; Loubinoux et al, 2003; Nudo et al, 1996). Perilesional structural reorganization leading to an enlargement and rearrangement of receptive fields has been described in the somatosensory cortex of monkeys and rats (Jenkins and Merzenich, 1987; Reinecke et al, 2003; Schiene et al, 1999), in the motor cortex of monkeys (Frost et al, 2003) and the visual cortex of cats (Eysel and Schweigart, 1999; Zepeda et al, 2004). In these studies the cortical representations shifted towards the vicinity of the lesion. Ablation of these perilesional areas in rats showing functional recovery after a previous motor cortex lesion reinstated the initial functional deficit (Castro-Alamancos and Borrel, 1995).

Several functional MRI studies in patients with hemiparetic stroke clearly demonstrated bilateral activation patterns during movements of the affected hand involving contralesional premotor or motor cortical areas (Johansen-Berg et al, 2002; Seitz et al, 1998; Weiller et al, 1992). It was therefore suggested that these alterations in the undamaged hemisphere contribute to the motor recovery. Experimental findings support these observations demonstrating bilateral functional MRI activation patterns also after middle cerebral artery occlusion (MCAO) in rats. A recent study by Biernaskie et al (2005) further supported the relevance of the contralesional cortex for functional recovery. The authors observed reinstatement of the previous functional deficit when they blocked neuronal activity by application of lidocaine into the contralateral cortex 3 – 4 weeks after MCAO. Interestingly, no reinstatement of the initial deficit was observed when contralesional hemisphere was

inactivated with a focal lesion, such as MCAO or electrolytic cortical damage (Andersen et al., 1991; Barth et al., 1990). However, in the neonatal brain, a second injury to the homotopic contralesional cortex appeared to cause bilateral deficits consistent with takeover of function (Barth and Stanfield, 1990). The extent to which the ipsilesional and contralesional alterations contribute to functional improvement is debatable and need to be further investigated. Induction of bilateral sequential cortical infarcts with clear functional sensorimotor deficits may help to elucidate the role of the contralesional hemisphere in functional recovery. Moreover, different time intervals between bilateral lesions could clarify whether a critical period does exist, in which the contralateral cortex contributes to the functional restoration.

Induction of the bilateral sequential infarcts is an appropriate model for the investigation of pathophysiological consequences of multiple infarcts. Several clinical studies indicated that patients already having stroke are at significantly increased risk for subsequent stroke (Brown et al., 2005; Vickrey et al., 2002). It is well known that multiple ischemic infarcts often correspond to widespread subcortical degeneration and vascular dementia that is characterized clinically by subacute onset of cognitive decline, stepwise deterioration, and focal neurological findings (Erkinjuntti et al., 1999). Patients with multiple large or small lacunar infarctions who became demented showed significantly larger cerebral atrophy than cognitively intact patients with similar cerebral infarctions (Salerno et al. 1992).

It is conceivable that induction of the subsequent focal ischemia could trigger similar pathophysiological processes and cause additional brain degeneration as well as cognitive impairment. Otherwise, some clinical studies demonstrated that transient ischemic attacks prior to stroke were significantly associated with less-severe strokes and improved functional outcome on follow-up that suggested ischemic tolerance in patients (Monkayo et al., 2000; Weih et al., 1999). Unfortunately, no systematic data

about the ratio between alterations induced by ischemic tolerance and progressive brain degeneration following sequential ischemic lesions are available as yet. Therefore, investigations of structural and functional consequences induced by repetitive ischemic infarcts might elucidate the complex interaction between protective and degenerative postischemic mechanisms.

2. Aims

The present study was designed to characterize the structural and behavioral consequences of cortical infarcts in the forelimb sensorimotor cortex (FL SMC). In order to analyze the role of functional alterations in the contralateral cortex the homotopic contralesional areas were systematically lesioned at different time points after the first infarct. The infarcts were photochemically induced allowing the placement of highly reproducible lesions in the forelimb sensorimotor cortex causing stable sensory and motor deficits of the corresponding forelimb. The study was addressed to the following questions:

1. What is the distribution and time-course of degenerative and inflammatory processes exerted by photothrombotic infarcts in the FL SMC?
2. What is the role of the contralateral homotopic cortex in functional recovery after infarcts in the FL SMC?
3. It there a specific time window, in which the contralateral homotopic cortex contributes to the functional recovery?
4. Do repetitive cortical infarcts influence the global brain volume?
5. What are the long-term consequences of bilateral sequential cortical infarcts on cognitive functions?

3. Material and Methods

3.1. Animal preparation and anesthesia

This study was performed in accordance with the guidelines of the German Animal Care and Use Committee. Adult male Wistar rats were used for the experiments. The animals were held under conditions with a room temperature of 22 – 24 °C, 60 - 80 % humidity and a 12 h light-night cycle. At the beginning of the study the animals weight was 250 – 330 g; that is average for the age of 2.5 – 3 months. The animals were housed in standard cages in groups of 4 – 5 rats per cage with access to water and food *ad libitum*.

Anesthesia was induced with 3.5 % enflurane (Abott GmbH, Germany) and maintained with 2.5 % enflurane in nitrous oxide and oxygen mixture (2 : 1) which was delivered through a closely fitting face mask. The body temperature was monitored with a rectal catheter and maintained at 37 $\pm$ 0.5 °C by means of a heating pad.

3.2. Induction of photothrombotic infarcts

Focal neocortical infarcts were induced using the photothrombosis model as described by Watson et al. (1985), with only minor modifications (Shanina et al., 2005). The anesthetized animals were placed in a stereotaxic frame, the scalp was incised and the cranial fronto-parietal convexities were exposed. A fiberoptic bundle (2.4 mm diameter) connected to the cold light source (Schott KL 1500, light intensity of 4.0 level) was positioned on the skull 0.5 mm anterior to Bregma and 3.7 mm lateral to the midline, aligned with the stereotaxic coordinates corresponding to the region of the forelimb sensorimotor cortex (Paxinos and Watson, 1986) (see Fig.

3.1). To induce focal lesions the photosensitive Rose Bengal dye (3,4,5,6,-tetrachloro-2',4',5',7'-tetrajodofluorescein disodium) (Sigma-Aldrich, Taufkirchen, Germany) (1.3 mg/100 g body weight), dissolved in saline (1 mg/100 µl), was injected into the tail vein. Immediately after the injection of Bengal Rose the light was turned on for 20 min. The cold light induces the dye transformation into triplet excited state followed by the transfer of the energy to the molecular oxygen (O_2) dissolved in the blood. It leads to the formation of the active singlet state ($^1O_2$) that induces damage of endothelial cells and aggregation of thrombocytes resulting in a thrombosis of the illuminated blood vessels and following ischemia in the cortical area. After illumination the wounds were sewed and the animals were left to wake up. The sham procedure was identical except for illumination of the skull.

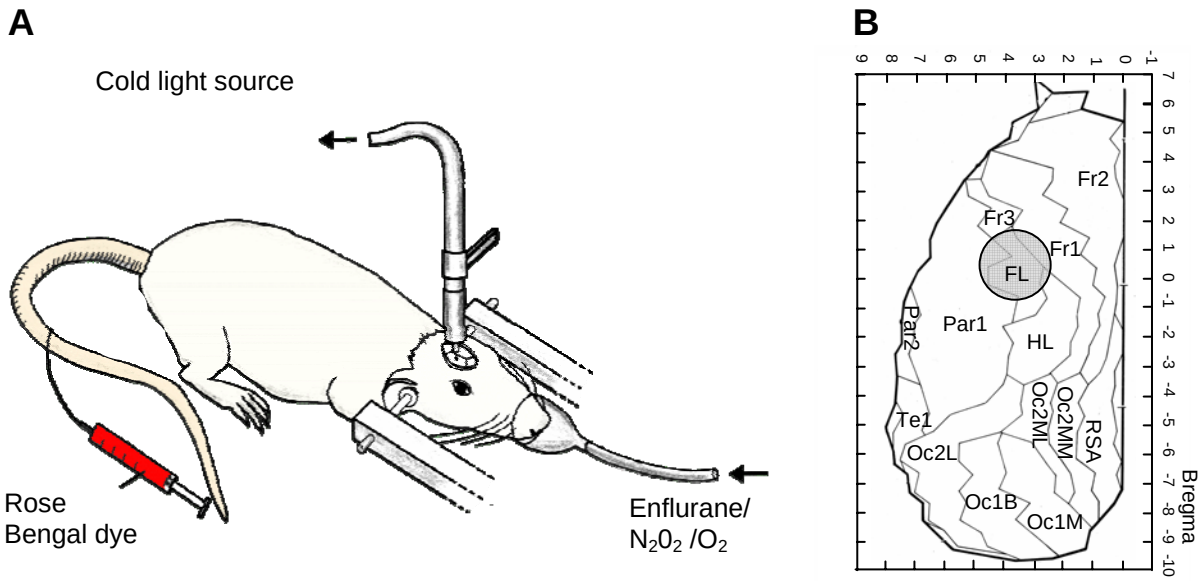

Fig. 3.1 A: Schematic illustration of induction of the photothrombotic lesion. **B:** Stereotaxic position of the photothrombotic infarct. The location of the lesion (grey circle) was chosen in the forelimb-sensorimotor cortex according to the atlas from Zilles (1985). FL forelimb sensorimotor cortex, HL hindlimb sensorimotor cortex, Fr1 frontal cortex, area 1 (primary motor cortex), Fr2 frontal cortex, area 2, Fr3 frontal cortex, area 3, Par1 parietal primary somatosensory cortex, Oc1 primary visual cortex, Oc2 secondary visual cortex.

3.3. Experimental design

In order to evaluate the histological alterations in brain structures not directly damaged by either single unilateral or sequential bilateral focal cortical ischemia, different morphological techniques were performed. The Fluoro-Jade B staining combined with 4'-6-diamidino-2-phenylindole (DAPI) was used to assess the level of neuronal degeneration after photothrombotic infarcts, triple immunofluorescence using antibodies to CD68 (marker for activated microglia/macrophages) and glial fibrillary acidic protein (GFAP) that is an astroglial marker, accompanied by DAPI staining (cell nuclei marker) was performed to evaluate the postischemic inflammation. The neuroanatomic connections of the FL SMC were investigated using the retrograde tracer Fluoro-Gold retrograde marker (description of these methods is given in the following). For this study the animals were divided into the following groups. In one group the animals received unilateral single photothrombotic infarct in the FL SMC (SL group, n = 32), whereas in other rats two sequential bilateral photothrombotic infarcts were induced with time intervals of 2 (DL2 group, n = 24) or 6 (DL6 group, n = 19) days between the lesions. Sham-operated animals (*n* = 3) served as controls and were sacrificed on day 7 after the surgery. In order to investigate the time-course of alterations in the lesion volume in the unilaterally and bilaterally impaired brains the animals were sacrificed according to the following scheme (Fig. 3.2): SL-animals were perfused on day 2 (*n* = 4), 4 (*n* = 4), 6 (*n* = 5), 8 (*n* = 5), 10 (*n* = 6), 14 (*n* = 4) or 28 (*n* = 4) post-surgery. The DL2 group was examined histologically on day 2 after the induction of the second infarct, corresponding to day 4 after the first one i.e. day 4(2) (n = 4). Other DL2-animals were tested on day 6(4) (*n* = 4), 8(6) (*n* = 4), 10(8) (*n* = 6) and 28(26) (*n* = 6). Animals from the DL6 group were sacrificed on day 2 after induction of the second

lesion, corresponding to day 8 after the first one (8(2) day) (n = 4), and further on day 10(4) (*n* = 4), 14(8) (*n* = 7) or 28(22) (*n* = 4).

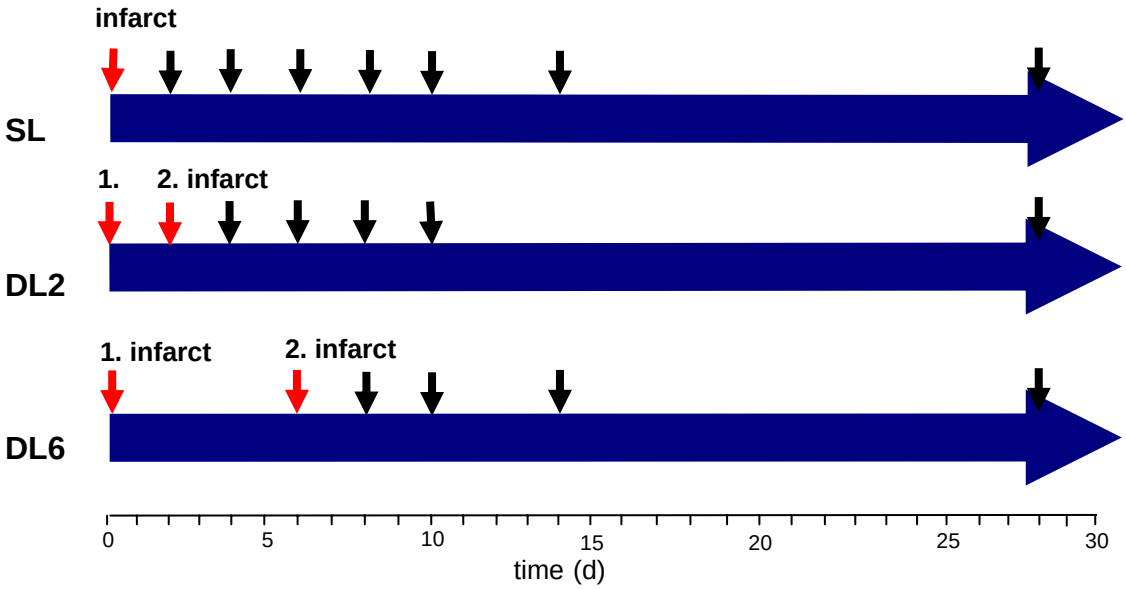

Fig. 3.2. Experimental design of the study of the remote postischemic alterations. The animals were divided into 3 experimental groups: SL, DL2 and DL6. Control animals received a sham-operation. Red arrows indicate the time point of infarct induction, black arrows indicate the time point of histological analysis.

The sensorimotor recovery of animals with single unilateral and sequential bilateral cortical infarcts was analyzed in a second series of experiments using a battery of sensorimotor behavioral tests for forelimb functions. In this study the animals were divided into five groups (Fig. 3.3). In one group (n = 8), a single photothrombotic infarct (SL) was induced. Four other groups received two sequential bilateral lesions (DL), with the second infarct induced either immediately after the first infarct (DL0, n = 4), or 2 days (DL2, n = 9), 7 days (DL7, n = 8), or 10 days (DL10, n = 9) later. The side for the induction of the first photothrombotic infarct was varied in all groups. The second lesion was produced in an identical way in the homotopic cortex of the contralateral hemisphere. The control group received a sham-operation (CTRL, n = 6) as described above.

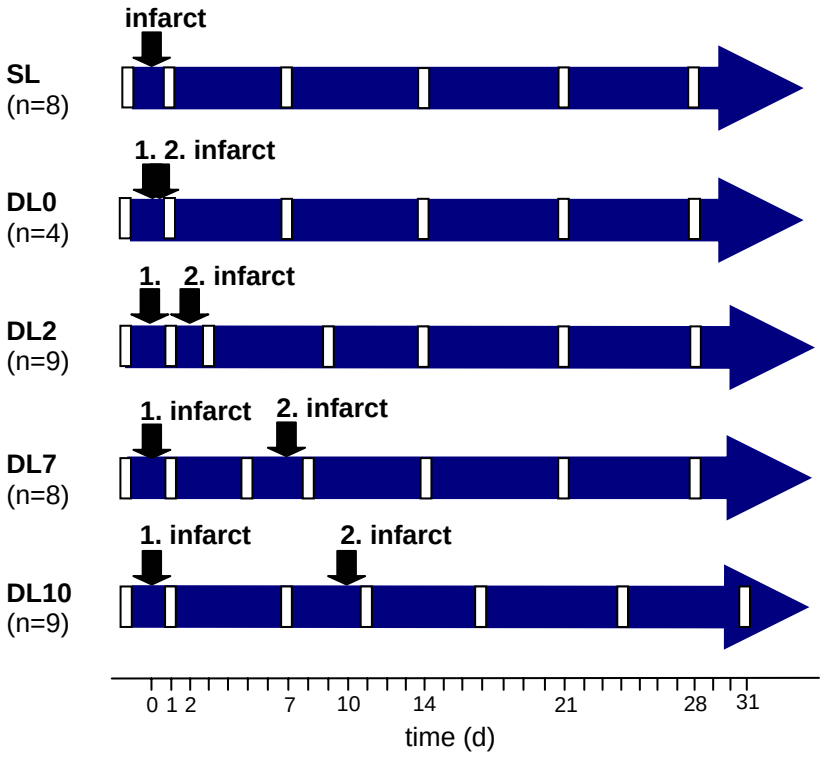

Fig. 3.3. Schematic illustration of the experimental design in the study of sensorimotor recovery after sequential bilateral photothrombotic infarcts. In one group (n = 8), a single photothrombotic infarct (SL) was induced. Four other groups received two sequential bilateral lesions (DL), with the second infarct induced in the homotopic contralateral cortex either immediately after the first infarct (DL0), 2 days (DL2), 7 days (DL7), or 10 days (DL10) later. The control group received only a sham-operation (CTRL). Black arrows designate induction of the photothrombotic lesions, whereas white bars mark the time points of the behavioral testing (forelimb activity and sliding test, foot-fault-test).

In order to assess the long-term consequences in brain volume and lesion size a third study with volumetric analysis was performed. In addition, the cognitive functions of the animals with single unilateral and sequential bilateral lesions were tested in the Morris watermaze. Figure 3.4 illustrates the distribution of the animals in the study with the volumetric analysis. Briefly, the group with unilateral single lesions (SL) includes 7 animals, whereas the DL0 - 6 animals, DL2 – 5 animals, DL7 – 6 animals and DL10 – 6 animals. The second photothrombotic lesion was identically produced in the homotopic cortex of the contralateral hemisphere. The side for the induction of the first photothrombotic infarct was varied in all groups. Control animals (CTRL, n = 6) received sham-operation. For the volumetry the DL-animals (i.e. DL0,

DL2, DL7 and DL10) were sacrificed 31 days after the second lesion. The animals from SL and CTRL group were analyzed on day 31 after surgery.

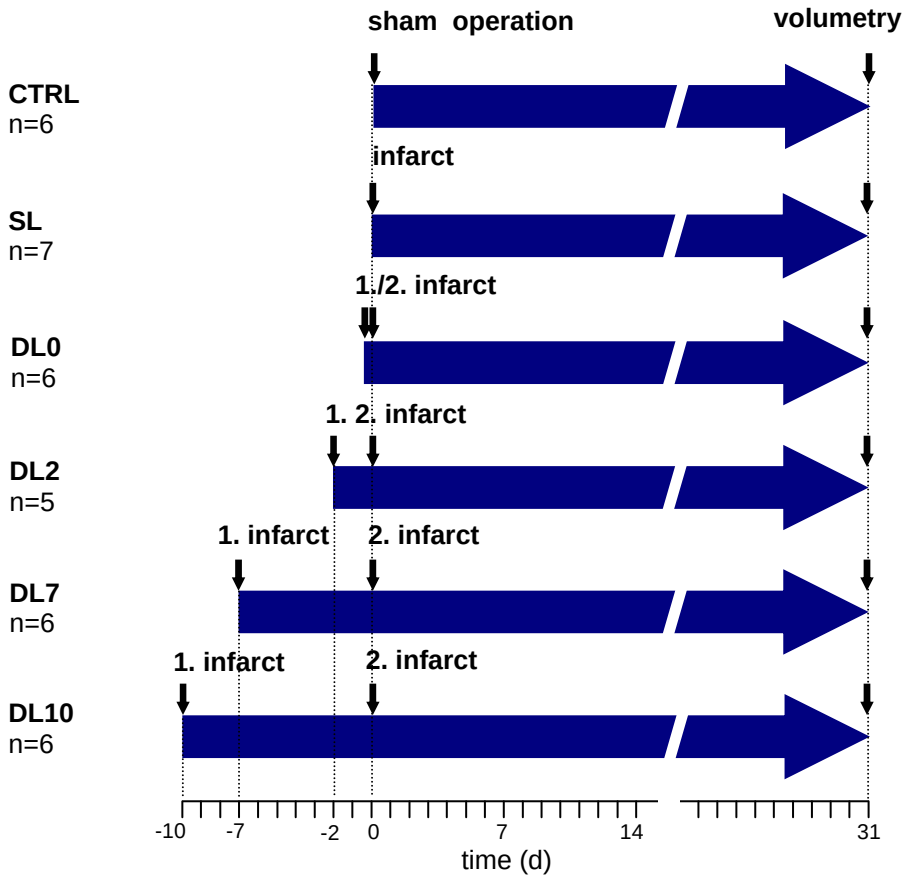

Fig. 3.4. Schematic illustration of the different experimental groups investigated volumetrically. Black arrows mark the induction of the first and second infarct or sham-operation. Volumetry was performed in all groups on day 31 after induction of the last surgery (marked with black arrows).

3.4. Histological processing

The animals were anesthetized with ether narcosis. The extremities of the animals were fixed in the perfusion-bath and the median incision was made from the abdomen to the sternum. The ribs were removed to access the heart area. The perfusion needle was inserted through the open left ventricle and moved into the aorta. After the incision in the right atrium the animal was perfused with 75 ml of 0.1 M phosphate buffer (PBS) followed by 300 ml of 4 % paraformaldehyde dissolved

in 0.1 M PBS. The normal continuous liquid flow of 35.0 ml/min was provided by the perfusion pump (505S, Watson-Marlow, England). Thereafter, brains were carefully removed from the skull, postfixed in 4 % paraformaldehyde solution overnight at 4 °C and submerged in 10 % sucrose in 0.1 M PBS for 24 h. The tissue was then transferred to a 30 % sucrose/PBS solution for 24 – 48 hours. The brains were frozen and stored at -75 °C. Sixty μm thick coronal sections were cut using a freezing microtome (Microm, Walldorf, Germany). For Nissl-staining every second slice was mounted onto a gelatinized slide and allowed to dry at room temperature. For this staining the brain slices were incubated in Cresyl-violet solution at 60 °C for 5 min. After a brief rinse in distilled water the slices were immersed in the ascending alcohol set (70 %, 96 %, 100 % Isopropanol). Finally, they were incubated in xylene and mounted with toluene (Entellan; Merck, Darmstadt, Germany).

3.5. Measurement of infarct volume

Using a charge-coupled device (CCD) camera and National Institute of Health (NIH), USA image software the area of the cortical infarct as well as that of each hemisphere (mm^2) was measured by tracing these regions on the computer screen. The area of the remaining tissue was calculated by subtracting the area of the infarction from that of the whole hemisphere. Every fourth section (60 μm) was volumetrically analyzed between Bregma +4.70 and -2.12 mm (schematic presentation of measurement is shown in Fig. 3.5). Volumes (mm^3) were determined by multiplying the appropriate area by the section interval thickness (240 μm).

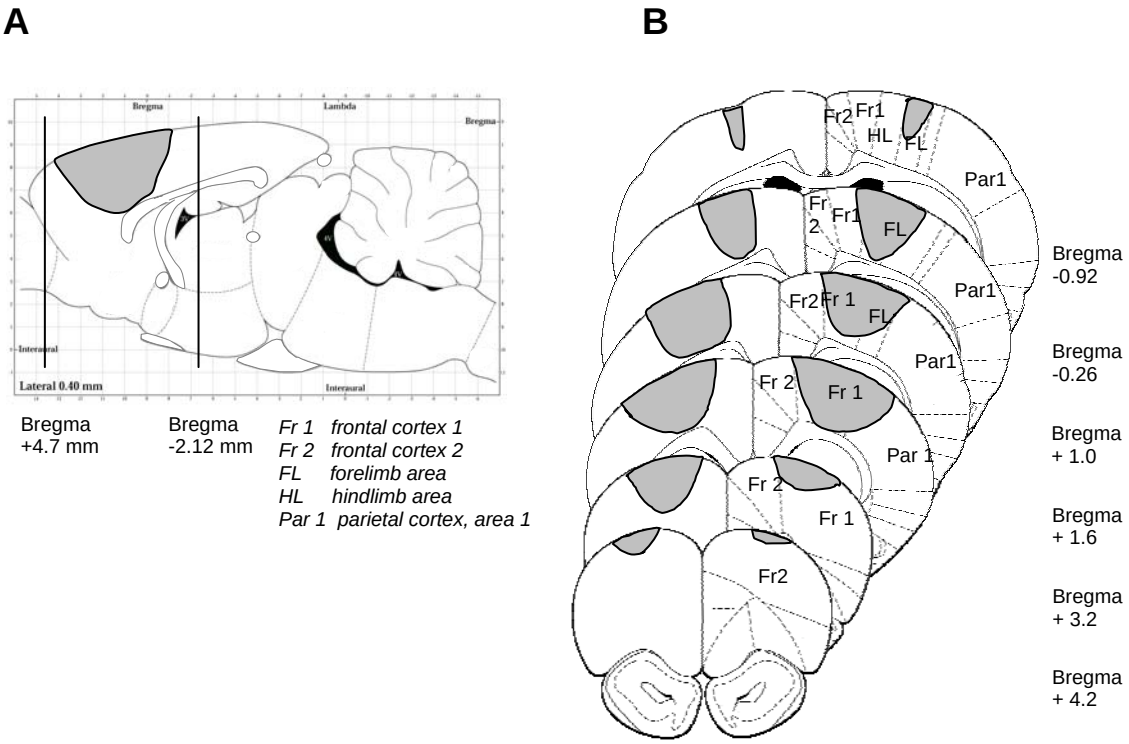

Fig. 3.5. Schematic presentation of the volumetric evaluation of the photothrombotic infarcts. **A:** Sagital view of rat brain (based on Paxinos and Watson, 1986). Black vertical lines designate the position of the first (Bregma +4.7 mm) and last (Bregma -2.12 mm) slices analyzed by volumetry. Photothrombotic infarcts marked with gray color always lay between these lines. **B:** Frontal slices of rat brain analyzed volumetrically. Photothrombotic lesions marked with gray color were predominantly located in the sensorimotor forelimb cortex.

3.6. Immunofluorescence

3.6.1. Fluoro-Jade B and DAPI staining

Coronal slices from animals used in the ***study of the histological alterations in remote brain structures*** after sequential bilateral infarcts (SL, DL2, DL6 as well as sham-operated) were used for Fluoro-Jade B staining (Histochem Jefferson AK, USA) combined with nuclear staining with DAPI. Fluoro-Jade B is an anionic tribasic fluorescein derivative with a molecular weight of 445 daltons. It is a dark red powder that has a green iridescence with excitation peak at 480 nm and emission at 525 nm. Fluoro-Jade B is a fluorescent marker for the identification of cell degeneration, preferentially in brain neurons, which was originally developed by Schmued and co-

workers and was shown to have a similar sensitivity to suppressed silver staining techniques (Schmued et al., 1997). Fluoro-Jade has since then been successfully used for depicting neuronal death after exposure to various neurotoxic agents (Eisch et al., 1998; Freyaldenhoven et al., 1997; Zuch et al., 2000), after mild brain injuries (Allen et al., 2000) and after cerebral ischemia induced by MCAO (Pennypacker et al., 2000). Fluoro-Jade staining detects degenerating neuronal cells, as well as their dendrites, axons and axon terminals. Quite recently it was reported that staining with TUNEL and Fluoro-Jade respectively shows a remarkable overlap (Kundrotiene et al., 2004; Zuch et al., 2000).

Staining was performed as described by Schmued et al. (1997) on 4 % PFA-fixed 40 μm thick coronal slices with some modifications. The tissue sections were washed in 0.1 M PBS, mounted onto gelatinized slides and allowed to dry at room temperature. After rinsing in PBS (3 times for 10 min) the slides were briefly incubated for 10 min in 4'-6-diamidino-2-phenylindole (DAPI, Sigma-Aldrich, Taufkirchen, Germany) solution, which allows visualization of the cell nuclei. DAPI is known to form fluorescent complexes with natural double stranded DNA. Cell nuclei are considered to have the normal phenotype when glowing brightly and homogeneously. Then the sections were rinsed in 0.9 % saline 3 times for 10 min. Finally, the slides were incubated with 0.0001 % solution of Fluoro-Jade B 30 min at 4 °C, rinsed in PBS and air dried for 20 – 30 min. The slides were mounted in D.P.X., neutral mounting medium (Sigma-Aldrich, Munich, Germany) and processed for fluorescence microscopy. The fluorescence filter used for visualizing Fluoro-Jade B was a (fluorescein-isothiocyanate) FITC filter that resulted in a green emission color of slices. The staining with Fluoro-Jade B allows detection of somata and processes of degenerating neurons that compared to the normal tissue have strong green fluorescence on the slides. DAPI-positive fluorescence was elicited by excitation light

with 372 nm wave length that resulted in the emission at 456 nm. Cells with strong Fluoro-Jade fluorescence accompanied by the fragmented morphology of nuclear bodies revealed by DAPI were counted as degenerating neurons. To evaluate the degeneration in the thalamus every eighth coronal slice from Bregma -1.8 mm to Bregma -4.16 mm was analyzed under an Axioplan 2 imaging microscope (Zeiss, Jena, Germany) and the number of degenerative cells for all thalamic nuclei was calculated and summarized per brain.

3.6.2. Triple immunofluorescence (CD68, GFAP, DAPI)

To analyze the processes of inflammation and gliosis after the induction of brain ischemia, immunostaining with the antibodies against rat CD68 (Serotec, Duesseldorf, Germany), GFAP (Advanced ImmunoChemical, USA) and DAPI was performed on coronal brain slices (40 μm). CD68 is a 110 kD transmembrane glycoprotein which is highly expressed in the majority of tissue macrophages and activated microglia that are main effectors of brain inflammation and is weakly represented in the peripheral blood granulocytes. This antigen is predominantly present on the lysosomal membranes of these cells and weakly expressed on the cell surface. Glial fibrillary acidic protein (GFAP) is a class-III intermediate filament that is expressed in astrocytes and serves to distinguish them from other glial cells and neurons. Free floating slices were rinsed 6 times for 10 min in Tris-buffer solution (TBS), then incubated in the Tris-Triton buffer (TBS plus) containing blocking serum (normal donkey serum, 3 %) for 30 min and treated with the mouse polyclonal anti rat CD68 and guinea pig monoclonal anti rat GFAP antibodies diluted in the TBS plus in ratio 1 : 500 and 1 : 1000, respectively overnight at 4 °C. The next day slices were rinsed 3 times for 10 min. After preincubation with TBS plus for 15 min, slides were

incubated with secondary antibodies for 2 hours at room temperature. In order to visualize CD68 antigen the secondary donkey anti-mouse antibodies coupled with Alexa Fluor 488 fluorochrome (Molecular Probes, Leiden, Netherlands) were used diluted in ratio 1 : 250, whereas donkey Rhodamine Red X-conjugated anti-guinea pig secondary antibodies (Dianova, Hamburg, Germany) identified GFAP-antigens. After rinsing in TBS 4 times for 10 min slides were mounted onto gelatinized slides and allowed to dry at room temperature. Then the slides were washed 2 times for 10 min, incubated in the DAPI solution for 10 min, rinsed 3 times for 10 min and allowed to dry at room temperature. Mounted with Moviol-DABCO (Sigma-Aldrich, Taufkirchen, Germany), the brain slices were analyzed with confocal laser microscopy (LSM 510 Meta, Zeiss, Jena, Germany). CD68 and GFAP-positive cells were colocalized with DAPI staining and counted. Values were presented as a cell number per 100 DAPI-positive cells. The evaluation was performed in the areas of the ventral posterolateral thalamic nucleus (VPL) and the posterior nuclear thalamic group (Po) at the level corresponding to Bregma -3.14 mm or -3.30 mm, where the maximal glial activation was observed.

3.7. Fluoro-Gold-tracing

Intact animals were used to study the thalamo-cortical connections (n = 3). Fluoro-Gold (hydroxystilbamidine) (Fluorochrome, LLC, Denver, USA), a retrograde neuronal marker, is able to stain the neurons having projections to the injected brain area. Anesthetized as described above, the animals were placed in a stereotaxic frame, the skull was bored at the following coordinates: Bregma: +0.5 mm; lateral from the midline: 3.7 mm that corresponded to the FL SMC area. The tracer application was made by means of a glass microelectrode (diameter 0.03 mm) filled

with 2 % Fluoro-Gold solution that was introduced in the skull hole and was lowered to 1.5 mm beneath the cortex surface. The current of 11 μA was elicited every 20 sec within 10 min. Then the skull was closed with bone wax, the head skin was sutured and animals were allowed to survive for 3 days.

To study the possible postischemic alterations of the anatomical relationship between the cortex and the thalamus, animals received a photothrombotic unilateral infarct (*n* = 4) in the FL SMC and were injected with Fluoro-Gold solution 34 days later. The tracer was applied with a glass microelectrode filled with Fluoro-Gold solution that was introduced in the contraleral to the lesion cortex at the following coordinates: Bregma: +0.5 mm; lateral from the midline: 3.7 mm; 1.5 mm beneath the cortex surface. The current of 11 μA was elicited every 20 sec for 10 min. The anesthetized animals were perfused 3 days later with fixation solution containing 4 % paraformaldehyde and 2.5 % acrolein (Sigma-Aldrich, Steinheim, Germany) in PBS. Then the brains were postfixed in the same solution and further brain tissue processing was carried out as described before. The free floating coronal brain sections (40 μm) were rinsed 6 times for 10 min with Tris-buffer (Tris saline, pH 7.4, 0.2 % Triton X - 100), immersed for 20 min in the sodium borohydride solution (10 % in Tris-buffer without Triton X - 100) and washed 8 times in wash-buffer until no small vesicles were observed. After 15 min incubation in 1 % H_2O_2 the sections were rinsed 3 times for 10 min and performed for 1 h to the Tris-buffer with 1.5 % goat serum. Then the slides were incubated with primary antibody solution containing 1.5 % goat serum and rabbit polyclonal antibodies for the Fluoro-Gold (Chemicon, Hampshire, UK) (1 : 6000) dissolved in Tris-buffer for 2 days at 4 °C. On the third day the sections were rinsed 6 times for 10 min and incubated for 1 h with secondary biotynilated goat anti-rabbit antibodies (Jackson Immunoresearch, West Grove, PA, USA) (1 : 500) dissolved in the Tris-buffer containing 1.5 % goat serum at room

temperature. After rinsing 3 times for 10 min the slides were immersed for 30 min in avidin-biotin-peroxidase complex solution (Vectastain Elite Kit, Vector Laboratories, Birlingame, CA, USA) and processed using 3´-3´-diamino-benzidine hydrochloride (DAB, Sigma-Aldrich, Munich, Germany) as a chromogen. The sections were mounted onto gelatin-coated slides, air-dried and coverslipped with Entellan (Merck, Darmstadt, Germany). The thalamo-cortical anatomic connections were analyzed using an Axioplan 2 imaging microscope.

3.8. Behavioral assessment

3.8.1. Time schedule of sensorimotor behavioral tests

All animals in the sensorimotor behavioral study were tested pre- and postoperatively using forelimb preference and sliding test in glass cylinder and a foot-fault test (see Fig. 3.3). The animals in the CTRL, SL, and DL0 groups were tested 1, 7, 14, and 21 days after the surgery. In the DL2 group animals received postoperative tests on day 1 after the first lesion and day 1 after the second infarct corresponding to day 3 after the first one. The testing was then continued on day 9(7), day 14(12), and day 21(19). For the DL7 group the tests were performed on day 1 and 5 after the first surgery, and then again on day 1 after the second infarct as well as on days 14(7), 21(14), and 28(21), respectively. The DL10-animals were tested on day 1 and 7 after the first lesion and on days 11(1), 24(14), and 31(21) after the second lesion.

3.8.2. Forelimb preference and sliding test

Forelimb use during spontaneous vertical exploration was analyzed based on the method described by Schallert et al. (2000b). The rats were videotaped in a

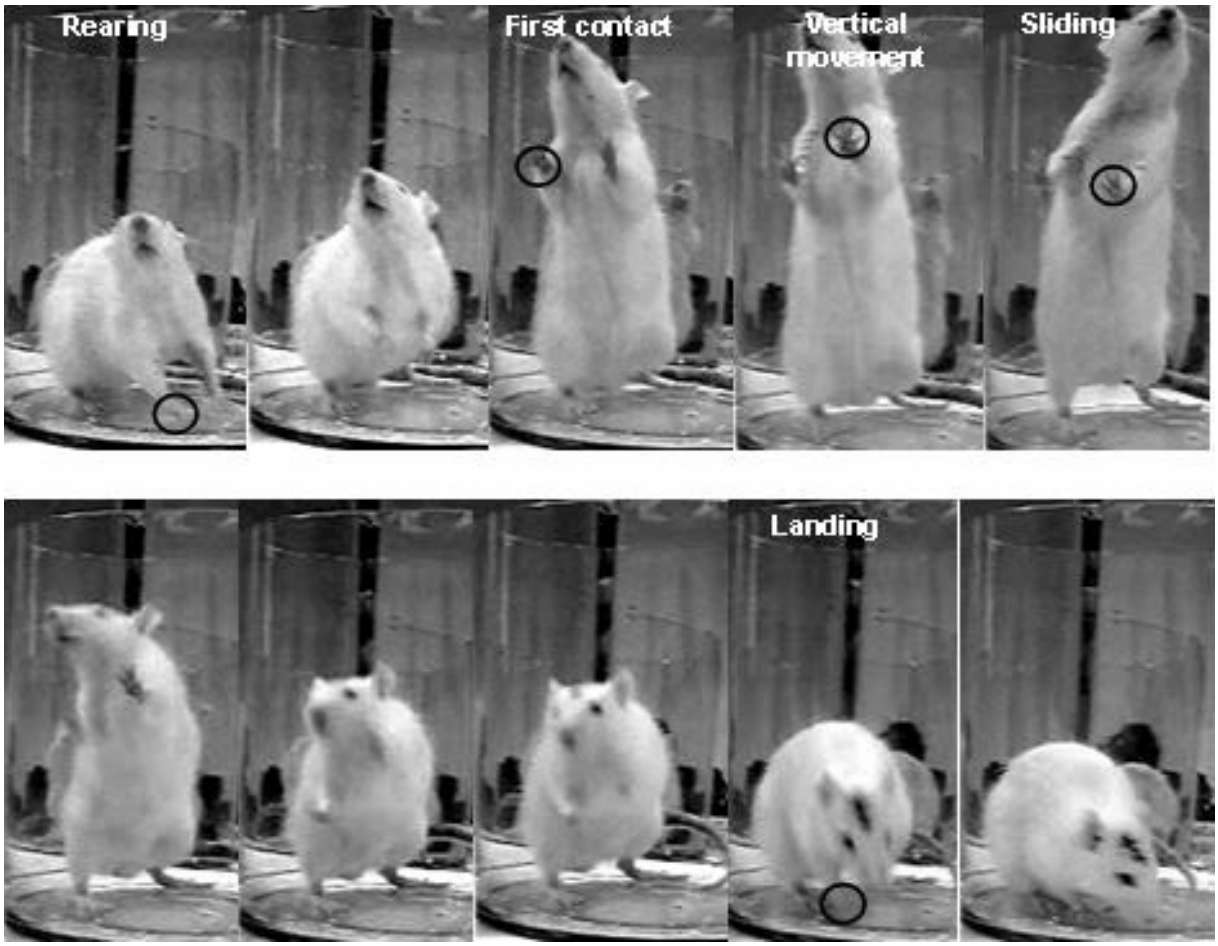

Fig. 3.6. Glass cylinder test. Series of video recordings of the forelimb preference and sliding test. Characteristic behavioral elements are marked with a black circle.

transparent glass cylinder for 3 – 10 min depending on the degree of activity during the trial (Fig. 3.6). Two mirrors set at an angle of 90 ° were placed behind the glass cylinder allowing the recording of forelimb movements even when the animal turned away from the camera. Several behavioral elements were scored to determine the extent of forelimb impairment during spontaneous exploration of the glass cylinder. The independent or simultaneous use of the left or right forelimb was analyzed (a) at first contact with the wall, (b) during vertical and horizontal movements along the wall, and (c) also sliding movements of each forelimb at the wall of the cylinder were scored (Fig. 3.6). In case where the animals used both forelimbs simultaneously it

was counted as half for each limb. Forelimb activity (FLA) was evaluated for each forelimb using the following formula:

$$\text{forelimb activity} = \frac{\text{first contact movements} + \text{horizontal movements} + \text{vertical movements}}{\text{number of rearings}}$$

In addition, the frequency of sliding movements which occurred during vertical activity at the wall of the glass cylinder was assessed for each forelimb using the following score:

$$\text{sliding score (\%)} = \frac{\text{sliding movements}}{\text{first contact movements} + \text{horizontal movements} + \text{vertical movements}} \times 100$$

In order to illustrate the time course of behavioral alterations in these tests data in figures are presented as the percentage difference between the preoperative baseline and the results at different time points after the infarcts.

3.8.3. Foot-fault test

The foot-fault test allows the assessment of asymmetry in limb-use for fore- and hindlimbs on an elevated grid (Barth et al., 1990). The animals have to coordinate paw movements to gain footholds on the wire frame. Inaccurate placement leads to a slipping through the openings (3 x 3 cm) in the grid (i.e. a “foot-fault”, Fig. 3.7). Naive animals rarely show mistakes which are symmetric for both limbs. All animals had to walk from one end of the grid to the home cage at the other end five times. The movements were recorded using a videotape and analyzed in slow-motion offline for every limb separately. A score of “foot-faults” was calculated for every limb using the following formula:

$$\text{foot fault score}\,(\%) = \frac{\text{foot faults per limb}}{\text{steps per limb}} \times 100$$

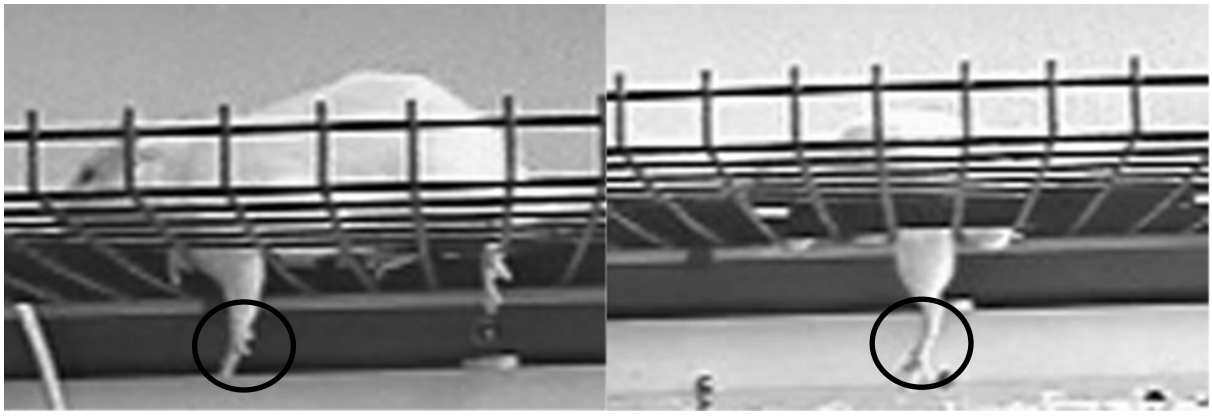

Fig. 3.7. Foot-faults during walking on the grid. A step error was counted when the paw slipped completely through the grid openings. The photographs here present an example of forelimb (left) and hindlimb (right) step errors.

3.8.4. Morris water maze

The Morris water maze (Morris, 1981) was used to test spatial learning acquisition and cognitive functions in additional groups of animals with single infarcts (SL, n = 5) and two sequential lesions (DL2, n = 10) as well as sham-operated controls (CTRL, n = 10). The test was carried out 8 weeks after the sham-surgery or single infarct for the CTRL and SL animals or 8 weeks after the second lesion for the DL2 group. The maze (diameter: 181 cm, height: 60 cm) used for the experiments was gray like the escape platform and was situated in a room with posters, lamps and other distal cues. The escape platform was placed 2 cm beneath the water surface and kept in a constant position during the acquisition trials. The temperature of the water was 20 ± 1 °C at beginning of the testing period. The rats' swim paths were tracked using a video camera located perpendicularly above the center of the pool and analyzed using EthoVision software, version 2.3 (Noldus Information Technology, Wageningen, Netherlands).

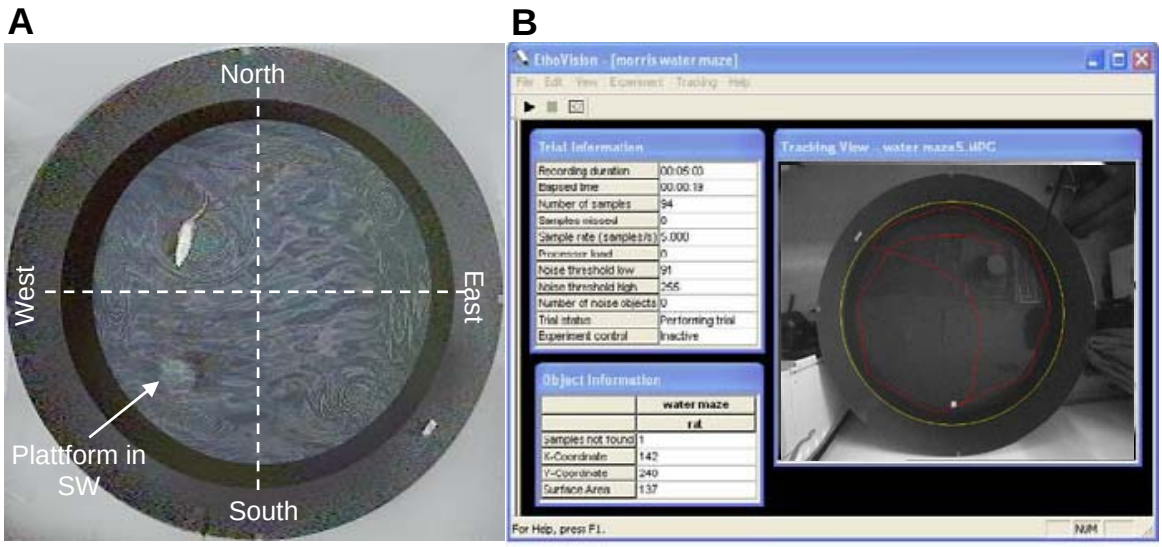

Fig. 3.8. Morris water maze test. **A:** A rat placed in watermaze has to learn the location of the invisible platform to escape from water. **B:** Ethovision program allows tracking of the swimming path of the rat (red curve) and gives information about latency (time between start of trial and escape on the platform), path length and swimming speed.

At the beginning of each trial the animals were placed into the water at one of the four designated points marked North, East, South and West. A different start location was used for each trial within one session. The rat was trained to swim to the underwater platform. The location of the platform was varied between rats but remained in the same quadrant during all acquisition sessions. Different start and platform positions were equally distributed in the experimental groups. The rats were allowed to swim for a maximum time period of 90 sec. The trial was stopped either when the animal had reached the platform and climbed onto it or after the time period expired. Animals that failed to find the escape platform within this time period were manually guided to it. After reaching the platform, each animal was allowed to rest for 20 s. All groups of animals were tested on 6 consecutive days with 4 trials per training day. The time (escape latency, s) that animals needed to reach the platform was measured for each trial. On day 7 one acquisition trial was performed with the platform located in the training quadrant as usual. Then the platform was removed and the swim path in each of the four quadrants was recorded for 60 sec. For this

probe trial, each rat was placed at a start position directly opposite to the platform. Rats that had learned the precise location of the platform usually spent most of their time in the quadrant, where the platform had been formerly located. The percentage of time spent in each quadrant was calculated for all groups of animals.

3.9. Statistical analysis

All data are presented as mean ± SEM unless otherwise noted. Statistical significance between SL and DL-animals in the ***study of histological alterations in remote brain structures*** after sequential bilateral photothrombotic infarcts was analyzed with the non-parametric Mann-Whitney U-test using SPSS 11.5 for Windows (SPSS Inc., Chicago, USA). The number of Fluoro-Jade or CD68-positive cells was compared between hemispheres in the DL-animals and with SL-animals at the corresponding time after induction of the lesions. For instance, the number of positive cells found on day 8 in the SL group was compared with the number of cells on day 8(6) for the firstly impaired hemisphere and day 10(8) for the secondly impaired hemisphere in the DL2 group.

In the ***study of sensorimotor recovery*** after sequential bilateral photothrombotic infarcts behavioral alterations to the preinfarct baseline in the glass cylinder and during the foot-fault test were assessed with nonparametric Wilcoxon matched pairs test using SPSS 11.5 for Windows (SPSS Inc., Chicago, IL, USA) and Bonferroni-Holm post hoc test for multiple comparisons (alpha-level: 0.05). Differences between groups were assessed using the Kruskal-Wallis test (nonparametric ANOVA) followed by Dunn's multiple comparisons post-test. The statistical significance of alterations between the volumes of lesioned and control brains in the ***study of long-term consequences of sequential bilateral photothrombotic infarcts on brain***

volume and cognitive function was assessed using one-way analysis of variance (ANOVA) with the Dunnett multiple comparisons test (GraphPad Software, Inc., USA). Statistical analysis of the behavioral data collected in the water maze was made with one-way analysis of variance (ANOVA) with the Tukey-Kramer post t-test. A level of $p \leq 0.05$ was considered statistically significant.

3.10. Solutions

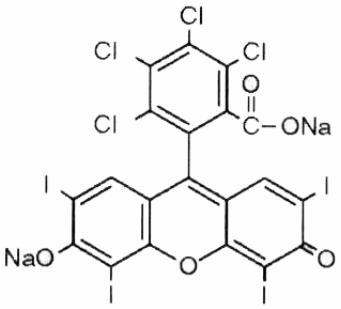

Chemical formula of Bengal rose dye

1) Bengal rose dye (3,4,5,6,-tetrachloro-2',4',5',7'-tetrajodofluorescein disodium): 1mg dissolved in 100 µl of saline. Final concentration: 1.3 mg/100 g body weight.

2) O,1 M phosphate buffer saline (PBS): stock I base: (a) 28.392 g Na_2HPO_4 + 158.957 g NaCl solved in 2000 ml Aqua bidest.; stock II acid: (b) 13,799 g NaH_2PO_4 * H_2O + 79.478 NaCl solved in 1000 ml Aqua bidest. 1400 ml Aqua bidest. + 35 ml Stock II was titrated with ca. 165 ml Stock I to pH 7.4.

3) 4 % paraformaldehyde solution: 500 ml 0.1 M PBS + 40 g paraformaldehyde (Merck) (solved in 300 ml Aqua bidest. at 60 °C and clarified with a few drops of NaOH) + Aqua bidest until 1000 ml in volume and filtrated.

4) 10 % and 30 % sucrose solution: sucrose 10 g or 30 g dissolved in 90 ml or 70 ml of PBS respectively.

5) Stock Tris-buffer 10x: 60,55 g Tris(hydroxymethyl)-aminomethane (ICN) + 73,8 g NaCl; filled with 1000 ml Aqua bidest.

6) Tris-buffer solution (TBS): Tris-buffer-Stock solution diluted 1:10 and titrated with HCl to pH 7,4.

7) TBS plus: 3 % normal donkey serum with 0.1 %Triton X - 100 (Merck) diluted in TBS.

8) Gelatine solution for mounting the slides: 1g gelatine; 0.1 g Chrome-(III) Potassium sulfate; 200 ml Aqua bidest; the solution was warmed to 37 - 42 °C.

9) Cresyl-Violet solution: 300 ml Aqua bidest; 1.6326 Sodium acetate (water free); 2.88 glacial acetic acid; 100 g Cresyl-Violet. The solution was mixed approximately for 15 min at 60 °C and then filtrated.

10) DAB-solution: 50 mg 3,3-Diaminobenzidine (Sigma-Aldrich) + 1 ml Aqua bidest.

11) Fluoro-Jade B stock solution 0.01 %: Fluoro-Jade B (Chemicon) 50g + 500 ml Aqua bidest.

12) Fluoro-Jade B (FJ) staining solution: FJ stock solution 20ml + 0.1 % acetic acid 180 ml.

13) 4,6-Diamino-2-phenyl-indol (DAPI) staining solution: for stock solution 1 mg 4,6-Diamino-2-phenyl-indol was dissolved in 1 ml Aqua bidest and stored at -20 °C. For staining solution 1 ml stock solution was diluted in 500 ml PBS.

14) Acrolein-containing fixation solution: 25 ml acrolein (H_2C=CHCHO) was diluted in 1000 ml of the fixation solution containing 4 % of PFA.

4. Results

4.1. Histological alterations in remote brain regions after sequential bilateral photothrombotic infarcts

The remote effects of unilateral single and bilateral sequential infarcts induced with an interval of 2 or 6 days between the infarcts were analyzed using morphological and immunohistological techniques. In this study neuronal degeneration and activation of glial cells were investigated in the areas not directly impaired by the ischemic lesion.

4.1.1. Morphology of photothrombotic infarcts

All animals which received either a single unilateral photothrombotic lesion (SL) or two bilateral sequential lesions (DL) recovered quickly without suffering from weight loss or any severe functional impairment. Histological processing revealed well-defined cortical infarcts in all SL or DL animals. The lesions were located in the forelimb sensorimotor cortex (FL SMC) with some extensions to Fr1, Fr3, and Par1 areas according to the rat brain atlas from Paxinos and Watson (1986) and Zilles (1985) (Fig. 4.1). The infarcts involved all cortical layers with no damage to the underlying white matter in the majority of animals. In sham-operated controls no structural alterations were observed.

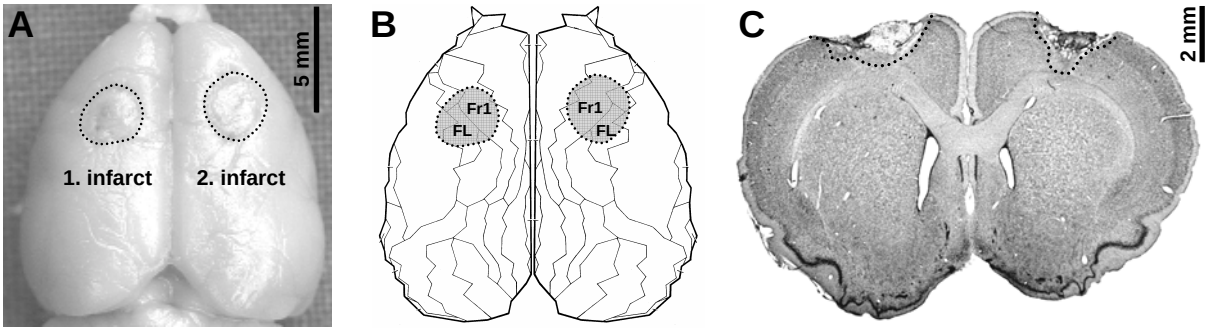

Fig. 4.1. Location of the bilateral photothrombotic infarcts in the forelimb sensorimotor cortex (FL SMC) of the rat. **A:** The photograph displays the morphology of the infarcts 28 days after induction of the second lesion in the adult rat brain. **B:** Schematic diagram illustrates the location of the photothrombotic lesion in the forelimb sensorimotor cortex according to the atlas of Zilles (1985). **C:** A coronal Nissl-stained brain section including the lesions is shown. The cortical infarcts affected all cortical layers while the subcortical white matter remained mostly intact. The infarct extents are marked with black points.

In the SL-animals the volume of the photothrombotic infarcts in the FL SMC was maximal on day 2 (24.0 ± 1.6 mm^3) and gradually decreased until day 28 (8.3 ± 0.7 mm^3) (Fig. 4.2). In both DL2 and DL6-animals the volume of all secondly induced lesions was significantly elevated at early time points compared to animals with single infarcts, probably due to the stronger postischemic edema. This difference has not been observed anymore following day 8 after induction of the second lesion. At the end of the experiment (28 day) the size of the lesions did not differ significantly between the DL and SL groups. However, within the DL2-animals the secondly induced infarct was significantly bigger than the first one, (10.0 ± 2.6 mm^3 versus 7.3 ± 1.9 mm^3, $p = 0.031$), whereas in the DL6 group the size difference between the lesions was reversed (6.5 ± 2.3 mm^3 versus 7.7 ± 2.6 mm^3 , not significant) (Fig. 4.2).

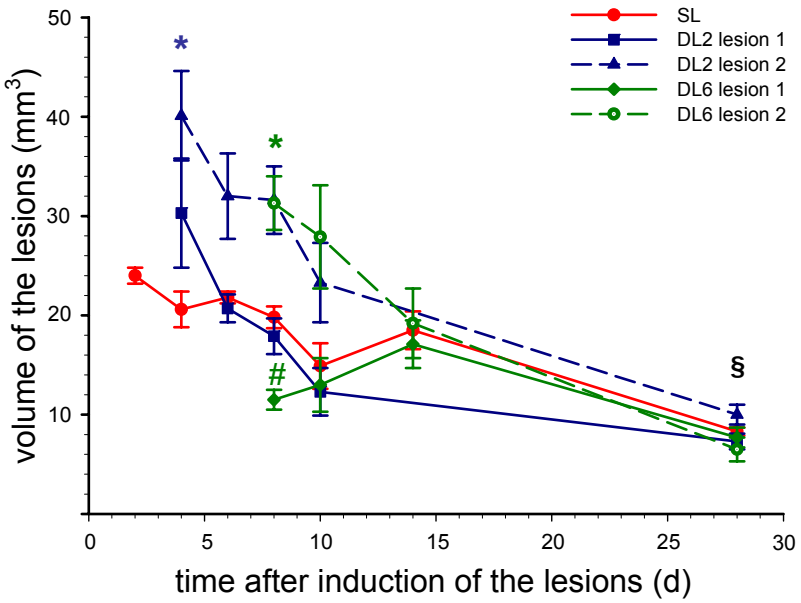

Fig. 4.2. Time course of photothrombotic lesions in the SL and DL-animals. The absolute volume (mm^3) of the lesions was measured from the Cresyl violet stained slices (40 μm). Data are presented as mean ± SEM. Non-parametric Mann-Whitney U-test revealed significant differences between volumes of the second lesion in the DL2-animals on day 4(2) and 8(6) and the corresponding lesion in the SL-animals on day 2 and 6, respectively (*, $p < 0.05$). The firstly induced lesion in the DL6 group on day 8(2) was significantly smaller compared to the corresponding lesion in the SL-animals on day 8 (#, $p < 0.05$). On day 28(26) DL2-animals demonstrated a significantly increased volume of the secondly induced infarct compared to the first infarct (§, $p < 0.05$).

4.1.2. Remote neuronal degeneration after brain ischemia

In subcortical brain regions of ipsilateral hemisphere a massive degeneration of neurons revealed by bright Fluoro-Jade B (FJ) fluorescence was found colocalized with DAPI staining demonstrating fragmented cell nuclei (Fig. 4.3). FJ-positive cells were observed in the laterodorsal thalamic nucleus (LD), lateroposterior (LP), ventroanterior nucleus (VA), posterior thalamic nuclear group (Po), ventral posterolateral (VPL), and ventrolateral (VL) thalamic nuclei. Degenerating FJ-positive fibers were found in the laterodorsal part of the striatum and the internal capsule of striatum. No FJ-positive cells were observed in the contralateral hemisphere in SL or sham-operated animals. First signs of neuronal degeneration in the thalamus were

detected on day 4 after induction of the unilateral single or bilateral sequential infarcts, whereas the maximal number of degenerating cells in the SL-animals was observed on day 8 (Fig. 4.4). In DL2-animals the number of degenerating neurons in the thalamus affected by the second infarct was significantly increased at day 10(8) compared to the SL-group. While in SL-animals the maximal cell degeneration was observed on day 8, animals from the DL6 group demonstrated significantly less thalamic degeneration in both, the firstly and the secondly affected hemispheres on days 8(2) and 14(8), respectively (Fig. 4.4). On day 28 no difference was observed between the SL and DL-animals.

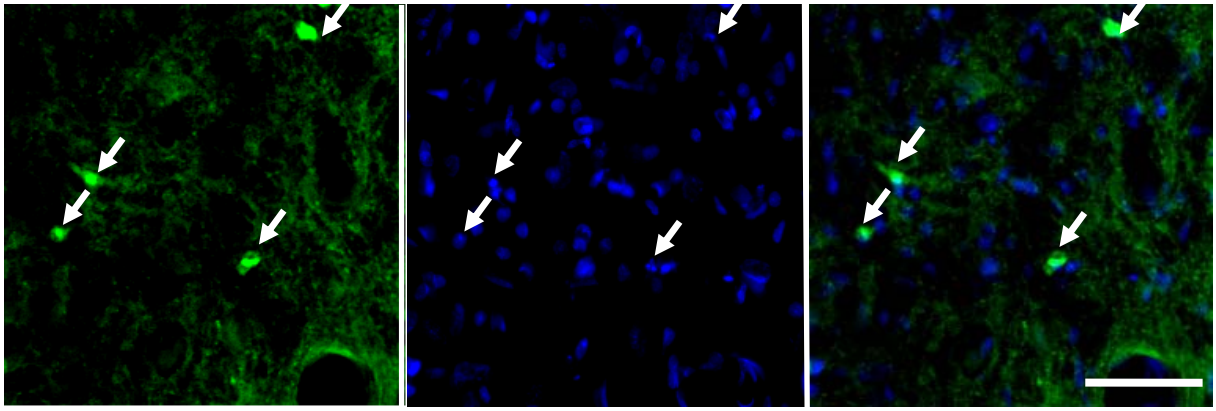

Fig. 4.3. Fluoro-Jade positive cells in the thalamus. The degenerating cells were recognized by bright green Fluoro-Jade B fluorescence accompanied by defragmented nuclei stained with DAPI. White arrows illustrate degenerating cells. White bar = 40 μm.

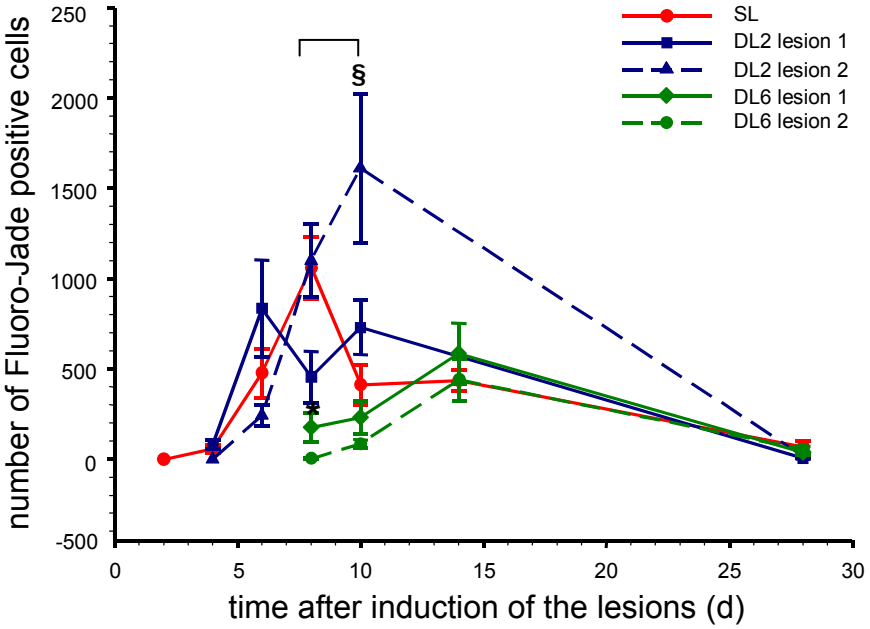

Fig. 4.4. Time course of remote degeneration in the thalamic nuclei after photothrombotic lesions in the FL SMC. The general number of Fluoro-Jade positive cells was assessed through all thalamic nuclei on every eighth slice (40 μm) from Bregma -1.8 mm to -4.16. Data are presented as mean ± SEM. The number of degenerating cells in thalamus affected by the second infarct in DL2-animals was significantly bigger on day 10 compared to SL-animals on day 8 (§, $p < 0.05$). The level of the FJ-positive cells in the thalamus ipsilateral to the primarily impaired FL SMC in the DL6-animals was significantly reduced on day 8(2) compared to the SL group (*, $p < 0.05$).

4.1.3. Thalamo-cortical connectivity of contralateral FL SMC after photothrombotic infarcts

To determine whether this remote secondary cell death in subcortical structures is due to progressive transsynaptic neuronal degeneration, retrograde tracing study was performed in intact animals using application of the retrograde neuronal tracer Fluoro-Gold in the FL SMC. Three days after the tracer application Fluoro-Gold-positive neurons were observed in the cortex surrounding the injection site, secondary somatosensory (Par2) and auditory ipsilateral cortex, contralateral homotopic cortical areas, ipsilateral ventral anterior (VA), ventral posterolateral (VPL), ventrolateral (VL) and posterior (Po) thalamic nuclei. These data suggested

that the neuronal damage revealed by Fluoro-Jade staining might be caused by the retrograde degeneration of neurons in the areas projecting to the FL SMC.

In order to determine whether cortical infarcts change the connectivity of the deafferented sensory thalamus, the animals with unilateral photothrombotic lesions were injected with Fluoro-Gold retrograde neuronal tracer on day 34 in the contralateral FL SMC area.

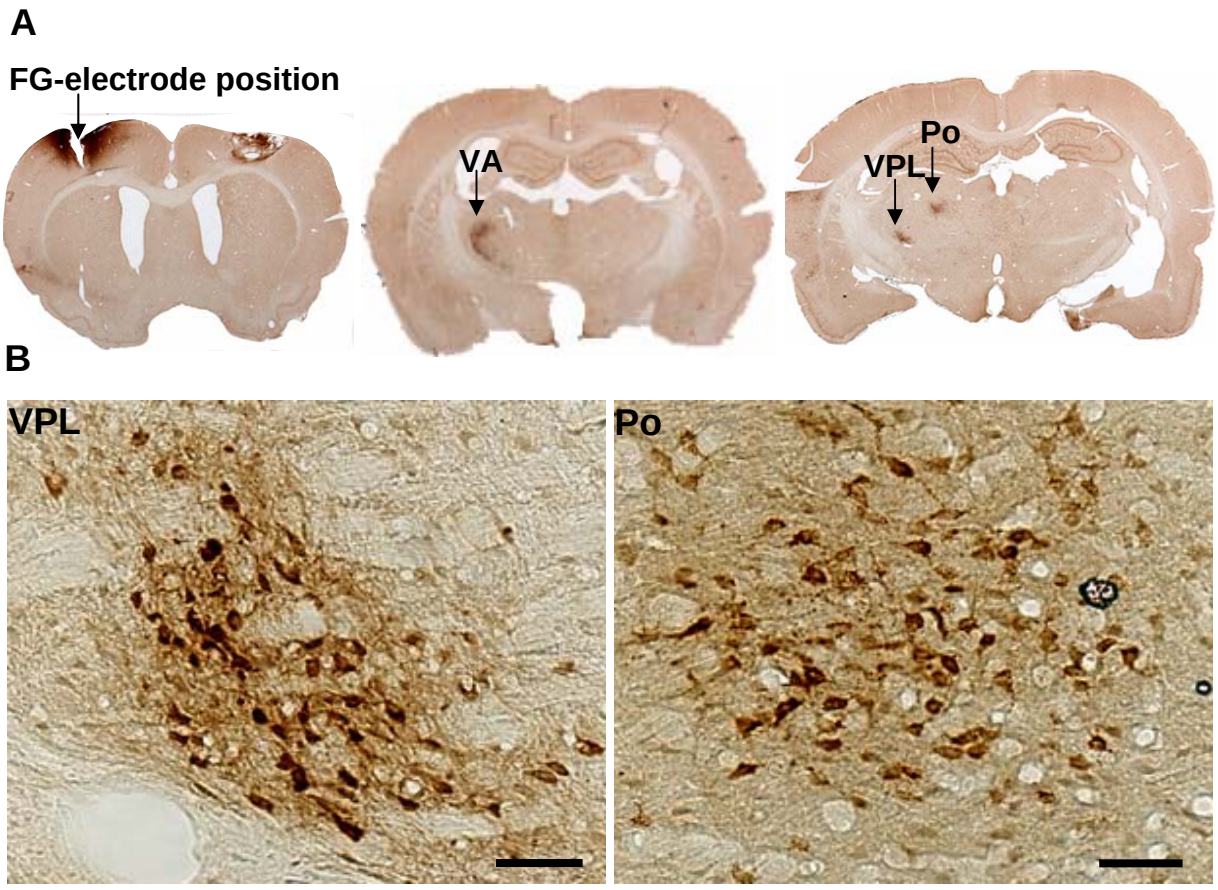

Fig. 4.5. Thalamo-cortical connections. The connections between the sensorimotor rat cortex and the thalamus were visualized with retrograde tracing of the FL SMC using Fluoro-Gold. **A:** A series of photographs presents the site of Fluoro-Gold iontophoretic application in the FL SMC (Bregma: +0.5 mm; 3.7 mm lateral to midline; 1.5 mm below surface) (left slide), a coronal slice on the level Bregma -2.8 mm (middle) demonstrating positive staining of ventroanterior thalamic nucleus (VA) and a slice on the level Bregma -3.6 mm (right slide), where positive Fluoro-Gold neurons were found in the VPL and Po thalamic nuclei. **B:** The microphotographs demonstrate the Fluoro-Gold-positive neurons in the VPL and Po at the higher magnification (black bar = 50 μm).

It is known, that the somatosensory thalamus projects to the ipsilateral FL SMC, HL, Par1, and Par2 areas (Paxinos and Watson, 1995). Induction of the photothrombotic infarct in the FL SMC did not cause alterations in the thalamo-cortical connections and as in the intact animals, the FG-positive neurons were observed only in the contralesional (i.e. ipsilateral to the application site) thalamic nuclei. No positive staining was detected in the thalamus ipsilateral to the FL SMC lesion (Fig. 4.5).

4.1.4. Activation of glial cells in remote brain areas

The first signs of microglial activation have been demonstrated in the infarct core as early as 4 hours after induction of brain ischemia (Schroeter et al, 1999). In our study on day 2 after induction of the photothrombotic lesion massive CD68-positive cell invasion was observed in the infarct core as well as on the boundary of the lesion. Microglia activation was observed in the dorsal striatum, internal capsule, laterodorsal thalamus (LD), ventrolateral (VL), ventral posterolateral (VPL) and posterior (Po) thalamic nuclei (Fig. 4.6). In the sham-operated animals and in the unlesioned hemispheres of the SL group no CD68-positive cells were detected. First signs of remote inflammation were observed on day 2 in the dorsal part of the striatum, where a few CD68-positive round shaped cells were revealed both in the SL and DL-animals.

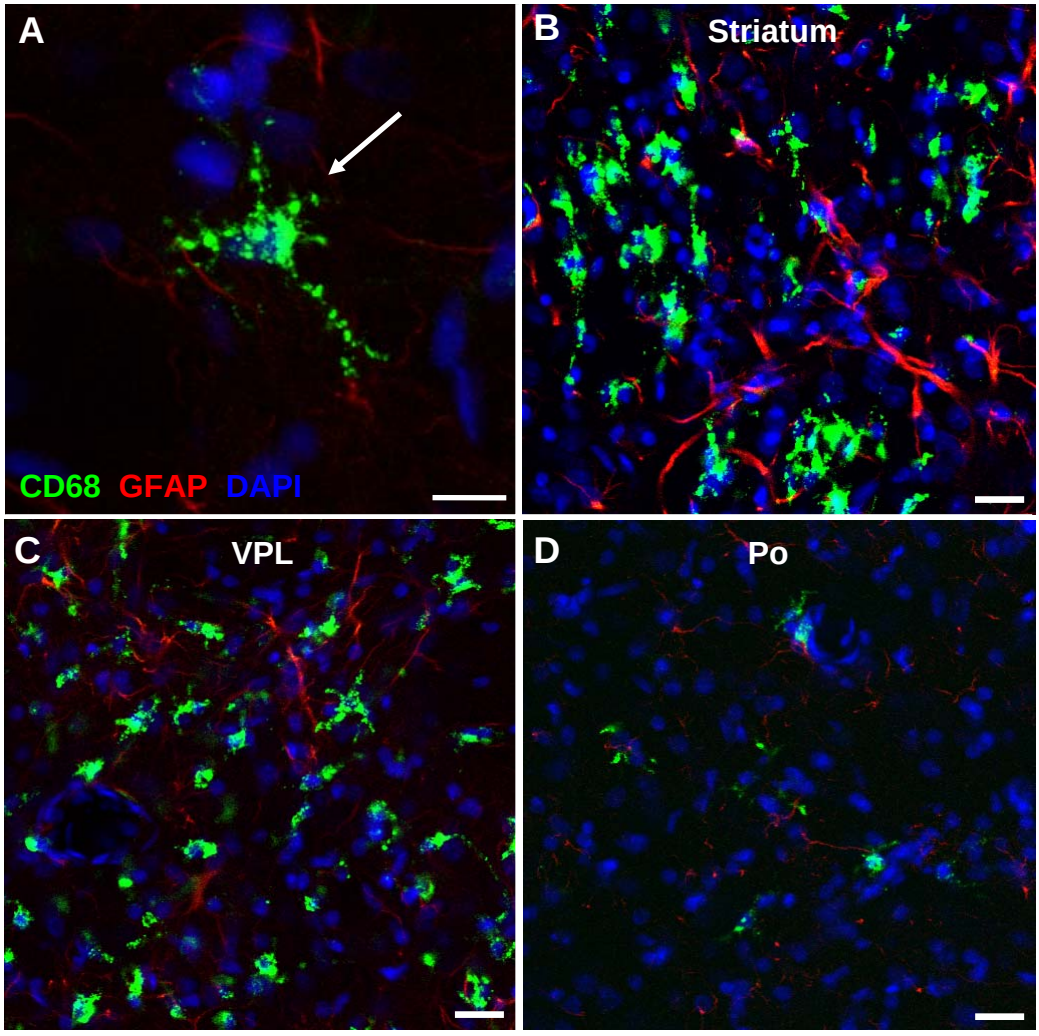

Fig. 4.6. A: CD68-positive microglial cell (shown with white arrow) at higher magnification. Bar = 10 μm. Photomicrographs of representative sections made by confocal microscope 10 days after induction of the photothrombotic lesion in the **B:** dorsal striatum; **C:** ventral posterolateral thalamic nucleus; **D:** posterior thalamic nucleus. CD68-positive cells appear as green, GFAP-positive cells have red fluorescence, DAPI (blue) stains all cell nuclei. Bar = 20 μm.

Since most microglial activation was observed in the VPL and Po thalamic nuclei the number of CD68-positive cells was evaluated in these areas. The first signs of microglial activation in the thalamus ipsilateral to the infarct were detected on day 6 in the VPL of SL and DL-animals. This was followed by the microglial response in the Po on day 8 and 10. In the SL-animals the number of CD68-positive cells in the VPL increased continuously, achieving a higher level on day 28 (Fig. 4.7 A), whereas in the Po microglial activation evolved after a delay (Fig. 4.7 B).

The time-course of the microglial activation in the VPL in the DL2 and DL6-animals was similar to that in the SL group and statistical analysis did not revealed any differences in the number of CD68-positive cells between SL and DL-animals (DL2, DL6), although on day 28 the number of CD68-positive cells in the VPL tended to be less in the SL-animals than in the DL-animals.

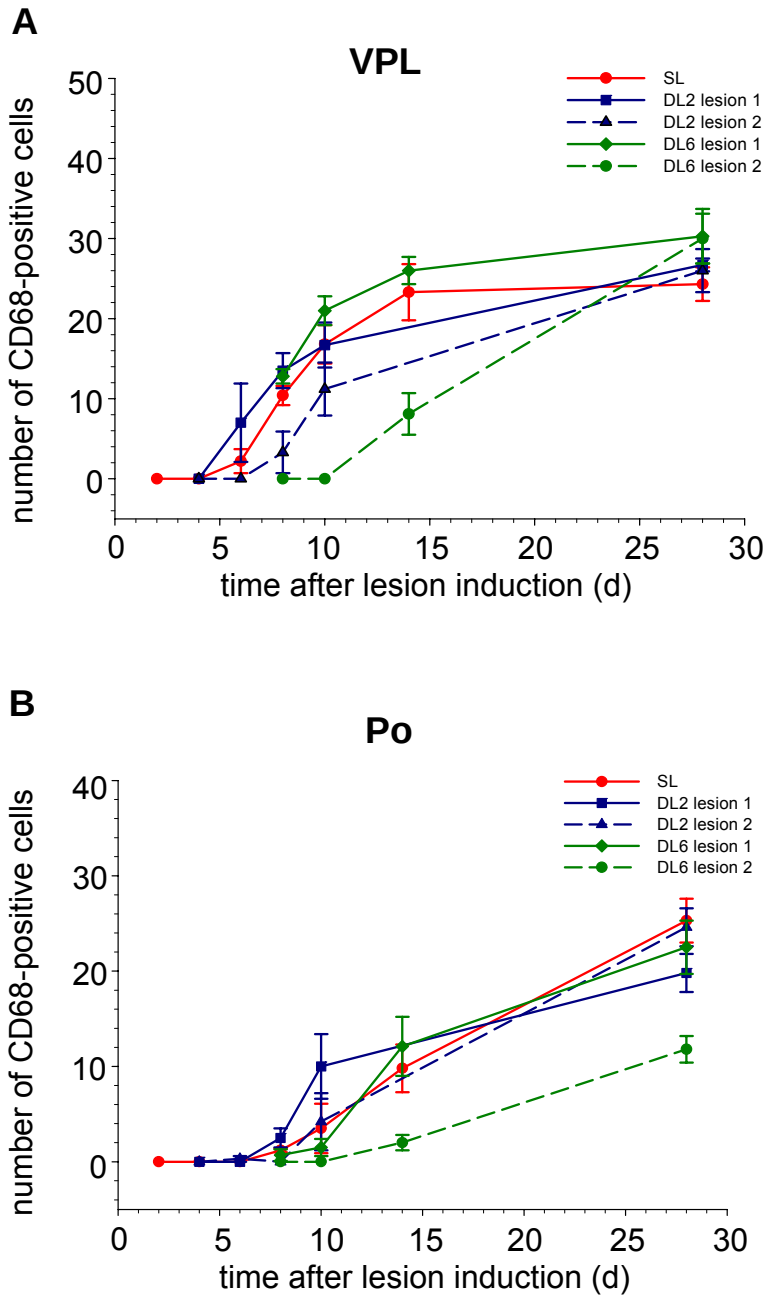

Fig. 4.7. The number of CD68-positive cells (activated microglia/macrophages) in the thalamus. **A:** in the VPL; **B:** and Po. Expression of CD68 lysosomal marker was detected in the VPL earlier (day 6) than in the Po (day 8) in both the SL and DL groups.

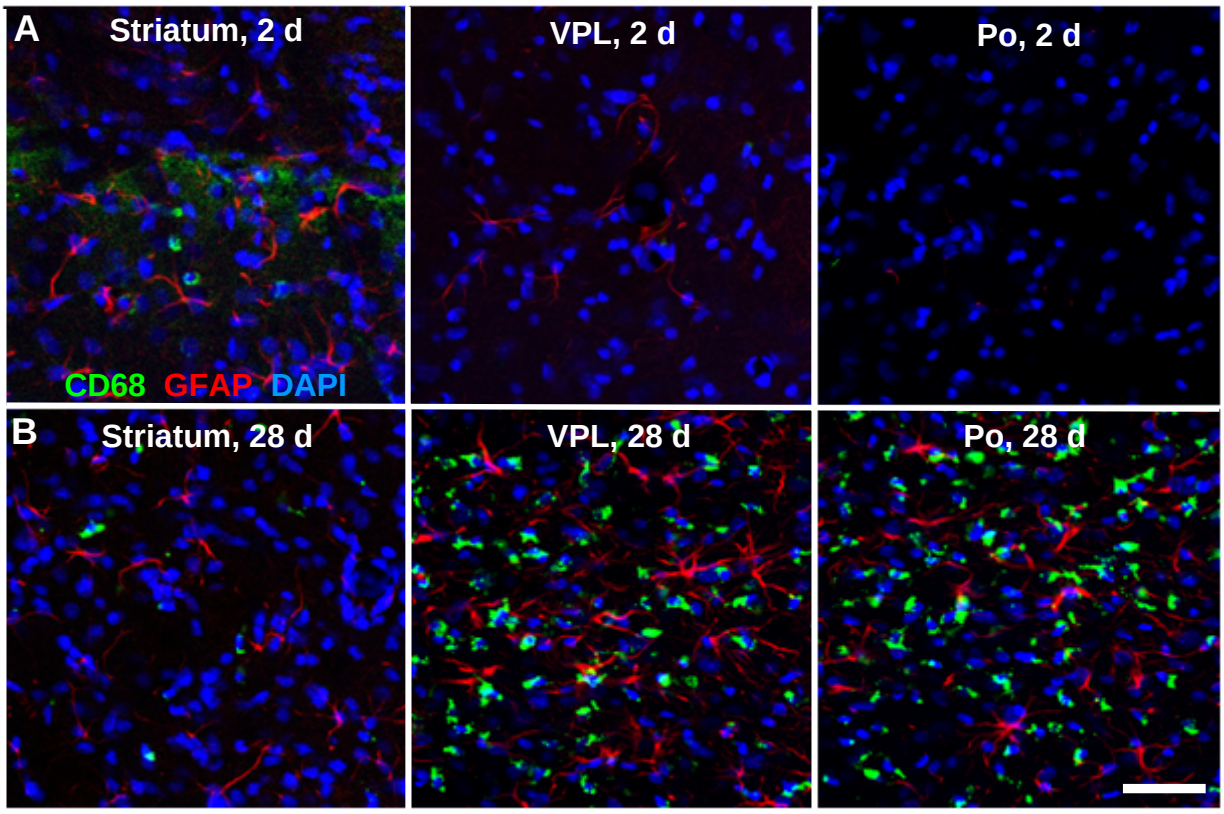

Fig. 4.8. Expression of activated microglia and astrocytes in the remote brain areas after unilateral single photothrombotic infarcts. **A:** ipsilateral dorsal striatum, VPL and Po in the SL-animals 2 days after induction of the infarct; **B:** ipsilateral dorsal striatum, VPL and Po in the SL-animals 28 days after induction of the infarct. Activated microglia/macrophages (CD68) expressed green fluorescence, astrocytes (GFAP) showed red fluorescence and cells nuclei (DAPI) appeared blue. Bar = 50 μm.

Astroglial activation visualized by the increased expression of GFAP was observed in the dorsal striatum ipsilateral to the photothrombotic lesion beginning from day 2 in SL-animals (Fig. 4.8). The strong GFAP expression in the corresponding striatum was also detected on day 2 after the second lesion in DL2 and DL6-animals (day 4(2) and 8(2), respectively). On day 28 all groups (SL and DL) demonstrated activated astrocytes in the dorsal striatum (Fig. 4.8 B and 4.9 A, B). In the VPL, pronounced GFAP immunoreactivity was detected beginning from day 6, whereas in the Po the first signs of reactive astroglial response were revealed on day 8-10 after induction of photothrombotic infarcts. At the end of the experiment (day 28) the hypertrophic

astrocytes in both the VPL and the Po strongly expressed GFAP, forming a network and surrounding microglial aggregates (Fig. 4.8 B and 4.9 A, B). No significant differences between SL, DL2, or DL6-animals were observed in the thalamus regarding the number of GFAP-positive cells (data not shown).

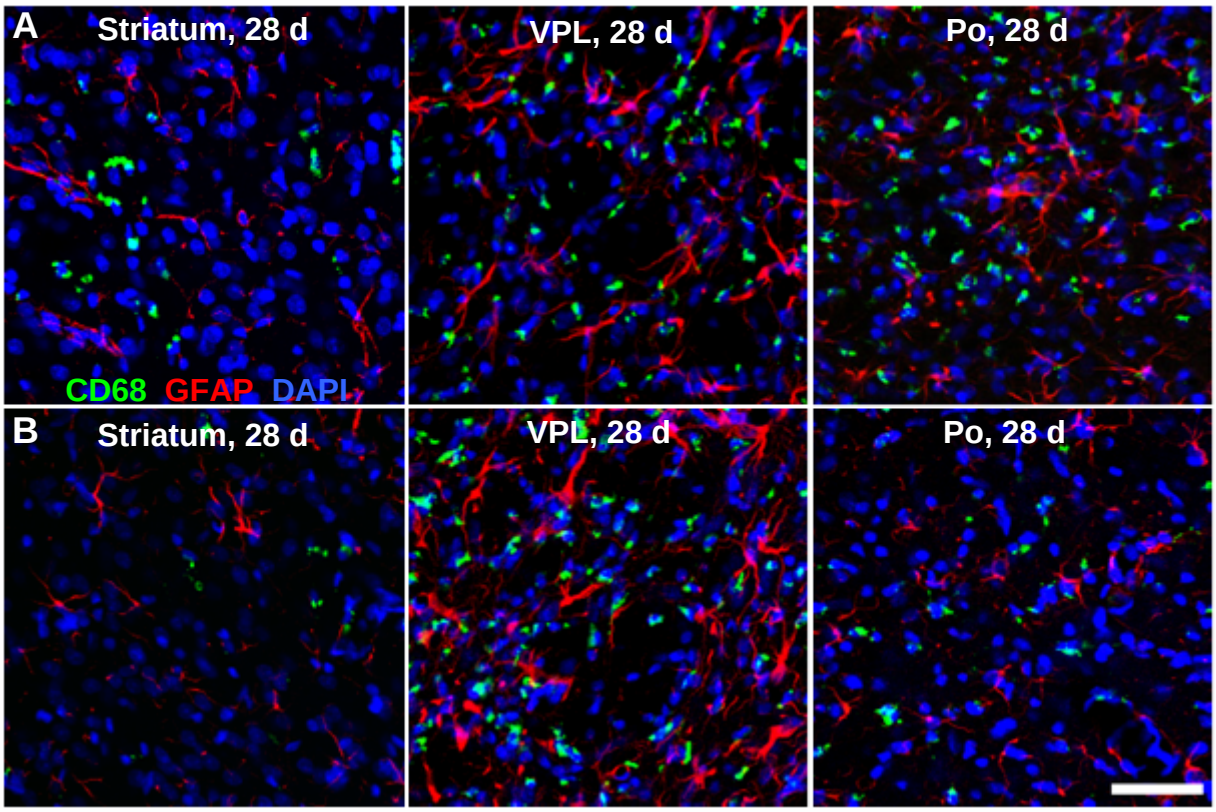

Fig. 4.9. Expression of activated microglia and astrocytes in the remote brain areas after bilateral sequential photothrombotic infarcts. **A:** ipsilateral to the firstly induced infarct dorsal striatum, VPL and Po in the DL2-animals on 28 day; **B:** ipsilateral to the firstly induced infarct dorsal striatum, VPL and Po in the DL6-animals on 28 day. Activated microglia/macrophages (CD68) expressed green fluorescence, astrocytes (GFAP) showed red fluorescence and cells nuclei (DAPI) appeared blue. Bar = 50 μm.

4.2. Sensorimotor recovery after sequential bilateral photothrombotic infarcts

4.2.1. Sensorimotor performance in sham-operated controls

Sensorimotor deficits and recovery of forelimb functions after unilateral single or bilateral sequential lesions induced with different intervals (immediately, 2, 7 or 10 days) between the lesions were compared using a battery of behavioral sensorimotor tests.

After being placed in the glass cylinder, sham-operated controls (n = 6) actively explored the cylinder, reared and supported their body against the walls with their forelimbs. Sham-operated animals did not show any asymmetry in forelimb use when they initiated a rearing movement. They used either the right or the left forepaw equally to push off from the ground. There was no difference in limb use before and after the surgery (see Tab. 4.1). For vertical explorative activity, i.e. the first contact with the cylinder wall after rearing and the following movements along the wall, all control rats used both forelimbs symmetrically. Sliding of a forelimb occurred in only approximately 20 % of movements in sham-operated controls with no difference between limbs. The animals did not show any significant asymmetry in forelimb use when they landed with their paws on the floor of the cylinder. In addition, sham-operated animals also showed only a few misplacements before and after the surgery when they walked along the grid in the foot-fault test (Tab. 4.1).

Tab. 4.1. Behavioral scores in the different experimental groups.

	forelimb activity		sliding		foot-fault test	
	1st FL	2nd FL	1st FL	2nd FL	1st FL	2nd FL
	mean ± SEM	mean ± SEM	mean ± SEM	mean ± SEM	mean ± SEM	mean ± SEM
CTRL *(n = 6)*						
day 0	3.4 ± 1.3	2.9 ± 1.4	23.0 ± 14.3	29.1 ± 14.4	5.5 ± 3.6	6.0 ± 2.2
day 1	3.1 ± 1.3	2.8 ± 1.4	18.1 ± 6.3	21.5 ± 5.3	6.9 ± 4.0	6.8 ± 3.5
day 7	3.0 ± 0.7	3.2 ± 1.1	16.9 ± 7.7	19.5 ± 9.0	6.3 ± 3.8	8.8 ± 7.5
SL *(n = 8)*						
day 0	3.4 ± 0.8	3.4 ± 1.4	22.5 ± 6.4	31.8 ± 9.6	8.8 ± 5.4	6.1 ± 4.4
day 1	1.5 ± 0.7*	3.4 ± 1.4	59.4 ± 20.4**	23.0 ± 10.2	25.7 ± 7.0 ***	10.1 ± 5.7
day 7	2.5 ± 0.5	4.9 ± 1.5	50.4 ± 9.2**	21.3 ± 12.3	15.1 ± 6.1	6.8 ± 3.1
day 14	3.4 ± 1.1	4.3 ± 1.1	31.5 ± 12.8	24.1 ± 8.4	7.3 ± 5.0	5.9 ± 3.8
day 21	3.2 ± 1.3	4.3 ± 1.2	21.4 ± 8.9	14.9 ± 8.8	10.1 ± 6.1	10.1 ± 2.0
DL0 *(n = 4)*						
day 0	3.0 ± 1.3	2.2 ± 0.6	18.2 ± 9.1	28.4 ± 10.3	6.8 ± 5.2	6.9 ± 3.6
day 1	1.8 ± 0.8	1.5 ± 0.3	46.6 ± 18.8	42.0 ± 23.5	28.6 ± 6.8*	17.5 ± 7.9
day 7	1.8 ± 1.1	2.2 ± 1.0	48.5 ± 12.4	39.3 ± 7.9	10.5 ± 5.0	10.5 ± 7.1
day 14	1.8 ± 0.7	2.1 ± 0.6	32.3 ± 13.0	26.9 ± 13.1	18.2 ± 4.2	16.6 ± 8.9
day 21	1.6 ± 0.8	2.5 ± 0.7	28.3 ± 17.1	17.9 ± 11.1	16.6 ± 10.2	11.2 ± 5.7
DL2 *(n = 9)*						
day 0	2.9 ± 1.0	2.9 ± 1.5	22.3 ± 12.1	23.1 ± 9.9	7.1 ± 4.6	8.0 ± 4.7
day 1	2.0 ± 1.2	2.8 ± 1.3	53.4 ± 22.0**	20.5 ± 11.6	25.6 ± 5.7***	6.2 ± 4.0
day 3(1)	2.0 ± 0.7	1.6 ± 0.6	54.9 ± 19.7**	64.2 ± 25.2*	19.2 ± 5.6**	14.3 ± 3.6**
day 9(7)	2.1 ± 1.4	2.4 ± 1.2	34.4 ± 17.3	26.7 ± 17.6	13.5 ± 4.9*	10.5 ± 5.3
day 14(12)	2.1 ± 0.7	2.5 ± 0.8	23.1 ± 9.8	16.5 ± 14.6	9.6 ± 6.8	11.8 ± 6.2
day 21(19)	1.8± 0.7	2.1± 1.0	25.9± 7.6	22.0± 19.1	8.5± 5.2	11.4± 6.0
DL7 *(n = 8)*						
day 0	2.8 ± 0.9	2.6 ± 1.1	23.3 ± 9.8	23.3 ± 10.1	6.2 ± 3.6	9.8 ± 2.7
day 1	0.9 ± 0.4**	2.8 ± 1.5	65.2 ± 20.4***	18.9 ± 13.2	22.4 ± 6.0***	7.9 ± 2.9
day 5	2.0 ± 0.7	3.3 ± 1.2	41.0 ± 11.0**	17.2 ± 15.7	16.7 ± 5.8**	9.5 ± 6.9
day 8(1)	1.1 ± 0.5**	1.2 ± 0.7**	46.2 ± 13.3**	63.6 ± 16.9***	13.1 ± 4.7	20.8 ± 4.1***
day 14(7)	2.2 ± 0.9	2.3 ± 1.5	37.1 ± 14.8*	35.8 ± 16.6	13.5 ± 3.3*	15.2 ± 7.9*
day 21(14)	2.0 ± 0.9*	2.5 ± 0.9	23.4 ± 12.3	22.1 ± 13.0	10.7 ± 6.1	15.8 ± 6.0*
day 28(21)	1.9 ± 0.8	2.1 ± 0.7	33.1 ± 28.0	28.8 ± 13.2	8.9 ± 2.0	8.8 ± 2.5
DL10 *(n = 9)*						
day 0	3.1 ± 1.4	3.0 ± 1.1	21.7 ± 9.5	22.7 ± 8.5	6.5 ± 4.8	6.9 ± 2.4
day 1	2.1 ± 1.0	3.1 ± 1.9	54.1 ± 12.9**	21.1 ± 11.4	22.6 ± 10.3**	5.1 ± 4.2
day 7	2.9 ± 1.1	3.9 ± 1.6	37.5 ± 12.2**	24.6 ± 12.1	14.4 ± 5.0	4.5 ± 4.8
day 11(1)	2.9 ± 0.8	1.7 ± 0.6*	24.4 ± 11.7	58.5 ± 19.7***	9.1 ± 7.2	20.7 ± 5.9**
day 17(7)	2.7 ± 0.4	1.8 ± 1.0*	29.9 ± 11.6	40.8 ± 18.6	9.6 ± 2.7	18.9 ± 7.8**
day 24(14)	2.8 ± 0.6	2.1 ± 0.6	30.5 ± 15.6	31.2 ± 13.9	10.3 ± 7.3	9.4 ± 5.8
day 31(21)	2.4 ± 0.2	1.8 ± 1.0	29.5 ± 13.2	34.4 ± 15.0	9.9 ± 7.7	11.4 ± 3.7

The data are presented as mean ± SEM. For the forelimb activity (FLA) the number of forelimb movements on each side pro rear is shown. The sliding score is presented as a percentage of the number of slides for each forelimb per total number of forelimb movements (first touch, horizontal and vertical movements), whereas the foot-fault score demonstrates the percentage of foot-faults for each forelimb per total number of steps made with that paw. The postoperative behavioral data for each animal was compared to the baseline (day 0) for each side using the nonparametric Wilcoxon matched pairs test and Bonferroni-Holm post hoc test for multiple comparisons. Statistically significant differences are indicated with asterisks *$p < 0.05$, ** $p < 0.01$, ***$p < 0.001$.

4.2.2. Sensorimotor deficits induced by single unilateral and sequential bilateral lesions

All animals with unilateral single (SL) or bilateral sequential photothrombotic infarcts (DL0, DL2, DL7, DL10) demonstrated transient functional deficits of the affected forelimbs in the glass cylinder and foot-fault test. In all these animals the impaired functions detected by the behavioral tests showed a near complete recovery to baseline levels within 3 – 4 weeks after the injury.

Analysis of ***forelimb use*** during vertical exploration of the glass cylinder (Fig. 4.10 A) revealed a significant decrease in use of the impaired forelimb in animals with unilateral single infarcts (SL group) on day 1 after the photothrombotic infarct compared to the preoperative level (Fig. 4.10 B). This deficit disappeared completely within 2 weeks. SL-animals favored the unimpaired forelimb until day 21 after the lesion (Fig. 4.10 B). All animals with bilateral sequential infarcts (DL0, DL2, DL7, DL10) demonstrated a similar deficit of the affected forelimb after the first lesion accompanied by an increased activity of the ipsilesional unimpaired paw as described in animals with unilateral single infarcts (Tab. 4.1; Fig. 4.10 C). After induction of the second infarct in the contralateral cortex, the animals showed a decreased use of the secondly affected forelimb which was previously unimpaired. The deficit of this secondly impaired forepaw reached nearly the same extent as observed for the firstly affected forelimb (Tab. 4.1; Fig. 4.10 C). A compensatory overuse which was detected for the unimpaired forelimb after single unilateral lesions was not found for the firstly affected paw after the second contralateral lesion.

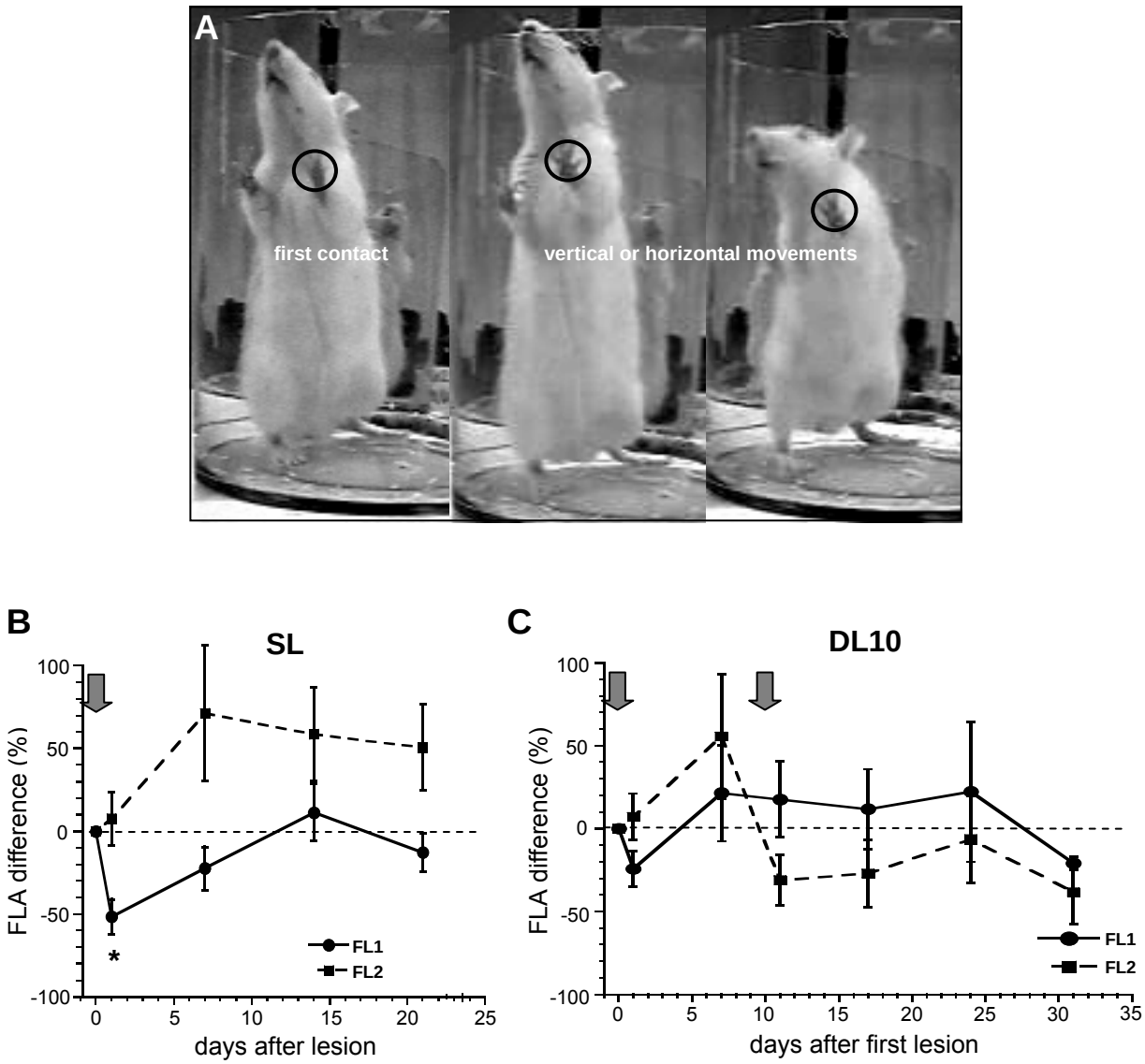

Fig. 4.10. Forelimb-activity in the glass cylinder test in animals with single unilateral (SL) and sequential bilateral (DL) infarcts in the FL SMC. **A:** Series of video recordings demonstrating a typical forelimb activity after rearing. The animal touched the wall of the cylinder with the left forelimb (black circle) and then made vertical and horizontal movements with the same paw. **B:** Relative alterations in forelimb activity compared to baseline levels after cortical infarcts in the SL-animals. Diagram illustrates the difference in forelimb use of the impaired (FL1) and unimpaired (FL2) paw in SL-animals during the first 21 days after lesion induction compared with the preoperative baseline. **C:** Relative alterations in forelimb activity to baseline levels after cortical infarcts in the DL10-animals. Diagram illustrates the difference in forelimb use of the firstly impaired (FL1) and secondly impaired (FL2) paw in DL10-animals over a period of 31 days after induction of the first lesion compared with the preoperative baseline. The grey arrows mark the time-points of lesion induction. Statistically significant differences to baseline ($p < 0.05$, Wilcoxon matched pairs test and Bonferroni-Holm post hoc test) are differentially indicated for the FL1 (*) and FL2 ($^{\#}$).

Quantitative evaluation of the ***sliding*** movements (Fig. 4.11 A) observed during explorative activity on the wall of the glass cylinder revealed an immediate increase

in the contralesional forelimb on day 1 after single unilateral lesions (SL) (Tab. 4.1; Fig. 4.11 B). The sliding score then decreased over the next two weeks, reaching the preoperative level on day 21 after the infarct. In the ipsilesional forelimb no significant changes were detected. In animals with bilateral sequential lesions (DL0, DL2, DL7, DL10) the functional deficit produced by the first photothrombotic infarct was very similar to that in the SL group (Tab. 4.1; Fig. 4.11 C). The second lesion then caused a significant increase in the sliding score of the corresponding forelimb and this functional deficit matched the impairment after the first lesion (Fig. 4.11 C).

To assess deficits in coordinated limb placing the ***foot-fault*** test was used in this study (Fig. 4.12 A). All animals with single and sequential infarcts demonstrated a significant deficit in forelimb placing with an increased number of foot-faults (Tab. 4.1; Fig. 4.12 A,B). In animals with single unilateral lesions the foot-fault score of the contralateral forelimb significantly increased on day 1 after the injury and then continuously recovered until day 14 (Fig. 4.12 B). In animals with sequential bilateral infarcts (DL0, DL2, DL7, DL10) similar deficits were detected for both forelimbs after the first and second lesion (Tab. 4.1; Fig. 4.12 C). These rats showed a significant increase in foot-fault score immediately after lesion induction which recovered within 14 – 21 days. Interestingly, the functional deficit produced by the second lesion was less pronounced in the DL2 group (Tab. 4.1).

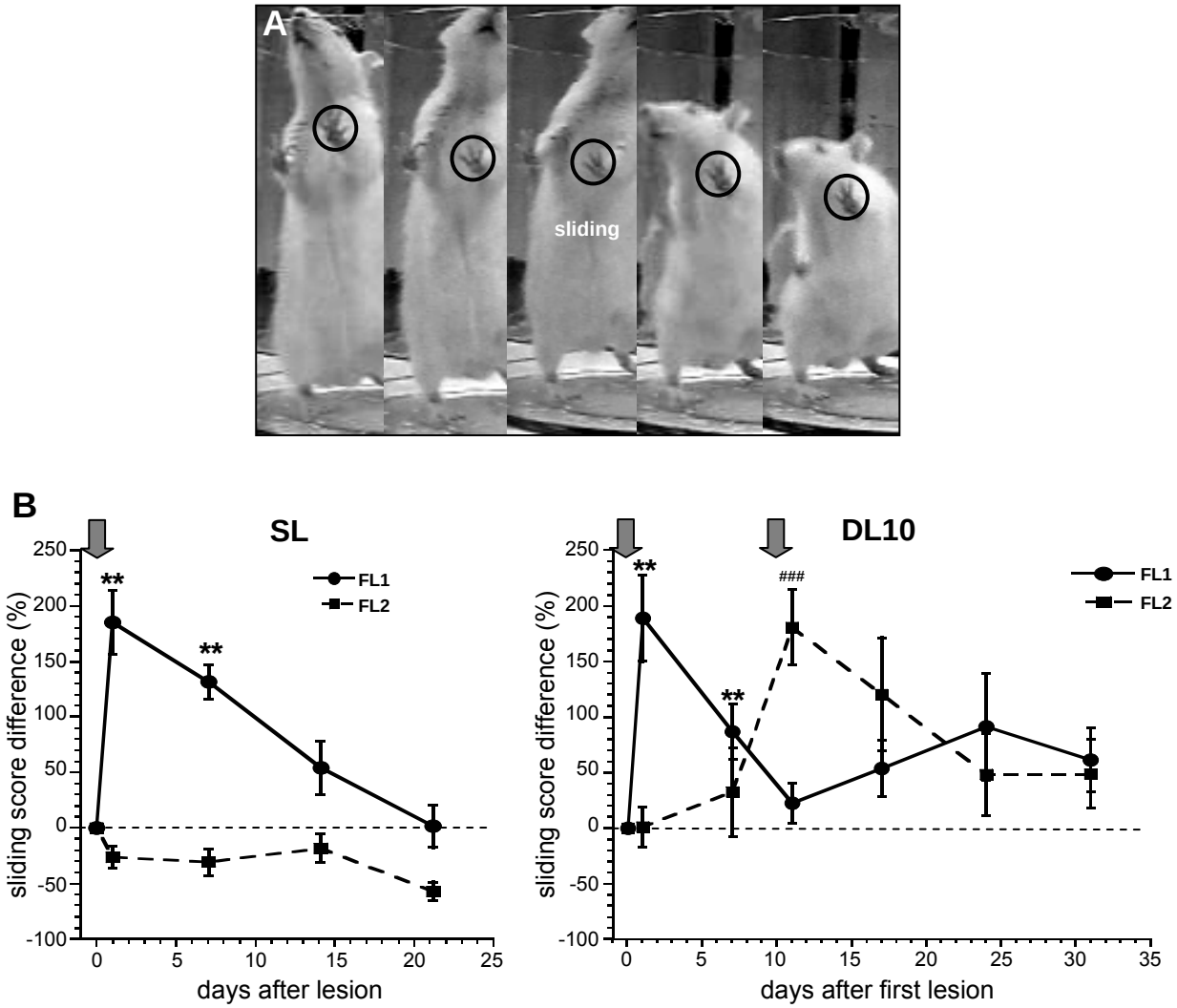

Fig. 4.11. Forelimb sliding in the glass cylinder test in animals with single unilateral (SL) and sequential bilateral (DL) infarcts in the FL SMC. **A:** Series of video recordings illustrating a typical sliding-movement of the left forelimb (black circle) during vertical explorative activity. **B:** Diagram of the relative alterations in forelimb sliding to baseline levels after cortical infarcts in the SL-animals. The diagram illustrates the difference in the sliding score of the impaired (FL1) and unimpaired (FL2) paw during the first 21 days after lesion induction compared with the preoperative baseline in the SL-animals. **C:** Diagram of the relative alterations in forelimb sliding compared to baseline levels after cortical infarcts in the DL10-animals. The diagram illustrates the difference in sliding score of the firstly impaired (FL1) and secondly impaired (FL2) forelimb during the 31 days after induction of the first lesion compared with the preoperative baseline in the DL10-animals. The grey arrows mark the time-points of lesion induction. Statistically significant differences to baseline ($p < 0.05$, Wilcoxon matched pairs test and Bonferroni-Holm post hoc test) are differentially indicated for the FL1 (*) and FL2 ($^{\#}$).

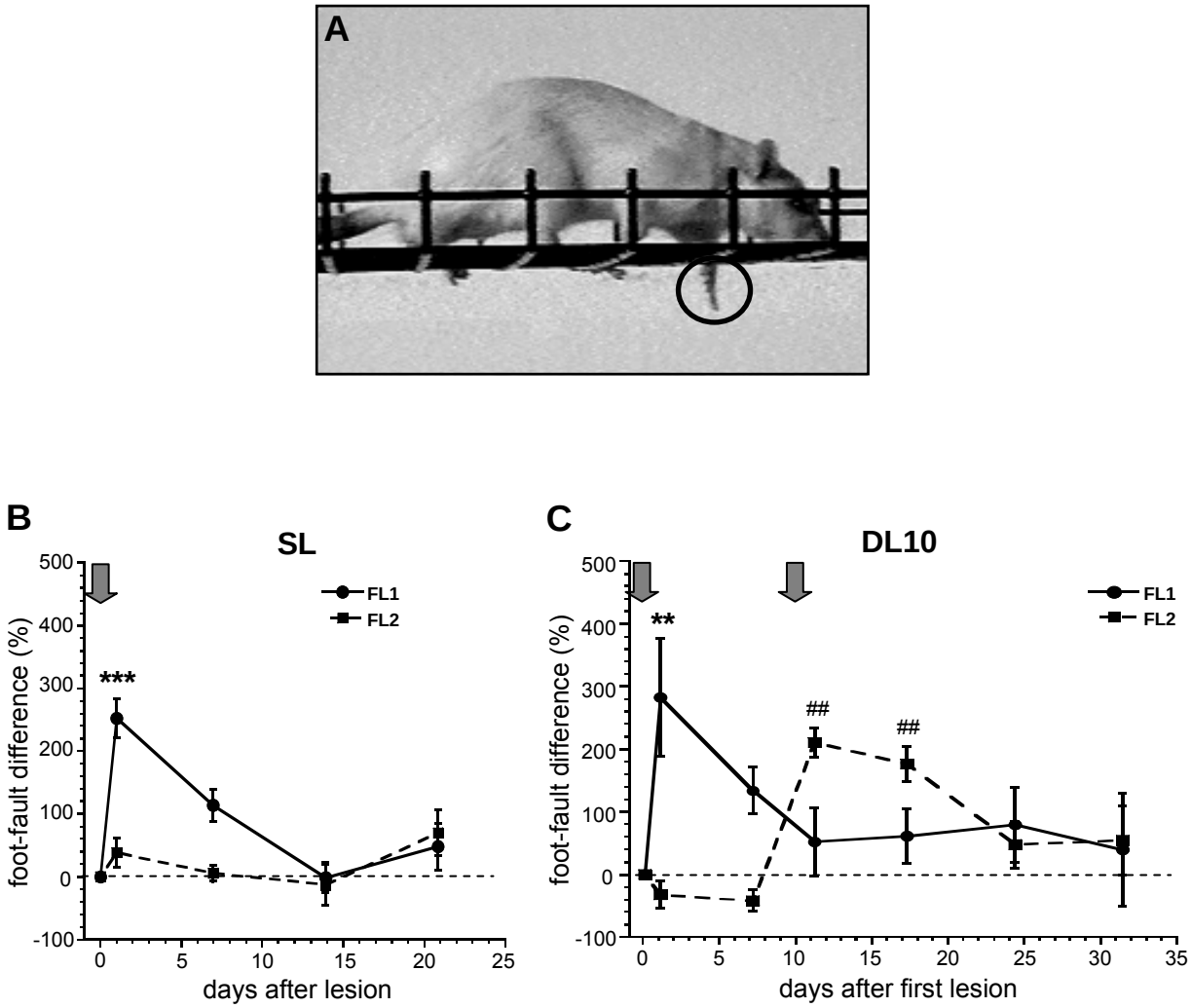

Fig. 4.12. Performance in the foot-fault test in animals with single unilateral (SL) and sequential bilateral (DL) infarcts in the FL SMC. **A:** Photograph illustrating a typical slip of the left forelimb through the opening of the grid (black circle). **B:** Diagram of the relative alterations in the foot-fault score in SL-animals. The diagram illustrates the difference in the foot-fault score of the impaired (FL1) and unimpaired (FL2) paw in the SL-animals during the first 21 days after lesion induction compared with the preoperative baseline. **C:** Diagram of the relative alterations in the foot-fault score in DL10-animals. The diagram illustrates the difference in the foot-fault score of the firstly impaired (FL1) and secondly impaired (FL2) paw in the DL10-animals over period of 31 days after induction of the first lesion compared with the preoperative baseline. The grey arrows mark the time-points of lesion induction. Statistically significant differences to baseline ($p < 0.05$, Wilcoxon matched pairs test and Bonferroni-Holm post hoc test) are differentially indicated for the FL1 (*) and FL2 ($^{\#}$).

4.2.3. Recovery after single unilateral and sequential bilateral lesions

To assess the effects of the homotopic contralateral cortex on sensorimotor recovery after the infarct the time course of functional improvement of the firstly impaired

forelimb was compared between animals with single unilateral and sequential bilateral lesions. After single cortical infarcts all animals showed a continuous recovery in forelimb activity of the impaired limb and a similar improvement in the sliding score and foot-fault test (Fig. 4.13, 4.14, 4.15). In animals with sequential cortical lesions (DL0, DL2, DL7, DL10) the time course of functional recovery of the firstly impaired forelimb did not significantly differ from animals with only single infarcts. Compared with unilaterally lesioned animals the progression of functional improvement in DL-animals varied to some extent but reached similar scores 2 weeks after the first infarct in the forelimb activity and sliding as well as the in the foot-fault tests (Fig. 4.13, 4.14, 4.15). Statistical analysis (Kruskal-Wallis test, Dunn's multiple comparisons) did not reveal any significant difference between the groups. It suggests that in animals with sequential bilateral lesions the second insult in the contralateral cortex did not impair the functional recovery after the first lesion.

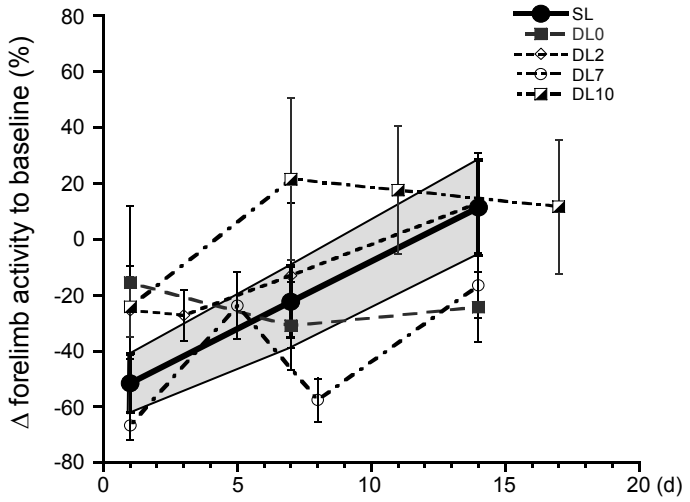

Fig. 4.13. Functional recovery in forelimb activity after unilateral and bilateral infarcts in the FL SMC. Comparison of the functional improvement of the contralesional forelimb of SL-animals with the primary affected forelimb in DL-animals. Data are given as mean ± S.E.M., the fat line demonstrates the time course of functional recovery in SL-animals (grey zone reflects S.E.M.). Statistical analysis (Kruskal-Wallis test, Dunn's post test) does not reveal any significant difference between these groups.

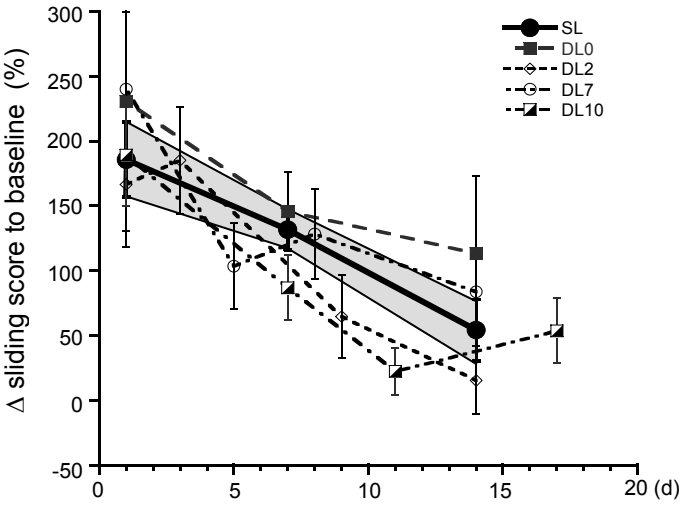

Fig. 4.14. Functional recovery in sliding score after unilateral and bilateral infarcts in the FL SMC. Comparison of the functional improvement of the contralesional forelimb of SL-animals with the firstly affected forelimb in DL-animals. Data are given as mean ± S.E.M., the fat line demonstrates the time course of functional recovery in SL-animals (grey zone reflects S.E.M.). Statistical analysis (Kruskal-Wallis test, Dunn's post test) does not reveal any significant difference between these groups.

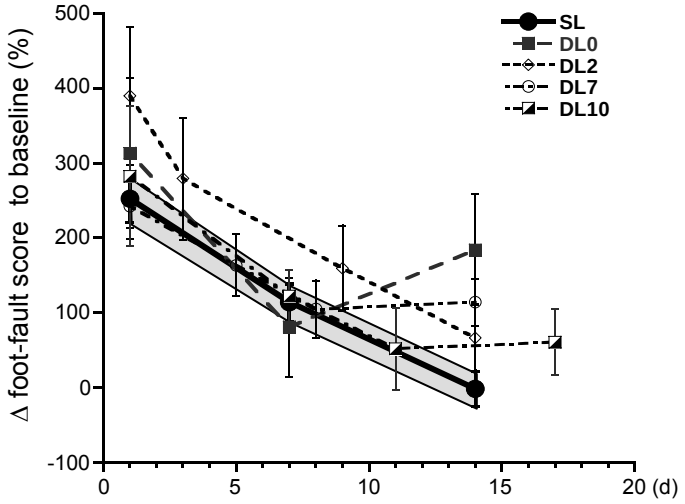

Fig. 4.15. Functional recovery in foot-fault score after unilateral and bilateral infarcts in the FL SMC. Comparison of the functional improvement of the contralesional forelimb of SL-animals with the firstly affected forelimb in DL-animals. Data are given as mean ± S.E.M., the fat line demonstrates the time course of functional recovery in SL-animals (grey zone reflects S.E.M.). Statistical analysis (Kruskal-Wallis test, Dunn's post test) does not reveal any significant difference between these groups.

4.3. Long-term consequences of sequential bilateral photothrombotic infarcts on brain volume and cognitive function

4.3.1. Effects of sequential bilateral photothrombotic infarcts on brain volume

To evaluate the interaction of sequential bilateral lesions induced at different intervals between the lesions and their influence on the remaining brain tissue a volumetric analysis was performed. All animals were tested histologically 31 days after the last injury or sham-operation. The effects of the sequential bilateral lesions on the cognitive performance were tested using the Morris water maze.

In animals with sequential lesions, on day 31 the sizes of the first and the second lesions were similar in all groups (DL0, DL2, DL10) except for those with a time interval of 7 days between acquisition of the lesions (cf. Fig. 4.16 B). In this group, the second lesion was 25.5 $\pm$ 31.6 % smaller than the first ($p < 0.05$).

Notably, the first as well as the second lesion were smaller than a single lesion on day 31 in all other groups with sequential lesions (DL0, DL2, DL10): e.g., when lesions were inflicted with an interval of ten days (DL10), the first and the second lesion had volumes of 3.7 $\pm$ 1.4 mm^3 and 4.2 $\pm$ 2.1 mm^3 respectively compared to a volume of 8.5 $\pm$ 3.5 mm^3 in animals with a single lesion (Fig 4.16 B). This indicates that the infliction of a second lesion affected the shrinkage of a previously obtained first lesion in these groups.

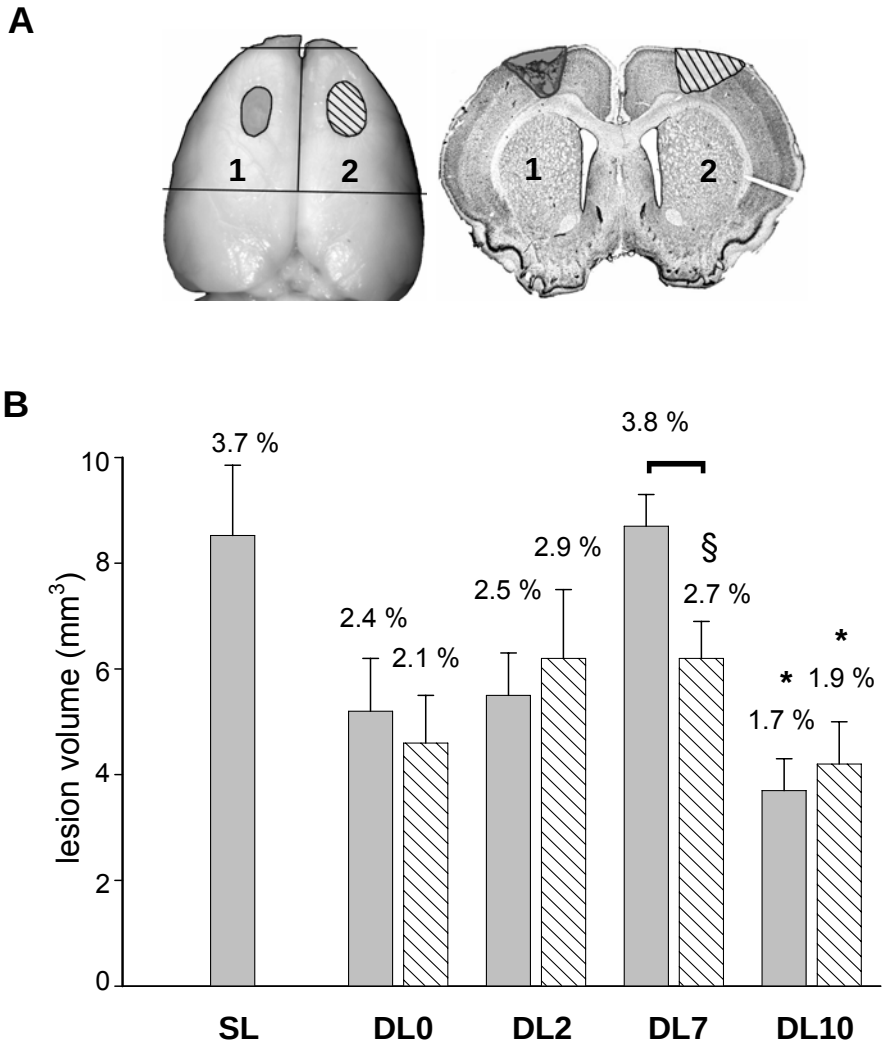

Fig. 4.16. Volumetric analysis of the infarct size (mean ± S.E.M.) on day 31 in animals with single unilateral and sequential bilateral photothrombotic lesions. **A:** On the left side an adult rat brain that received two photothrombotic lesions in sequence is shown. The first infarct is colored gray and the second one is hatched. The brain segment analyzed volumetrically is marked with black lines. The right side shows a Nissl stained coronal brain section of the same brain. The infarcts are indicated in the same way as on the left. **B:** Absolute infarct volumes (mm^3) in the SL and DL-animals. Gray columns indicate the first infarct, hatched ones the second. The relative volumes of the brain lesions to the analyzed brain segment are given on top of the columns (brackets). The mean infarct volume in the SL group tended to be bigger than that in the DL-animals. In the DL7 group the second lesion was significantly smaller compared to the first one ($^{\S}p < 0.05$). Both infarcts in the DL10-animals were significantly smaller than the single lesion ($^{*}p < 0.05$).

Since lesion size is affected by shrinkage of the scar, it does not necessarily reflect how much brain tissue was lost in the different groups of animals with sequential lesions. Therefore, evaluation of the amount of residual brain was performed (Fig. 4.17 A,B). Animals with a single lesion lost about 7.0 % of brain volume in the

afflicted hemisphere (cf. Fig. 4.17 C). The size of the non-lesioned hemisphere was not different from that of the sham animals. In animals with sequential lesions, the volume of the intact tissue 31 days after lesion induction was smaller than expected from the scar sizes: compared to the sham animals, there was a superadditive brain volume loss in all animals with sequential lesions. Thus, in the DL2-animals the loss of brain volume was 12.0 ± 5.5 % in the first affected hemisphere and 14.5 ± 6.1 % in the second.

A determination of brain volume including scar tissue (cf. Fig. 4.18 A,B) showed that the loss of brain tissue in animals with sequential lesions exceeded the loss of brain volume measured in animals with a single lesion: When the sequential lesions were induced with an interval of two days the brain volume loss compared to sham-operated animals was 9.9 ± 5.2 % in the first affected hemisphere and 11.9 ± 5.5 % in the second hemisphere, while in the animals with single lesions the loss of brain volume in the impaired hemisphere was only 3.4 ± 7.3 % (cf. Fig. 4.18).

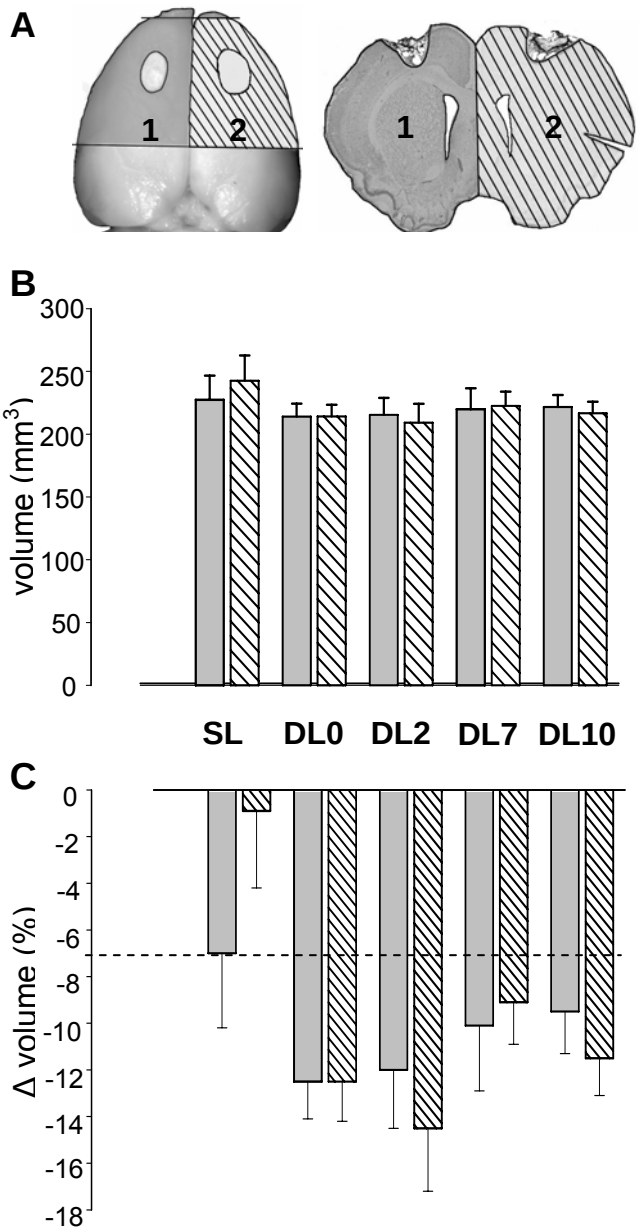

Fig. 4.17. Volume of the remaining brain tissue (mean ± S.E.M.) in animals with single unilateral and sequential bilateral photothrombotic infarcts. **A:** On the left side an adult rat brain that received two photothrombotic lesions in sequence is shown. The volume of the remaining brain tissue in the first infarcted hemisphere is indicated in gray and the volume of the second one is hatched. The brain segment analyzed volumetrically is marked with black lines. The right side shows a Nissl stained coronal brain section of the same brain. **B:** Absolute volume of the remaining brain tissue (mm^3) in SL and DL-animals. Gray columns indicate the volume of the remaining brain tissue in the hemisphere receiving the first lesion; hatched ones denote the volume in the second-lesioned hemisphere. **C:** The relative loss of remaining brain tissue in the groups with bilateral infarcts. The percentage difference (%) between the volume of the remaining brain tissue in hemispheres with unilateral and bilateral infarcts and the volume of the brain tissue in sham-operated animals is shown. Gray columns demonstrate the relative loss in volume in the hemisphere receiving the first lesion, hatched ones in hemisphere with the second lesion. In the SL group the gray column indicates the impaired hemisphere and the hatched column the non-ischemic hemisphere. The dotted line shows the loss of brain volume in the affected hemisphere of animals with unilateral infarcts (SL) emphasizing additional tissue loss in all DL-animals.

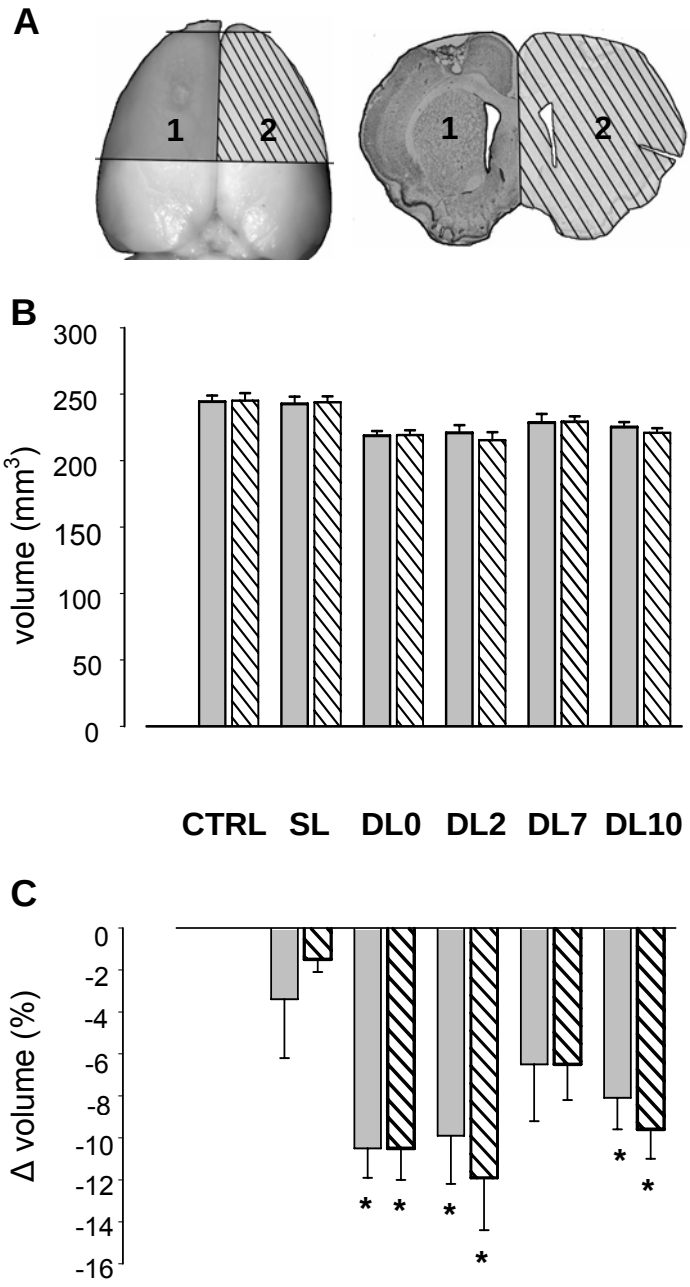

Fig. 4.18. Alterations of global brain volume in animals with single unilateral and sequential bilateral photothrombotic lesions. **A:** On the left side an adult rat brain that received two photothrombotic lesions in sequence is shown. The global volume of the first infarcted hemisphere is indicated in gray and the second one is hatched. The brain segment analyzed volumetrically is marked with black lines. The right side shows a Nissl stained coronal brain section of the same brain. The area of the hemispheres measured as global brain volume is indicated in the same way as on the left. **B:** Absolute global brain volume (mm^3) (mean ± S.E.M.) in SL and DL-animals. Gray columns indicate the global volume of hemisphere receiving the first lesion, hatched ones denote the volume of the second-lesioned hemisphere. **C:** The relative loss of tissue in the groups with single and the double lesions. The difference (%) between the global volume of hemispheres with uni- and bilateral infarcts and the global volume of hemispheres in sham-operated animals is shown. Gray columns demonstrate the relative loss in global volume in the hemispheres receiving the first lesions, hatched ones in hemispheres with the second lesions. Reduction of brain volume is observed in all DL-animals compared to sham-operated controls (CTRL) but not in the SL group.

4.3.2. Cognitive consequences of sequential cortical infarcts

The functional consequences of single and sequential brain lesions were analyzed by testing spatial learning with the Morris water maze. For purpose, two additional series of animals receiving either 2 photothrombotic infarcts with an interval of 2 days between the lesions (DL2; n = 11) or a single cortical infarct (SL; n = 5) were compared with sham-operated controls (CTRL; n = 10). The place navigation task was performed 2 months after the last surgery. At this time, there were no observed differences in swim speed between experimental and control groups.

Animals were trained daily for 7 consecutive days to reach the underwater platform. Following 4 days of training, sham-operated controls asymptotically approximated a latency of 12.9 ± 2.5 s (Fig. 4.19 A). At the same time point (4 day), the latency was 27.0 ± 5.6 s for DL-animals and 21.6 ± 5.7 s for single lesioned animals. In contrast to sham-operated controls, the learning curve of both the SL and DL2 groups was less inclined, showing their shortest latencies on day 6 and 7. Following 7 days of training, the latency of animals with single lesions (10.1 ± 3.8 s) was very similar to that of sham-operated controls (8.9 ± 1.1 s), whereas double-lesioned animals demonstrated a small but statistically significant performance deficit with a latency of 18.3 ± 2.5 s ($p < 0.05$).

To determine the learn curve differences between these 3 experimental groups the analysis of the areas below the learn curves was performed. The one-way ANOVA followed by Tukey-Kramer multiple comparisons post t-test demonstrated that the “learn curve area” in the CTRL-animals differed significantly from that of the DL-animals (125.8 ± 9.3 versus 183.4 ± 17.0, $p < 0.05$). At the same time comparison of the “learn curve area” in the SL group (138.5 ± 30.0) with other groups did not reveal any significant difference.

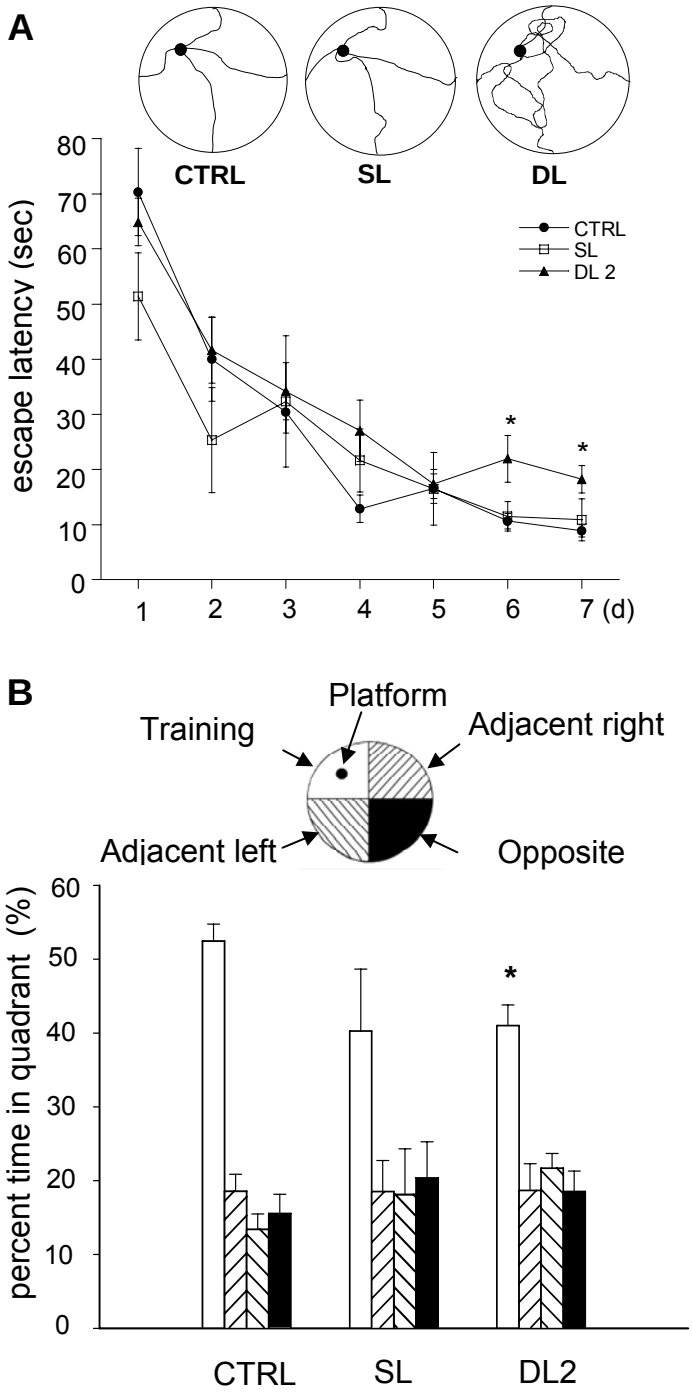

Fig. 4.19. Behavioral performance of animals with single unilateral and sequential bilateral photothrombotic lesions and sham-operated controls in the Morris water maze. **A:** Acquisition trial. Above, examples of typical swimming paths in Morris water maze of animals in sham- (CTRL), single- (SL) and double-lesioned (DL2) groups. Below is a graph, demonstrating latency (seconds) to find an invisible platform in Morris water maze during 7 consecutive days of acquisition training. The data are presented as mean ± S.E.M. Following 7 days of training the latency of animals with single lesions was very similar to sham-operated controls, whereas double-lesioned animals demonstrated a small but significant performance deficit (*$p < 0.05$). **B:** Probe trial. Mean ± S.E.M. percentage of time spent in each of the four quadrants during 60 s of probe trial. Each group spent the greatest percentage of time in the target quadrant, but sham-operated controls spent significantly more time in the target quadrant (*$p < 0.05$) than double-lesioned animals. Animals from the SL group spent less time in the target quadrant compared with sham-operated controls but not to a significant level.

On day 7 the platform was removed and probe trials were performed to test whether the animals remembered its location. These probe trials revealed that sham-operated controls spent significantly more time in the target quadrant 52.5 % ($p < 0.05$) (Fig. 4.19 B) than double-lesioned animals (41.0 %). In addition, animals from the SL group spent less time in the target quadrant (40.3 % (n.s.)) compared with sham-operated controls but this did not reach a significant level. These data indicate that performance in this spatial memory task was impaired in both groups of animals with focal cortical infarcts. However, non-memory cognitive impairments may have contributed to the differences (Day et al., 1999).

5. Discussion

Focal brain ischemia leads to widespread neuronal degeneration in remote subcortical structures. The present study demonstrated that a contralateral infarct induced 2 days after the first one (DL2) increased neuronal death in thalamic nuclei in the ipsilateral hemisphere, whereas in the animals with 6 days between the infarcts (DL6) a decreased neuronal degeneration was observed in both hemispheres. Neuronal degeneration in the striatum and thalamus was accompanied by massive activation of microglia and astrocytes. However, this inflammatory response did not differ between SL and DL groups. Investigations of forelimb sensorimotor functions using glass cylinder and foot-fault tests demonstrated no difference in time course and extent of functional recovery in SL and DL-animals. Even when the intervals between the infarcts were varied (0, 2, 7, or 10 days), the second infarct did not impair the functional recovery of the initially impaired forelimb. This finding provides further evidence that the contralesional cortex did not significantly contribute to the functional recovery of the impaired forelimb. However, evaluation of brain volume in DL-animals detected an additional reduction of global brain volume compared to the animals from the SL group with exception of the DL7-animals. Behavioral studies in the water maze further demonstrated that this loss of brain volume corresponded to a slight but significant cognitive impairment.

5.1. Remote neuronal degeneration after sequential bilateral photothrombotic infarcts

The present study clearly demonstrated that photothrombotic infarcts in the sensorimotor cortex induced delayed neuronal degeneration in remote subcortical

structures. Degenerating cells and/or fibers were found in the thalamic structures as well as in the dorsolateral striatum and the internal capsule of the striatum. These findings were in accordance with previous experimental studies that demonstrated a delayed cellular death in different thalamic nuclei and striatal structures in animal models of focal brain ischemia in the somatosensory and motor cortex (Dihne et al., 2002; Iizuka et al., 1990; Nagasawa and Kogure, 1990; Rupalla et al., 1998; Sharp et al., 1986; Sulejczak et al., 2004). Fluoro-Jade-positive cells were predominantly observed in the ventral anterior (VA), ventral posterolateral (VPL) and posterior (Po) somatosensory thalamus. These thalamic nuclei show strong thalamocortical connections to the sensorimotor cortex. This finding provides evidence for retrograde degeneration in the somatosensory thalamus after focal ischemia in the FL SMC. This was in accordance with a previous study from Sorensen et al. (1996) demonstrating that thalamo-cortical neurons prelabeled with Fluoro-Gold tracer degenerated following sensorimotor cortex ablation. Since the somatosensory thalamus and somatosensory cortex have reciprocal connections it is conceivable that the degenerating neurons found in this study undergo both retrograde and anterograde degeneration. There are different mechanisms that possibly contribute to thalamic neuronal death after cortical injury. Cortical ischemia leads to the direct injury of the axons projecting from the somatosensory thalamus followed by progressive retrograde degeneration of the cell bodies. Furthermore, Wallerian (anterograde) degeneration of the corticothalamic projections results in a massive release of excitatory amino acids and disturbance of reuptake mechanisms (Yoon and Ross, 1989; Young et al., 1981). This leads to an increase in excitability and an overexcitation of the thalamic neurons followed by their degeneration (Ross and Ebner, 1990). Additionally, Wallerian degeneration of corticothalamic projections leads to massive deafferentation of the thalamic relay neurons. Despite many

proposed hypotheses, the pathophysiological mechanisms of the delayed thalamic degeneration after cortical injury are still only poorly understood.

This study demonstrated that after induction of a second lesion in the DL2 group the number of Fluoro-Jade-positive cells in the ipsilateral thalamus was considerably bigger compared to the degeneration induced by a single lesion, probably due to the triggering of deleterious pathophysiological mechanisms following repetitive brain ischemia. Interestingly, in the DL6 group the number of degenerating thalamic neurons was significantly reduced for both the firstly and secondly impaired hemispheres on day 8 compared to the SL-animals that could be mediated by neuroprotective mechanisms of ischemic preconditioning, which will be discussed later (Dirnagl et al., 2003; Kirino, 2002).

5.2. Inflammatory response in remote brain areas

In response to an injury, including focal ischemia, the brain is subjected to an inflammatory reaction (Feuerstein et al., 1998). Activated microglia and hematogenous macrophages as well as activated astrocytes produce proinflammatory cytokines, chemoattractants and metalloproteinases that sustain the inflammatory response (for review see Dirnagl and Priller, 2005). Activated glial cells are thought to take part in secondary neuronal degeneration within subcortical structures after focal brain ischemia (Block et al., 2005). Astroglial and microglial activation was detected within the ventroposterior thalamic nuclei 2 to 3 days after middle cerebral artery occlusion (MCAO) or photothrombotic stroke in the parietal cortex by upregulation of GFAP or OX-42 immunohistochemistry respectively (Rupalla et al., 1998; Schroeter et al., 1999; Sorensen et al., 1996). After ablation of the hindlimb sensorimotor cortex the activation of microglia in the thalamus detected

by tomato lectin immunoreactivity was observed from day 3, increased up to day 14 and progressively decreased to day 30 (Vela et al., 2002). In the present study only a few CD68 positive cells were found in the dorsal striatum on day 2 after induction of the infarct followed by maximal expression of these cells on days 10 and 14. In the thalamus, VPL demonstrated first signs of microglial activation on day 6, whereas in Po this activation occurred later (day 8 or 10) accompanied with GFAP overexpression. The strong activation of microglia/macrophages and reactive astrocytes was still observed on day 28 in the VPL and Po providing evidence of further ongoing processes of postischemic inflammation. CD68-immunoreactivity characterizes the phagocytic activity of microglial cells or hematogenous macrophages that preceded by common microglial activation. Use of other microglial markers as described above could explain some delay in expression of CD68-positive cells found in this study.

The present study provides further evidence that microglia as well as astroglia is activated in remote brain areas after focal cerebral ischemia. We showed the detailed time-course of the glial response in the subcortical structures remote from the lesion site such as the striatum and the thalamus. In contrast to the increased neuronal degeneration in the DL2 group, no significant differences were observed in the inflammatory response between SL and DL groups. The number of tissue macrophages and/or activated microglia (CD68-positive cells) in the degenerating thalamus did obviously not correspond to the neuronal cell death. Possibly, the immunohistological approach was not sensitive enough to detect this difference.

5.3. Sensorimotor deficits after focal ischemic cortical lesions

Following lesions in the FL SMC functional impairment of the corresponding forelimb has been previously described in different injury models and behavioral tests. One sensitive parameter for functional impairment is the measurement of forelimb preference during exploratory behaviour in the glass cylinder (Jones and Schallert, 1992; 1994; Kozlowski et al., 1996; Schallert et al., 2000b). Animals preferentially use the unimpaired ipsilesional forepaw for rearing and support during exploratory activity in the glass cylinder (Hsu and Jones, 2005; Schallert et al., 2000b). In accordance with these previous reports asymmetric use of the forelimbs with significant impairment of the paw contralateral to the lesion was observed. Furthermore, animals with photothrombotic lesions showed significantly increased sliding movements of the impaired forelimb during vertical exploration of the glass cylinder. Sham-operated animals usually placed their forelimbs accurately on the wall of the glass cylinder and held it on the same position until the next movement. In contrast animals with infarcts in the FL SMC were not able to keep this position gliding down with their impaired forelimb. Increased sliding movements were only observed in the affected forelimb indicating that they were not caused by unspecific effects of the anesthesia and/or surgical procedure. Moreover, an increase in the sliding score did not occur after sham surgery. It is conceivable, that the sliding movements were primarily caused by the paresis following corticospinal tract damage but also sensory impairment might contribute to this dysfunction. Therefore, increased sliding movements were a sensitive marker for impaired forelimb function. However, this increase in sliding movements was transient and declined to baseline at two weeks after the infarct that correlates with functional recovery in other sensorimotor tests.

Animals with infarcts in the FL SMC additionally showed functional deficits in the foot-fault test during skilled walking on a regular grid. This finding is in accordance with previous studies demonstrating that rats with SMC lesions increasingly misplace the contralateral forelimb (Barth et al., 1990; Napielalski et al., 1998). Placing deficits were also caused by corticospinal tract injury and impairment of sensory function. In particular, deficits in proprioception might occur and the animals might lose the necessary feedback from the limbs when they slip too deep into the openings of the grid (Barth et al., 1990).

The tests used in this study focus on sensorimotor function during exploratory behavior and skilled walking and allow the assessment of both forelimbs. A very sensitive test for fine sensorimotor forelimb function is the single pellet reaching test (Whishaw et al., 1993) which has been shown to detect even slight deficits in grasping after different brain lesions (Gharbawie et al., 2005; Metz et al., 2005; Z'Graggen et al., 2000) However, increasing evidence indicates that the complex grasping movements learned in this test require the integrity of both hemispheres (Gonzalez et al., 2004). Moreover, the pellet reaching task additionally necessitates a training period prior to the lesion and only analyses the sensorimotor performance of a single (“trained”) forelimb. Since there are currently no additional sensitive tests available which allow the assessment of fine sensorimotor functions of both forelimbs it was not possible to evaluate these capabilities in the present study.

5.4. Role of the contralateral cortex for postlesional functional reorganization

Several animal and human studies on stroke recovery associate restoration of functions with reorganization in the brain (Dijkhuizen et al., 2001; 2003; Johansson, 2000; Kolb, 1995; Lee and van Donkelaar, 1995; Nudo and Friel, 1999; Weiller,

1992; 1993; 1998). Several functional MRI studies in patients with hemiparetic stroke clearly demonstrated bilateral activation patterns during movement of the affected hand, involving contralesional premotor or motor cortical areas (Johansen-Berg et al, 2002; Seitz et al., 1998; Weiller et al., 1992). On the other side, many experimental and clinical studies clearly demonstrate that significant adaptive changes take place in the direct vicinity of the infarct (Butz et al., 2004; Chollet et al., 1991; Loubinoux et al., 2003; Nudo et al., 1996). Despite explicit demonstration of stroke-induced plastic changes in the brain, the contribution of the ipsilateral and contralateral hemispheres to functional recovery are still not completely understood.

This study provides further evidence that the contralesional cortex did not significantly contribute to the functional recovery of the impaired forelimb. Lesions to the contralateral cortex homotopic to the initial infarct did not significantly influence the functional improvement of the initially affected forelimb. This was a surprising finding since several experimental and clinical studies indicate that alterations contralateral to the damaged hemisphere facilitate sensorimotor recovery after brain lesions (Butefisch et al., 2005; Cramer, 1999; Fisher, 1992; Fries et al., 1993; Johansen-Berg et al., 2002; Kato et al., 2001). Further support for this hypothesis came from a recent study by Biernaskie and colleagues (2005) analyzing sensorimotor function after endothelin-1 induced middle cerebral artery occlusion in rats and single intracortical application of the anesthetic lidocaine into the sensorimotor contralesional cortex 3 – 4 weeks later. Using this experimental approach they observed a reinstatement of the initial forelimb deficit in the pellet reaching task, suggesting that the contralesional cortex is recruited for functional recovery after focal brain ischemia. These findings are in contrast to a study by Andersen et al. (1991) who analyzed the sensorimotor performance in animals with a second middle cerebral artery occlusion induced contralaterally 28 days after the first

one. Following the second infarct the animals showed a deficit in removing an adhesive tape for the contralesional forelimb only, while the initially impaired limb was not (re-)affected. Using sequential bilateral electrolytic lesions of the FL SMC and behavioral analysis of coordinated forelimb placing Barth and colleagues (1990) demonstrated no reinstatement of the initial deficit either. The results of the present study are in accordance with these previous reports (Andersen et al., 1991; Barth et al., 1990).

Several differences in the experimental design such as the behavioral tests as well as permanent versus functional blockade of the contralesional cortex might explain the controversial findings of Biernaskie et al. (2005). Furthermore, lesion size and location are crucial factors for the sensorimotor deficits of the corresponding limb but also for functional alterations in the contralesional hemisphere. Functional magnetic resonance imaging studies on chronic stroke patients clearly demonstrated a bilateral activation when subcortical brain regions were involved, while in patients with cortical lesions predominantly ipsilesional activation was observed (Feydy et al., 2002; Luft et al., 2004). These data allow the hypothesis that the mechanisms of reorganization are dependent on lesion location. Considerable methodological differences complicate the direct transfer of functional activation patterns to behavioral findings after brain lesions in animals. However, the animal data strongly support the importance of the lesion site for functional recovery. The endothelin-1 induced MCAO model used by Biernaskie et al. (2005) damaged the primary somatosensory cortex including the barrel fields and subcortical areas whereas a considerable part of the FL SMC located in the vicinity remained intact. The subcortical damage in this model causing bilateral functional alterations might contribute to the reinstatement of the previous sensorimotor deficit after contralesional lidocaine application. In the present study as well as in the study of Barth et al. (1990), ischemic injury was restricted to

the sensorimotor cortex leaving subcortical structures intact. One possibility is that the reduced function in pellet reaching by the forelimb ipsilateral to the first infarct after the second infarct was due in part to impaired capacity in the opposite limb to support body weight, which is essential for proper use of the reaching forelimb. Pellet reaching requires use of both limbs. The animals must aim the reaching forelimb precisely without visual guidance, a movement that depends heavily on motor function in the non-reaching forelimb (Metz et al., 2005; Whishaw et al., 2002). Moreover, an increasing evidence indicates that the complex grasping movements learned in this test require the integrity of both hemispheres (Gonzalez et al., 2004).

Functional magnetic resonance imaging studies further indicate that contralesional activation patterns are temporally limited (Cao et al., 1998; Cramer et al., 1997; Luft et al., 2005). Dijkhuizen and colleagues (2003) demonstrated a bihemispheric activation of the FL SMC following sensory stimulation of the impaired forelimb only 1 and 3 days after transient MCAO in rats. Two weeks after the infarct, when functional recovery in gross locomotor activity tests was completed, the stimulation response only occurred in the ipsilesional hemisphere. These findings indicate that the contralesional activation patterns do not significantly correlate with functional recovery. The transient activation of the contralesional cortex, which increased with the size of the infarcts, might reflect postischemic cortical hyperexcitability, which definitely involves the undamaged hemisphere but probably also contributes to dysfunction and diaschisis (Buchkremer-Ratzmann et al., 1996; Reinecke et al., 1999; von Monakow, 1914; Witte et al., 1999; 2000).

Several experimental and clinical studies suggest that reorganization of lost sensorimotor functions after cortical lesions predominantly occurs in the direct vicinity of the damaged cortex (for review see Calautti and Baron, 2003; Nudo and Friel, 1999). Ablation of perilesional areas in rats that showed functional recovery after a

primary forelimb motor cortex lesion reinstated the initial functional impairment, while the same lesion in controls did not affect motor forelimb function (Castro-Alamancos and Borrel, 1995). Improvement in impaired limb functions have been found using facilitating stimulation of the perilesional cortex in humans (Fregni et al., 2005, Hummel et al., 2005), monkeys (Plautz et al., 2003) and rats (Adkins-Muir and Jones, 2003). Nudo and colleagues further demonstrated that cortical representations shift toward adjacent areas after motor cortex lesions and that these processes are training dependent (Frost et al., 2003; Nudo et al., 1996; Xerri et al., 1998). Similar processes occur after lesions in the visual cortex (Zepeda et al., 2003). Transcranial magnetic stimulation studies in humans further support the finding that perilesional cortical areas are predominantly involved in functional reorganization after stroke (Liepert et al., 2000). The retrograde tracing of the contralesional cortex performed in this study 2 months after induction of the infarct in the FL SMC demonstrated that no new thalamocortical projections arose from the deafferented thalamus to the contralateral cortex. This finding further supports the behavioral data that the contralateral cortex was not involved in functional recovery after focal ischemia.

The sensorimotor tests used in the present investigation did not reveal significant discrepancies between animals with different time intervals between sequential lesions. Thus, when the second lesion immediately followed the first (i.e. in the DL0 group), the deficit in the second forelimb was smaller in all tests, but the time-course of recovery did not differ significantly between both impaired forelimbs and SL-animals. In the other DL groups, which received sequential lesions with an interval of 2, 7 or 10 days, the recovery in the firstly and secondly impaired forelimbs varied to some extent but was not significantly different compared to the SL-animals. However, the tests was not capable to detect fine sensorimotor deficits.

The present study indicates that following small ischemic cortical infarcts in the FL SMC the contralateral cortex homotopic to the lesion did not significantly influence sensorimotor recovery of the contralesional forelimb. Even when the intervals between the infarcts varied, no effect of the second infarct on functional recovery of the initially impaired forelimb was observed. These findings suggest that there is no critical period for the involvement of contralateral homotopic cortex in functional recovery during the first ten days after the initial infarct. Together with the literature these findings might support the hypothesis that ipsilesional cortical reorganization predominantly facilitates functional recovery after ischemic cortical infarcts, and that the contralesional cortex may contribute to motor compensation in the better-functioning forelimb. However, it is also conceivable that the functional compensation after small cortical lesions may rely upon ipsilateral processes, whereas that of larger lesions might require plastic changes on the contralateral side. Additional studies are needed to elucidate these probably different reorganization patterns.

5.5. Loss of global brain volume following sequential ischemic infarcts

Interestingly, the evaluation of brain volume in the DL-animals detected an additional reduction of global brain volume compared to the animals from the SL group. Observed in this study loss in global brain volume in animals with sequential bilateral lesions could be explained in part by the processes of scar formation that occur after focal ischemic lesions. After ischemia, an irreversible cell death was observed, followed by the digestion of necrotic cells in the injured area and subsequent substitution of these cells with fibroblasts and glial elements. These processes induce a slight positional shift in the surrounding tissue and thereby alter the morphology of the lesioned hemisphere. However, this study demonstrated a loss of

volume in the remaining tissue in animals with sequential infarcts. This approach excluded the possibility that the observed decrease in global brain volume was caused by shifting of the lesion surround, which might be undetectable by the volumetric method.

The loss of global brain volume in DL-animals is probably associated with an increased thalamic degeneration detected by Fluoro-Jade marker in the DL2-animals. A loss of brain volume in the remaining, not directly lesioned, brain tissue was also described in the study by Kozlowski and colleagues (1996) demonstrating a reduction of volume in the ipsilateral forelimb sensorimotor cortex (FL SMC), posterior striatum and thalamus one month after unilateral electrolytic lesions. Chu and Jones (2000) reported a significant decrease in the cortical volume of the hindlimb sensorimotor area ipsilateral to electrolytic FL SMC lesions associated with a loss of neurons in the lesion surround. In the present study the loss of brain volume in the SL-animals was not significant. Only animals with sequential lesions showed a loss in global volume. This discrepancy might be explained by specific differences in the lesion models; specifically, the lesions in this study were comparably small and circumscribed.

5.6. Possible mechanisms

The consequences of focal cerebral ischemia evolve in time and space and are not limited to the lesion itself. They can also be observed in perilesional (penumbra) and widespread ipsi- and sometimes contralateral remote areas. These nonischemic changes in remote, indirectly affected areas can be caused by several factors such as brain edema, spreading depression, transsynaptic degeneration, reactive plasticity and systemic effects (Witte et al., 2000). Some of these mechanisms are

disadvantageous, whereas others facilitate plastic processes. Following focal ischemia, cortical excitability and inhibition are changed in widespread ipsi- and contralateral regions (Buchkraemer-Ratzmann et al., 1996; Qu et al., 1998; Que et al., 1999; Redecker et al., 2002; Reinecke et al., 1999). A considerable body of evidence shows that glutamate excitotoxicity contributes to neuronal damage at the primary lesion site as well as provides remote neuronal degeneration (Block et al., 2005; Dirnagl, 1999; Mergenthaler et al., 2004). Application of a glutamate receptor antagonist was demonstrated to reduce the secondary damage of substantia nigra after an excitotoxic lesion in the striatum (Block et al., 2004; DeGiorgio et al., 1999). Furthermore, there is increasing evidence that post-ischemic inflammation contributes to the brain injury both in the primary lesion site and remote regions (Feuerstein, 1998; Block et al., 2005). Several studies reported a widespread up-regulation of inflammatory mediators such as COX 1, 2, IL-1β, TNF-α after the focal ischemia in the activated microglia or reactive astrocytes (Davies et al., 1999; Mattson et al., 2001; Schwab et al., 2000; Yu and Lau, 2000). Interestingly, the delayed bilateral increase in IL-1β expression in the hippocampal neurons following MCAO could be prevented by the glutamate receptor antagonist MK-801. That assumes that glutamatergic overexcitation triggers remote inflammation after MCAO (Nolden-Koch et al., 2000). It is conceivable that induction of repetitive brain ischemia could cause an excessive overexcitation triggering additional neuronal degeneration and loss of brain volume as observed in this study.

The present study demonstrated that in the animals with 7 days between infarcts (DL7), the volume of the second lesion was smaller compared to that of the first. In this group, the loss of global volume was less prominent than in other groups with bilateral infarcts. This finding also corresponded to the significantly decreased neuronal degeneration in the DL6 group revealed by Fluoro-Jade staining. It

suggests that protective mechanisms might reduce the loss of brain volume associated with remote degeneration within a limited time-window. Several studies indicated that primary ischemia activates molecular cascades, which protect the surrounding and remote brain areas from subsequent ischemic injury (Dirnagl, 2003). The phenomenon of ischemic tolerance has been observed in the specific time-window after primary ischemia and varies depending on the duration, the interval, and models of ischemia (Kato et al., 1989; 1990). The mechanisms that are prominent during the excitotoxic phase of ischemic cell death are signals as well as targets of ischemic preconditioning. In many models, ischemic tolerance requires NMDA-receptor activation (Bond et al., 1999; Jiang et al., 2003). Spreading depression, which is one of the deleterious factors leading to cellular death in the penumbra and remote brain structures, was shown to induce ischemic tolerance in focal ischemia (Matsushima et al., 1996). Cortical spreading depression was also demonstrated to increase brain-derived neurotrophic factor (BDNF) levels that were consistent with induction of ischemic tolerance (Kawahara et al., 1997). Ischemic preconditioning could be also mediated by the up-regulation of different factors such as superoxide dismutases, stress proteins, and growth factors (e.g. FGF-2), but the underlying mechanisms are still not fully understood. In the present study, only animals that received the second infarct with an interval of about a week after the initial one showed a significant decrease in volume of the second lesion compared to the first. In the DL7-animals the loss of global brain volume was also less prominent compared with that of the other DL groups and this finding correlated with decreased neuronal degeneration in the thalamus of the DL6-animals, suggesting an ischemic preconditioning.

5.7. Correlation between cognitive performance and morphological finding

Analysis of cognitive function indicated that the loss of global volume in animals with sequential bilateral ischemic lesions was accompanied by a significantly impaired performance in the Morris water maze. These findings are in accordance with previously reported studies showing that bilateral photothrombotic infarcts in the frontal or parietal cortical areas induced spatial learning deficits that can be observed during the first week after ischemia (Kharlamov et al., 1994; Rogers et al., 1997). In the animals with single infarcts, no significant differences were observed in the water maze test compared to controls. The precise role of different cortical areas in the performance of spatial tasks is still a matter of some debate. There is evidence suggesting that frontal and parietal cortical areas are involved in spatial navigation (Kolb et al., 1994), but the influence of the FL SMC lesion on cognitive functions remains to be elucidated. The impairment in spatial learning was not due to slower swim speeds. Moreover, a test of forelimb use during exploration indicated that recovery of function occurred 2 – 3 weeks after the second infarct; that is, scores on forelimb activity in a glass cylinder and foot-fault test did not differ from the baseline score taken before the animals underwent their first operations (Shanina et al., 2006).

The additional loss in brain volume in DL2-animals associated with increased degeneration of neurons in the thalamus that have been observed in this study could explain the cognitive impairment of these animals in the water maze. In clinical studies, multiple ischemic infarcts are thought to be one of the factors triggering vascular dementia associated with cognitive deficits in the elderly. Poststroke dementia occurs in up to one third of patients with clinically eloquent ischemic strokes after age 65 years (Pohjasvaara et al., 1997). It is conceivable that additional

neuronal loss combined with cognitive impairment in the animals with sequential bilateral lesions could resemble to some extent a poststroke dementia in patients and the present model with sequential bilateral ischemic lesions might be useful for the investigation of long-lasting, pathophysiological mechanisms of postischemic brain degeneration or alternatively ischemic preconditioning.

6. Conclusions

1. Photothrombotic infarcts in the forelimb sensorimotor cortex induced delayed neuronal death in the remote subcortical structures such as the dorsolateral striatum and somatosensory thalamic nuclei accompanied by massive activation of microglia and astrocytes. The neuronal degeneration in the thalamus increased until day 8 and then declined, whereas activation of microglia as an important component of inflammation, started later and increased continuously until day 28. The extent of remote neuronal degeneration in the DL-animals was dependent on the time intervals between sequential infarcts. However, the inflammatory response did not differ between SL and DL groups.
2. Following small ischemic cortical infarcts in the FL SMC, the contralateral cortex homotopic to the lesion did not significantly influence sensorimotor recovery of the initially impaired forelimb. This finding supports the hypothesis that ipsilesional cortical reorganization predominantly facilitates functional recovery after ischemic cortical infarcts.
3. Induction of the second infarct at different intervals (0, 2, 7, or 10 days) after the first injury did not influence the time course and extent of functional recovery in the DL-animals indicating that there was no critical time window in which the contralateral homotopic cortex is involved in restoration of sensorimotor functions.
4. Animals with different time intervals between sequential bilateral cortical lesions demonstrated reduced infarct size compared to the SL group. There was no significant difference in volume between the first and second

infarcts in DL groups. Only in animals with interval of 7 days (DL7) the second infarct was significantly smaller, providing further evidence for ischemic tolerance. However, the global brain volume of DL-animals was reduced compared to SL-animals.

5. Behavioral studies in the Morris water maze demonstrated that the loss of brain volume in DL-animals was associated with a slight but significant impairment in spatial learning.

7. Reference List

Adkins-Muir DL and Jones TA (2003) Cortical electrical stimulation combined with rehabilitative training: enhanced functional recovery and dendritic plasticity following focal cortical ischemia in rats. *Neurol.Res.* **25:** 780-788.

Allen GV, Gerami D, Esser MJ (2000) Conditioning effects of repetitive mild neurotrauma on motor function in an animal model of focal brain injury. *Neuroscience* **99:** 93-105.

Andersen CS, Andersen AB, Finger S (1991) Neurological correlates of unilateral and bilateral "strokes" of the middle cerebral artery in the rat. *Physiol Behav.* **50:** 263-269.

Barth TM and Stanfield BB (1990) The recovery of forelimb-placing behavior in rats with neonatal unilateral cortical damage involves the remaining hemisphere. *J.Neurosci.* **10:** 3449-3459.

Barth TM, Jones TA, Schallert T (1990) Functional subdivisions of the rat somatic sensorimotor cortex. *Behav.Brain Res.* **39:** 73-95.

Biernaskie J and Corbett D (2001) Enriched rehabilitative training promotes improved forelimb motor function and enhanced dendritic growth after focal ischemic injury. *J.Neurosci.* **21:** 5272-5280.

Biernaskie J, Szymanska A, Windle V, Corbett D (2005) Bihemispheric contribution to functional motor recovery of the affected forelimb following focal ischemic brain injury in rats. *Eur.J.Neurosci.* **21:** 989-999

Block F, Dihne M, Loos M (2005) Inflammation in areas of remote changes following focal brain lesion. *Prog.Neurobiol.* **75:** 342-365.

Block F, Loos M, Frohn C, Schwarz M (2004) Association between inflammation and nigral neuronal damage following striatal excitotoxic lesion. *Brain Res.* **998:** 29-35.

Bogdan C, Paik J, Vodovotz Y, Nathan C (1992) Contrasting mechanisms for suppression of macrophages cytokine release by transforming growth factor-beta and interleukin-10. *J.Biol.Chem.* **267:** 23301-23308.

Bond A, Lodge D, Hicks CA, Ward MA, O'Neill MJ (1999) NMDA receptor antagonism, but not AMPA receptor antagonism attenuates induced ischaemic tolerance in the gerbil hippocampus. *Eur.J.Pharmacol.* **380:** 91-99.

Brown DL, Lisabeth LD, Royhoudhury C, Ye Y, Morgenstern LB (2005) Recurrent stroke risk is higher than cardiac event risk after initial stroke/transient ischemic attack. *Stroke* **36:** 1285-1287.

Buchkremer-Ratzmann I, August M, Hagemann G, Witte OW (1996) Electrophysiological transcortical diaschisis after cortical photothrombosis in rat brain. *Stroke* **27:** 1105-1109.

Butefisch CM, Kleiser R, Korber B, Muller K, Wittsack HJ, Homberg V, Seitz RJ (2005) Recruitment of contralesional motor cortex in stroke patients with recovery of hand function. *Neurology* **64:** 1067-1069.

Butz M, Gross J, Timmermann L, Moll M, Freund HJ, Witte OW, Schnitzler A (2004) Perilesional pathological oscillatory activity in the magnetoencephalogram of patients with cortical brain lesions. *Neurosci.Lett.* **355:** 93-96.

Calautti C and Baron JC (2003) Functional neuroimaging studies of motor recovery after stroke in adults: a review. *Stroke* **34:** 1553-1566.

Cao Y, D'Olhaberriague L, Vikingstad EM, Levine SR, Welch KM (1998) Pilot study of functional MRI to assess cerebral activation of motor function after poststroke hemiparesis. *Stroke* **29:** 112-122.

Carmichael ST and Chesselet MF (2002) Synchronous neuronal activity is a signal for axonal sprouting after cortical lesions in the adult. *J.Neurosci.* **22:** 6062-6070.

Castro-Alamancos MA and Borrel J (1995) Functional recovery of forelimb response capacity after forelimb primary motor cortex damage in the rat is due to the reorganization of adjacent areas of cortex. *Neuroscience* **68:** 793-805.

Chollet F, DiPiero V, Wise RJ, Brooks DJ, Dolan RJ, Frackowiak RS (1991) The functional anatomy of motor recovery after stroke in humans: a study with positron emission tomography. *Ann.Neurol.* **29:** 63-71.

Chollet F and Weiller C (1994) Imaging recovery of function following brain injury. *Curr.Opin.Neurobiol.***4:** 226-230.

Chu CJ and Jones TA (2000) Experience-dependent structural plasticity in cortex heterotopic to focal sensorimotor cortical damage. *Exp.Neurol.* **166:** 403-414.

Cramer SC (1999) Stroke recovery. Lessons from functional MR imaging and other methods of human brain mapping. *Phys.Med.Rehabil.Clin.N.Am.* 10: 875-86.

Cramer SC, Nelles G, Benson RR, Kaplan JD, Parker RA, Kwong KK, Kennedy DN, Finklestein SP, Rosen BR (1997) A functional MRI study of subjects recovered from hemiparetic stroke. *Stroke* **28:** 2518-2527.

Davies CA, Loddick SA, Toulmond S, Stroemer RP, Hunt J, Rothwell NJ (1999) The progression and topographic distribution of interleukin-1beta expression after permanent middle cerebral artery occlusion in the rat. *J.Cereb.Blood Flow Metab.* **19:** 87-98.

Day LB, Weisand M, Sutherland RJ, Schallert T (1999)The hippocampus is not necessary for a place response but may be necessary for pliancy. *Behav.Neurosci.* **113:** 914-924.

DeGiorgio LA, DeGiorgio N, Volpe BT (1999) Dizocilpine maleate, MK-801, but not 2,3-dihydroxy-6-nitro-7-sulfamoyl-benzo(f)quinoxaline, NBQX, prevents transneuronal degeneration of nigral neurons after neurotoxic striatal-pallidal lesion. *Neuroscience* **90:** 79-85.

Dihne M, Grommes C, Lutzenburg M, Witte OW, Block F (2002) Different mechanisms of secondary neuronal damage in thalamic nuclei after focal cerebral ischemia in rats. *Stroke* **33:** 3006-3011.

Dijkhuizen RM, Ren J, Mandeville JB, Wu O, Ozdag FM, Moskowitz MA, Rosen BR, Finklestein SP (2001) Functional magnetic resonance imaging of reorganization in rat brain after stroke. *Proc.Natl.Acad.Sci.U.S.A.* **98:** 12766-12771.

Dijkhuizen RM, Singhal AB, Mandeville JB, Wu O, Halpern EF, Finklestein SP, Rosen BR, Lo EH (2003) Correlation between brain reorganization, ischemic damage, and neurologic status after transient focal cerebral ischemia in rats: a functional magnetic resonance imaging study. *J.Neurosci.* **23:** 510-517.

Dirnagl U, Iadecola C, Moskowitz MA (1999) Pathobiology of ischaemic stroke: an integrated view. *Trends Neurosci.* **22:** 391-397.

Dirnagl U and Priller J (2005) Focal cerebral ischemia: the multifaceted role of glial cells. In: Kettenmann H & Ransom BR Neuroglia *Oxford University Press Inc:* 511-520.

Dirnagl U, Simon RP, Hallenbeck JM (2003) Ischemic tolerance and endogenous neuroprotection. *Trends Neurosci.* **26:** 248-254.

Eisch AJ, Schmued LC, Marshall JF (1998) Characterizing cortical neuron injury with Fluoro-Jade labeling after a neurotoxic regimen of methamphetamine. *Synapse* **30:** 329-333.

Erkinjuntti T, Bowler JV, DeCarli CS, Fazekas F, Inzitari D, O'Brien JT, Pantoni L, Rockwood K, Scheltens P, Wahlund LO, Desmond DW (1999) Imaging of static brain lesions in vascular dementia: implications for clinical trials. *Alzheimer Dis.Assoc.Disord.* **13:** 81-90.

Eysel UT and Schweigart G (1999) Increased receptive field size in the surround of chronic lesions in the adult cat visual cortex. *Cereb.Cortex* 9**:** 101-109.

Feuerstein GZ, Wang X, Barone FC (1998) The role of cytokines in the neuropathology of stroke and neurotrauma. *Neuroimmunomodulation* **5:** 143-159.

Feydy A, Carlier R, Roby-Brami A, Bussel B, Cazalis F, Pierot L, Burnod Y, Maier MA (2002) Longitudinal study of motor recovery after stroke: recruitment and focusing of brain activation. *Stroke* **33:** 1610-1617.

Fisher CM (1992) Concerning the mechanism of recovery in stroke hemiplegia. *Can.J.Neurol.Sci.* **19:** 57-63.

Fregni F, Boggio PS, Mansur CG, Wagner T, Ferreira MJ, Lima MC, Rigonatti SP, Marcolin MA, Freedman SD, Nitsche MA, Pascual-Leone A (2005) Transcranial

direct current stimulation of the unaffected hemisphere in stroke patients. *Neuroreport* **16:** 1551-1555.

Freyaldenhoven TE, Ali SF, Schmued LC (1997) Systemic administration of MPTP induces thalamic neuronal degeneration in mice. *Brain Res.* **759:** 9-17.

Fries W, Danek A, Scheidtmann K, Hamburger C (1993) Motor recovery following capsular stroke. Role of descending pathways from multiple motor areas. *Brain* **116:** 369-382.

Frost SB, Barbay S, Friel KM, Plautz EJ, Nudo RJ (2003) Reorganization of remote cortical regions after ischemic brain injury: a potential substrate for stroke recovery. *J.Neurophysiol.* **89:** 3205-3214.

Gharbawie OA, Gonzalez CL, Whishaw IQ (2005) Skilled reaching impairments from the lateral frontal cortex component of middle cerebral artery stroke: a qualitative and quantitative comparison to focal motor cortex lesions in rats. *Behav Brain Res* 156**:** 125-137.

Gonzalez CL, Gharbawie OA, Williams PT, Kleim JA, Kolb B, Whishaw IQ (2004) Evidence for bilateral control of skilled movements: ipsilateral skilled forelimb reaching deficits and functional recovery in rats follow motor cortex and lateral frontal cortex lesions *Eur J Neurosci* 20**:** 3442-3452.

Hagemann G, Redecker C, Neumann-Haefelin T, Freund HJ, Witte OW (1998) Increased long-term potentiation in the surround of experimentally induced focal cortical infarction. *Ann.Neurol.* **44:** 255-258.

Hsu JE and Jones TA (2005) Time-sensitive enhancement of motor learning with the less-affected forelimb after unilateral sensorimotor cortex lesions in rats. *Eur.J.Neurosci.* **22:** 2069-2080.

Hummel F, Celnik P, Giraux P, Floel A, Wu WH, Gerloff C, Cohen LG (2005) Effects of non-invasive cortical stimulation on skilled motor function in chronic stroke. *Brain* **128:** 490-499.

Iizuka H, Sakatani K, Young W (1990) Neural damage in the rat thalamus after cortical infarcts. *Stroke* **21:** 790-794.

Jenkins WM and Merzenich MM (1987) Reorganization of neocortical representations after brain injury: a neurophysiological model of the bases of recovery from stroke. *Prog. Brain Res.* **71:** 249-266.

Jiang X, Zhu D, Okagaki P, Lipsky R, Wu X, Banaudha K, Mearow K, Strauss KI, Marini AM (2003) N-methyl-D-aspartate and TrkB receptor activation in cerebellar granule cells: an in vitro model of preconditioning to stimulate intrinsic survival pathways in neurons. *Ann.N.Y.Acad.Sci.* **993:**134-145.

Jones TA and Schallert T (1992) Overgrowth and pruning of dendrites in adult rats recovering from neocortical damage. *Brain Res.* **581:** 156-160.

Jones TA and Schallert T (1994) Use-dependent growth of pyramidal neurons after neocortical damage. *J. Neurosci.* **14:** 2140-2152.

Johansen-Berg H, Rushworth MF, Bogdanovic MD, Kischka U, Wimalaratna S, Matthews PM (2002) The role of ipsilateral premotor cortex in hand movement after stroke. *Proc.Natl.Acad.Sci.U.S.A.* **99:** 14518-14523.

Johansson BB (2000) Brain plasticity and stroke rehabilitation. The Willis lecture. *Stroke* **31:** 223-230.

Kato H, Izumiyama M, Shiga Y, Saito N, Koizumi H, Takahashi A, Itoyama Y (2001) Hand motor cortical area reorganization following cerebral infarction evaluated with functional MRI, near infrared spectroscopic imaging, and transcranial magnetic stimulation. *No To Shinkei* **53:** 869-874.

Kato H and Kogure K (1990) Neuronal damage following non-lethal but repeated cerebral ischemia in the gerbil. *Acta Neuropathol.(Berl)* 79: 494-500.

Kato H, Kogure K, Nakano S (1989) Neuronal damage following repeated brief ischemia in the gerbil. *Brain Res.* **479:** 366-370.

Kawahara N, Croll SD, Wiegand SJ, Klatzo I (1997) Cortical spreading depression induces long-term alterations of BDNF levels in cortex and hippocampus distinct from lesion effects: implications for ischemic tolerance. *Neurosci.Res.* **29:** 37-47.

Kharlamov A, Zivkovic I, Polo A, Armstrong DM, Costa E, Guidotti A (1994) LIGA20, a lyso derivative of ganglioside GM1, given orally after cortical thrombosis reduces

infarct size and associated cognition deficit. *Proc.Natl.Acad.Sci.U.S.A.* **91:** 6303-6307.

Kirino T (2002) Ischemic tolerance. *J.Cereb.Blood Flow Metab.* **22:** 1283-1296.

Kitagawa K, Matsumoto M, Tagaya M, Hata R, Ueda H, Niinobe M, Handa N, Fukunaga R, Kimura K, Mikoshiba K (1990) 'Ischemic tolerance' phenomenon found in the brain. *Brain Res.* 528: 21-24.

Kolb B (1995) Brain plasticity and behavior. *Hillsdale, NJ:* Lawrence Erlboum.

Kolb B, Buhrmann K, McDonald R, Sutherland RJ (1994) Dissociation of the medial prefrontal, posterior parietal, and posterior temporal cortex for spatial navigation and recognition memory in the rat. *Cereb.Cortex* **4:** 664-680.

Kozlowski DA, James DC, Schallert T (1996) Use-dependent exaggeration of neuronal injury after unilateral sensorimotor cortex lesions. *J.Neurosci.* **1:** 4776-4786.

Kundrotiene J, Wagner A, Liljequist S (2004) Fluoro-Jade and TUNEL staining as useful tools to identify ischemic brain damage following moderate extradural compression of sensorimotor cortex. *Acta Neurobiol.Exp.(Wars.).* **6:** 153-162.

Lee RG and van Donkelaar P (1995) Mechanisms underlying functional recovery following stroke. *Can.J.Neurol.Sci.* **22:** 257-263.

Liepert J, Bauder H, Wolfgang HR, Miltner WH, Taub E, Weiller C (2000) Treatment-induced cortical reorganization after stroke in humans. *Stroke* **31:** 1210-1216.

Linnik MD, Zahos P, Geschwind MD, Federoff HJ (1995) Expression of bcl-2 from a defective herpes simplex virus-1 vector limits neuronal death in focal cerebral ischemia. *Stroke* **26:** 1670-1674.

Loubinoux I, Carel C, Pariente J, Dechaumont S, Albucher JF, Marque P, Manelfe C, Chollet F (2003) Correlation between cerebral reorganization and motor recovery after subcortical infarcts. *Neuroimage* **20:** 2166-2180.

Luft AR, Forrester L, Macko RF, McCombe-Waller S, Whitall J, Villagra F, Hanley DF (2005) Brain activation of lower extremity movement in chronically impaired stroke survivors. *Neuroimage* **26:** 184-194.

Luft AR, Waller S, Forrester L, Smith GV, Whitall J, Macko RF, Schulz JB, Hanley DF (2004) Lesion location alters brain activation in chronically impaired stroke survivors. *Neuroimage* **21:** 924-935.

Matsushima K, Hogan MJ, Hakim AM (1996) Cortical spreading depression protects against subsequent focal cerebral ischemia in rats. *J.Cereb.Blood Flow Metab* **16:** 221-226.

Mattson MP, Duan W, Pedersen WA, Culmsee C (2001) Neurodegenerative disorders and ischemic brain diseases. *Apoptosis* **6:** 69-81.

Mergenthaler P, Dirnagl U, Meisel A (2004) Pathophysiology of stroke: lessons from animal models. *Metab Brain Dis.* **19:** 151-167.

Metz GA, Antonow-Schlorke I, Witte OW (2005) Motor improvements after focal cortical ischemia in adult rats are mediated by compensatory mechanisms. *Behav.Brain Res.* **162:** 71-82.

Moncayo J, de Freitas GR, Bogousslavsky J, Altieri M, van Melle G (2000) Do transient ischemic attacks have a neuroprotective effect? *Neurology* **54:** 2089-2094.

Morris R (1981) Spatial localization does not require the presence of local cues. *Learning motivation* **12:**239-260.

Nagasawa H and Kogure K (1990) Exo-focal postischemic neuronal death in the rat brain. *Brain Res.* **524:** 196-202.

Napieralski JA, Banks RJ, Chesselet MF (1998) Motor and somatosensory deficits following uni- and bilateral lesions of the cortex induced by aspiration or thermocoagulation in the adult rat. *Exp.Neurol.* 154**:** 80-88.

Neumann-Haefelin T, Hagemann G, Witte OW (1995) Cellular correlates of neuronal hyperexcitability in the vicinity of photochemically induced cortical infarcts in rats in vitro. *Neurosci.Lett.* **193:** 101-104.

Nolden-Koch M, Breuer E, Block F (2000) Expression of the IL-1β in the hippocampus following focal ischemia. *J Neurol.* **247**: 129.

Nudo RJ and Friel KM (1999) Cortical plasticity after stroke: implications for rehabilitation. *Rev.Neurol.(Paris)* **155:** 713-717.

Nudo RJ, Wise BM, SiFuentes F, Milliken GW (1996) Neural substrates for the effects of rehabilitative training on motor recovery after ischemic infarct. *Science* **272:** 1791-1794.

Paxinos G and Watson C (1986) The rat brain in stereotaxic coordinates. *Academic Press, Inc*: London.

Pennypacker KR, Eidizadeh S, Kassed CA, O'Callaghan JP, Sanberg PR, Willing AE (2000) Expression of fos-related antigen-2 in rat hippocampus after middle cerebral arterial occlusion. *Neurosci.Lett.* **289:** 1-4.

Plautz EJ, Barbay S, Frost SB, Friel KM, Dancause N, Zoubina EV, Stowe AM, Quaney BM, Nudo RJ (2003) Post-infarct cortical plasticity and behavioral recovery using concurrent cortical stimulation and rehabilitative training: a feasibility study in primates. *Neurol.Res.* **25:** 801-810.

Pohjasvaara T, Erkinjuntti T, Vataja R, Kaste M (1997) Dementia three months after stroke. Baseline frequency and effect of different definitions of dementia in the Helsinki Stroke Aging Memory Study (SAM) cohort. *Stroke* **28:** 785-792.

Qu M, Mittmann T, Luhmann HJ, Schleicher A, Zilles K (1998) Long-term changes of ionotropic glutamate and GABA receptors after unilateral permanent focal cerebral ischemia in the mouse brain. *Neuroscience* **85:** 29-43.

Que M, Schiene K, Witte OW, Zilles K (1999) Widespread up-regulation of N-methyl-D-aspartate receptors after focal photothrombotic lesion in rat brain. *Neurosci.Lett.* **27:** 77-80.

Redecker C, Wang W, Fritschy JM, Witte OW (2002) Widespread and long-lasting alterations in GABA(A)-receptor subtypes after focal cortical infarcts in rats: mediation by NMDA-dependent processes. *J.Cereb.Blood Flow Metab.* **22:** 1463-1475.

Reinecke S, Dinse HR, Reinke H, Witte OW (2003) Induction of bilateral plasticity in sensory cortical maps by small unilateral cortical infarcts in rats. *Eur J Neurosci* **17:** 623-627.

Reinecke S, Lutzenburg M, Hagemann G, Bruehl C, Neumann-Haefelin T, Witte OW (1999) Electrophysiological transcortical diaschisis after middle cerebral artery occlusion (MCAO) in rats. *Neurosci.Lett.* **261:** 85-88.

Rogers DC and Hunter AJ (1997) Photothrombotic lesions of the rat cortex impair acquisition of the water maze. *Pharmacol.Biochem.Behav.* **56:** 747-754.

Ross DT and Ebner FF (1990) Thalamic retrograde degeneration following cortical injury: an excitotoxic process? *Neuroscience* **35:** 525-550.

Rupalla K, Allegrini PR, Sauer D, Wiessner C (1998) Time course of microglia activation and apoptosis in various brain regions after permanent focal cerebral ischemia in mice. *Acta Neuropathol.(Berl).* **96:** 172-178.

Salerno JA, Murphy DG, Horwitz B, DeCarli C, Haxby JV, Rapoport SI, Schapiro MB (1992) Brain atrophy in hypertension. A volumetric magnetic resonance imaging study. *Hypertension* **20:** 340-348.

Schallert T, Leasure JL, Kolb B (2000a) Experience-associated structural events, subependymal cellular proliferative activity, and functional recovery after injury to the central nervous system. *J.Cereb.Blood Flow Metab.* **20:** 1513-1528.

Schallert T, Fleming SM, Leasure JL, Tillerson JL, Bland ST (2000b) CNS plasticity and assessment of forelimb sensorimotor outcome in unilateral rat models of stroke, cortical ablation, parkinsonism and spinal cord injury. *Neuropharmacology* 39**:** 777-787.

Schiene K, Staiger JF, Bruehl C, Witte OW (1999) Enlargement of cortical vibrissa representation in the surround of an ischemic cortical lesion. *J.Neurol.Sci.* **162:** 6-13.

Schmued LC, Albertson C, Slikker W, Jr. (1997) Fluoro-Jade: a novel fluorochrome for the sensitive and reliable histochemical localization of neuronal degeneration. *Brain Res.* **751:** 37-46.

Schroeter M, Jander S, Witte OW, Stoll G (1999) Heterogeneity of the microglial response in photochemically induced focal ischemia of the rat cerebral cortex. *Neuroscience* **89:** 1367-1377.

Schwab JM, Nguyen TD, Postler E, Meyermann R, Schluesener HJ (2000) Selective accumulation of cyclooxygenase-1-expressing microglial cells/macrophages in lesions of human focal cerebral ischemia. *Acta Neuropathol.(Berl)* **99:** 609-614.

Seitz RJ, Hoflich P, Binkofski F, Tellmann L, Herzog H, Freund HJ (1998) Role of the premotor cortex in recovery from middle cerebral artery infarction. *Arch.Neurol.* **55:** 1081-1088.

Shanina EV, Redecker C, Reinecke S, Schallert T, Witte OW (2005) Long-term effects of sequential cortical infarcts on scar size, brain volume and cognitive function. *Behav. Brain Res.* **158:** 69-77.

Shanina EV, Schallert T, Witte OW, Redecker C (2006) Behavioral recovery from unilateral photothrombotic infarcts of the forelimb sensorimotor cortex in rats: Role of the contralateral cortex. *Neuroscience*

Sharp FR and Gonzalez MF (1986) Adult rat motor cortex connections to thalamus following neonatal and juvenile frontal cortical lesions: WGA-HRP and amino acid studies. *Brain Res.* **395:** 169-187.

Sorensen JC, Dalmau I, Zimmer J, Finsen B (1996) Microglial reactions to retrograde degeneration of tracer-identified thalamic neurons after frontal sensorimotor cortex lesions in adult rats. *Exp.Brain Res.* **112:** 203-212.

Sulejczak D, Czarkowska-Bauch J, Macias M, Skup M (2004) Bcl-2 and Bax proteins are increased in neocortical but not in thalamic apoptosis following devascularizing lesion of the cerebral cortex in the rat: an immunohistochemical study. *Brain Res.* **1006:** 133-149.

Vela JM, Yanez A, Gonzalez B, Castellano B (2002) Time course of proliferation and elimination of microglia/macrophages in different neurodegenerative conditions. *J.Neurotrauma* **19:** 1503-1520.

Vickrey BG, Rector TS, Wickstrom SL, Guzy PM, Sloss EM, Gorelick PB, Garber S., McCaffrey DF, Dake MD, Levin RA (2002) Occurrence fo secondary ischemic events among persons with atherosclerotic vascular disease. *Stroke* **33:** 901-906.

von Monakow C (1914) Die Lokalisation im Grosshirn un der Abbau der Funktion durch kortikale Herde. *Bergmann JF*: Wiesbaden 26-34.

Watson BD, Dietrich WD, Busto R, Wachtel MS, Ginsberg MD (1985) Induction of reproducible brain infarction by photochemically initiated thrombosis. *Ann Neurol* **17:** 497-504.

Weih M, Kallenberg K, Bergk A, Dirnagl U, Harms L, Wernecke KD, Einhaupl KM (1999) Attenuated stroke severity after prodromal TIA: a role for ischemic tolerance in the brain? *Stroke* **30:** 1851-1854.

Weiller C (1998) Imaging recovery from stroke. *Exp.Brain Res.* **123:** 13-17.

Weiller C, Chollet F, Friston KJ, Wise RJ, Frackowiak RS (1992) Functional reorganization of the brain in recovery from striatocapsular infarction in man. *Ann.Neurol.* **31:** 463-472.

Weiller C, Ramsay SC, Wise RJ, Friston KJ, Frackowiak RS (1993) Individual patterns of functional reorganization in the human cerebral cortex after capsular infarction. *Ann.Neurol.* **33:** 181-189.

Whishaw IQ, Pellis SM, Gorny B, Kolb B, Tetzlaff W (1993) Proximal and distal impairments in rat forelimb use in reaching follow unilateral pyramidal tract lesions. *Behav Brain Res* 56**:** 59-76.

Whishaw IQ, Suchowersky O, Davis L, Sarna J, Metz GA, Pellis SM (2002) Impairment of pronation, supination, and body co-ordination in reach-to-grasp tasks in human Parkinson's disease (PD) reveals homology to deficits in animal models. *Behav.Brain Res.* **133:** 165-176.

Wiessner C, Allegrini PR, Rupalla K, Sauer D, Oltersdorf T, McGregor AL, Bischoff S, Bottiger BW, van der Putten H (1999) Neuron-specific transgene expression of Bcl-

XL but not Bcl-2 genes reduced lesion size after permanent middle cerebral artery occlusion in mice. *Neurosc.Lett.* **268:** 119-122.

Witte OW, Bidmon HJ, Schiene K, Redecker C, Hagemann G (2000) Functional differentiation of multiple perilesional zones after focal cerebral ischemia. *J.Cereb.Blood Flow Metab.* **20:** 1149-1165.

Witte OW and Freund HJ (1999) Neuronal dysfunction, epilepsy, and postlesional brain plasticity. *Adv.Neurol.* **81:** 25-36.

Xerri C, Merzenich MM, Peterson BE, Jenkins W (1998) Plasticity of primary somatosensory cortex paralleling sensorimotor skill recovery from stroke in adult monkeys. *J.Neurophysiol.* **79:** 2119-2148.

Yoon M and Ross DT (1989) Reaction of protoplasmic astrocytes in the adult rat thalamus to ablation of the somatosensory cortex. *Anat.Rec.* **223:** 125A.

Young AB, Bromberg MB, Penney JB (1981) Decreased glutamate uptake in subcortical areas deafferented by sensorimotor cortical ablation in the cat. *J.Neurosc.* **1:** 241-249.

Yu AC and Lau LT (2000) Expression of interleukin-1 alpha, tumor necrosis factor alpha and interleukin-6 genes in astrocytes under ischemic injury. *Neurochem.Int.* **36:** 369-377.

Zepeda A, Sengpiel F, Guagnelli MA, Vaca L, Arias C (2004) Functional reorganization of visual cortex maps after ischemic lesions is accompanied by changes in expression of cytoskeletal proteins and NMDA and GABA(A) receptor subunits. *J.Neurosci.* **24:** 1812-1821.

Zepeda A, Vaca L, Arias C, Sengpiel F (2003) Reorganization of visual cortical maps after focal ischemic lesions. *J.Cereb.Blood Flow Metab.* **23:** 811-820.

Z'Graggen WJ, Fouad K, Raineteau O, Metz GA, Schwab ME, Kartje GL (2000) Compensatory sprouting and impulse rerouting after unilateral pyramidal tract lesion in neonatal rats. *J Neurosci* 20**:** 6561-6569.

Zilles K (1985) The Cortex of the Rat: A Stereotaxis Atlas. *Springer-Verlag*: Berlin.

Zuch CL, Nordstroem VK, Briedrick LA, Hoernig GR, Granholm AC, Bickford PC (2000) Time course of degenerative alterations in nigral dopaminergic neurons following a 6-hydroxydopamine lesion. *J.Comp Neurol.* **427:** 440-454.

8. Acknowledgements

Herrn Prof. Dr. med. O.W. Witte, Direktor der Neurologischen Klinik der Friedrich-Schiller-Universität Jena, danke ich für die Überlassung des Themas, für die exzellenten Arbeitsmöglichkeiten in seiner Klinik, für die Aufnahme und freundliche Hilfe bei der Integration in seinem Labor und die Betreuung meiner Arbeit.

Herrn PD Dr. med. C. Redecker, Oberarzt der Neurologischen Klinik der Friedrich-Schiller-Universität Jena, danke ich für die hervorragende Betreuung meiner Promotion. Seine wertvolle Ratschläge und kompetente Kritik haben mir sehr geholfen während meiner Arbeit im Labor und bei der Anfertigung dieser Doktorarbeit.

Herrn Prof. Dr. J. Bolz, Lehrstuhl für allgemeine Zoologie und Tierphysiologie an der Friedrich-Schiller-Universität Jena, danke ich für die Betreuung der Arbeit.

Besonders herzlich bedanken möchte ich mich bei meiner Kollegen aus meiner Arbeitsgruppe “Endogene neurale Stammzellen” Frau Dipl. Pharm. S. Grass, Herrn Dr. M. Kluska, Frau Dipl. med. F. Wurm, Herrn Dr. med. A. Kunze, Frau N. Manthei, Herrn M Sczuka, Frau N. Schlegel, Frau J. Oberland, die mich immer unterstützt haben und ein schönes Arbeitsklima geschaffen haben.

Allen Kollegen, Frau Dipl.-Biol. I. Antonow-Schlorke, Herrn Dipl.-Biol. S. Schmidt, Herrn Dr. C. Brühl, Frau S. Tausch, Herrn Dr. C. Schmeer, Herrn Dipl.-Biol. M. Knieling, Frau Dipl.-Biol. A. Urbach, Frau Dr. C. Frahm, Frau Dipl.-Biol. C. Haupt, Frau Dipl.-Biol. S. Wohl, Herrn Dipl.-Biol. L. Liebmann, Frau C. Sommer, Frau I. Ingrisch, Herrn PD G. Hagemann, danke ich für die ständige Bereitschaft zu Diskussion und Hilfestellung und für das sehr angenehme Arbeitsklima.

Ich möchte ganz besonders meinen Eltern Evgenia Shanina und Valerij Shanin und meinen Freund René Fiege für ihre Liebe und Unterstützung in meinem Leben danken.

9. Appendix

Abbreviations

Bcl-2	B-cell CLL lymphoma 2
BDNF	brain-derived neurotrophic factor
CNS	central nervous system
COX 1,2	cyclooxygenase 1,2
CTRL	sham-operated control animals control animals
DL	double lesion/ double-lesioned animals
FGF-2	fibroblast growth factor-2
FJ	Fluoro-Jade B
FL1/FL2	firstly/secondly affected forelimb
FL SMC	forelimb sensorimotor cortex
FLA	forelimb activity
Fr1	frontal motor cortex
GABA	γ-aminobutyric acid
GFAP	glial fibrilary acidic protein
HSP	heat shock protein
IL-1β	interleukin 1β
LD	laterodorsal thalamic nucleus
LP	lateral posterior thalamic nucleus
MCA	middle cerebral artery
MCAO	middle cerebral artery occlusion
MRI	magnetic resonance imaging

NGF	nerve growth factor
NMDA	N-metyl-D-aspartatic acid
NO	nitrate oxide
Par1	parietal primary somatosensory cortex
PBS	phosphate buffer saline
Po	posterior thalamic nuclear group
SL	single lesion/single-lesioned animals
TBS	Tris-buffer solution
TNF-α	tumor necrosis factor α
VA	ventral anterior thalamicnucleus
VL	ventrolateral thalamic nucleus
VPL	ventral posterolateral thalamic nucleus
VPN	ventroposterior nucleus thalamus

Curriculum vitae

Biographische Daten:

Name	Elena Chanina
Geburtsdatum	01.01.1974
Geburtsort	Kaluga, Rußland
Staatsgehörigkeit	russisch

Schulischer Werdegang:

1981 – 1991	Allgemeinbildende Mittelschule, Kaluga, Russland
1991	Hochschulreife (Note: sehr gut)

Hochschulausbildung:

09.1991 – 06.1997	Studium der Biochemie (Diplom) an der Russischen Staatlichen Medizinischen Universität in Moskau, Rußland. Schwerpunktfächer: Biologie, Biochemie, Medizin
09.1996 – 05.1997	Diplomarbeit in der Arbeitsgruppe von Herrn Prof. Dr. I.V. Victorov im Labor experimenteller Neurozytologie am Hirnforschungsinstitut der Russisch-Medizinischen Akademie der Wissenschaft, Moskau Thema: „Untersuchungen von Neuronen nach photothrombotisch induzierten ischemischen Läsionen des Rattenkortex (Note: sehr gut)
09.1997 – 12.1999	Wissenschaftliche Mitarbeiterin in der Arbeitsgruppe von Herrn Prof. Dr. I.V. Victorov im Labor experimenteller Neurozytologie im Hirnforschungsinstitut der Russischen Medizinischen Akademie der Wissenschaft, Moskau

Ab 01.2000	Promotion in der Arbeitsgruppe von Herrn Prof. Dr. med. O.W. Witte an der Neurologischen Klinik der Heinrich-Heine-Universität Düsseldorf Thema: „Neuronale Plastizität nach Hirnläsionen: Morphologische und verhaltensbiologische Untersuchungen zur Funktionserholung“
07.2001	Wechsel an die Neurologische Klinik der Friedrich-Schiller-Universität Jena (Direktor: Prof. Dr. med. O.W. Witte)

Jena, den 02.05.06

Publications

Ostrovskaya RU, Romanova GA, Barskov IV, Shanina EV, Gudasheva TA, Victorov IV, Voronina TA, Seredenin SB. (1999) Memory restoring and neuroprotective effects of the proline-containing dipeptide, GVS-111, in a photochemical stroke model. *Behavioural Pharmacology* Sep. **10(5):** 549-553.

Shanina E, Redecker C, Reinecke S, Schallert T, Witte OW (2005) Long-term effects of sequential cortical infarcts on scar size, brain volume and cognitive function. *Behavioural Brain Research* **158:** 69-77.

Shanina E, Schallert T, Witte OW, Redecker C (2006) Behavioral recovery from unilateral photothrombotic infarcts of the forelimb sensorimotor cortex in rats: role of the contralateral cortex. *Neuroscience* In press.

Shanina E, Witte OW, Redecker C (2006) Effects of sequential bilateral cortical infarcts on degeneration and inflammation in remote brain structures. Manuscript.

Poster presentations

Shanina E, Redecker C, Reinecke S, Schallert T, Witte OW (2002) Long-term effects of sequential cortical infarcts on brain infarct and cognitive function. Program No. 488.3. *Abstract Viewer/Itinerary Planner.* Orlando: Society for Neuroscience. Online.

Shanina E, Redecker C, Reinecke S. Schallert T, Witte OW, (2004) Influence of sequential ischemic lesions on functional outcome. Prog. No. 339. *Abstract.* Lissabon: FENS Forum.

Shanina E, Redecker C, Reinecke S, Schallert T, Witte OW (2004) Long-term effects of sequential cortical infarcts on brain infarct and cognitive function. *Abstract.* Jena: 49. Jahrestagung der DGKN.

Shanina E, Reinecke S, Schallert T, Witte OW, Redecker C, (2005) Effects of the contralateral cortex on sensorimotor recovery after cortical photothrombotic infarcts: functional evaluation of sequential bilateral lesions. Program No. 333.17. *Abstract Viewer/Itinerary Planner.* Washington DC: Society for Neuroscience. Online.

Ehrenwörtliche Erklärung

Hiermit erkläre ich, dass mir die Promotionsordnung der Biologisch-Pharmazeutischen Fakultät der Friedrich-Schiller-Universität bekannt ist,

ich die Dissertation selbst angefertigt habe und alle von mir benutzten Hilfsmittel, persönlichen Mitteilungen und Quellen in meiner Arbeit angegeben sind,

die Hilfe eines Promotionsberaters nicht in Anspruch genommen wurde und dass Dritte weder unmittelbar noch mittelbar geldwerte Leistungen von mir für Arbeiten erhalten haben, die im Zusammenhang mit dem Inhalt der vorgelegten Dissertation stehen,

dass ich die Dissertation noch nicht als Prüfungsarbeit für eine staatliche oder andere wissenschaftliche Prüfung eingereicht habe und

dass ich die gleiche, eine in wesentlichen Teilen ähnliche oder eine andere Abhandlung nicht bei einer anderen Hochschule als Dissertation eingereicht habe.

Jena, im Mai 2006 Elena V. Chanina